
THE UNIVERSITY
*of* EDINBURGH

# Borane-catalysed Alkyne Hydroboration


THE UNIVERSITY *of* EDINBURGH

Eduardo Nieto Sepúlveda

*Doctor of Philosophy*

The University of Edinburgh

2019

# Declaration

I declare that the work in this thesis was carried out by me under the supervision of Professor Guy Lloyd-Jones FRS and is in accordance with the requirement of the University of Edinburgh. This work is original, except where indicated by special reference in the text, and no part of the dissertation has been previously submitted for any other academic award.

Signed ……

Date ..……

# Publications

The work presented in Chapter 2 has been communicated:

*J. Am. Chem. Soc*. **2019,** 141 (46), 18600–18611.

# Abstract

Within the past few decades, organoboron compounds have become essential intermediates in organic and medicinal chemistry due to their unique advantages and versatility. Many synthetic approaches have been utilised to prepare these useful compounds, including several catalytic systems and diverse hydroborating agents. The hydroboration of terminal alkynes is one of the more common routes that provides alkenylboron reagents, allowing regio- and stereo-selective installation of the boron.

Alcoholysis of phosphine borane complex to generate a new metastable hydroborating agent has been studied. The effect of the alcohol and solvent used in the solvolysis reaction have been determined. The use of halogenated solvents removed the irreproducibility observed when an ethereal solvent is used on its own. Thus having a mixture of both solvents, produces an ideal media to stabilise dialkoxyborane species. All kinetic data obtained are consistent with a direct $SN_2$-like mechanism. A plausible mechanism has been proposed where an inconsistent generation of an ionic active species is likely to be causing the irreproducibility in the kinetic stability of the intermediate $HB(OEt)_2$.

The dicyclohexylborane-catalysed hydroboration of 4-fluoropheny-lacetylene with pinacolborane was used as a benchmark. The kinetic profile for all components, including intermediates and side-products, have also been established by using *in situ* $^{19}F$ NMR kinetic analysis and simulation. Isotope entrainment and stoichiometric studies employing isotopic labelling were used to characterise key steps of the borane-catalysed hydroboration reaction. The experimental evidence used to propose a thorough mechanism were also backed up by density functional theory (DFT) calculations. The mechanism includes the first true transborylation step, responsible of the regeneration of the catalyst ($HBCy_2$) *via* B-C-B transfer of the alkenyl group with retention of (*E*)-configuration.

# Lay Summary

Organoboranes are a versatile class of chemical compounds that have become essential intermediates in organic and medicinal chemistry as they possess wide applications in these fields. The contribution into this area was recognised with two Nobel Prizes awarded in 1979 to Herbert C. Brown and in 2010 to Akira Suzuki who both investigated the development of new synthetic tools for the introduction of boron atoms into organic molecules.

There has been plenty of research going into developing new systems to produce these types of reagents, especially those hydroboration reactions catalysed by expensive metals. Notably, only a few limited studies have been carried out into understanding how the accessible and versatile boron-catalyse hydroboration works.

This thesis is focused on the development in a new hydroborating agent by understanding the processes affecting its synthesis: nature of reagents and solvents. Furthermore, this work shows experimental evidence for a mechanistic proposal that accounts for the selectivity observed in the product of the boron-catalysed alkyne hydroboration reaction. Additionally, explains the side-products obtained and how to mitigate them, as well as the regeneration of the catalyst in the cycle.

# Acknowledgements

Firstly, I would like to thank Professor Guy Lloyd-Jones for his advice, support and trust on me. I am grateful for the acceptance and positive feedback that made a difference and encouraged me to always keep developing my project and strive for quality research work.

Secondly, I would like to thank Team Boron for taking me in when I joined the group, making me feel that I belonged, even with my lack of experience. I would also like to acknowledge all members of the GLJ group who have provided support and guidance, especially all post-docs with their invaluable knowledge that were always willing to share. Outside the group, I would like to thank the staff of the School of Chemistry that always helped with my queries and ensured the smooth running of a number of facilities.

Also, I would like to thank my family and friends for tolerating my absence over the past few years, while receiving me with such warmth and enthusiasm every time I had the opportunity to visit them. Thanks in particular to Alfonso for helping me through the unpredictability of my PhD and his unconditional support and confidence in me. I do not think I could have done this without you.

Lastly, I would to thank my parents and sister that have believed in me every step of the way and for always welcoming me home. Specially to my mum that has always been my motivation and role model, to whom I am greatly indebted. Therefore, I want to dedicate this thesis to her.

# Abbreviations

| | |
|---|---|
| Ac | acetyl |
| ACN | acetonitrile |
| bp | boiling point |
| BPO | benzoyl peroxide |
| cat | catechol |
| Cy | cyclohexyl |
| DABCO | 1,4-diazabicyclo[2.2.2]octane |
| DBU | 1,8-Diazabicyclo[5.4.0]undec-7-ene |
| DMF | N,N-dimethylformamide |
| DMSB | dimethyl sulphide borane complex |
| DMSO | dimethyl sulfoxide |
| Et | ethyl |
| equiv. | equivalents |
| h | hours |
| $^{i}$Pr | isopropyl |
| *J* | coupling constant |
| Me | methyl |
| min | minutes |
| mp | melting point |

| | |
|---|---|
| $^{n}$Bu | normal butyl |
| NHC | N-heterocylic carbenes |
| NMR | nuclear magnetic resonance |
| $^{n}$Pr | normal propyl |
| Ph | phenyl |
| pin | pinacol |
| ppm | parts per million |
| rt | room temperature |
| s | seconds |
| $^{s}$Bu | secondary butyl |
| SM | Suzuki-Miyaura |
| TBAC | tetrabutylammonium chloride |
| $^{t}$Bu | tertiary butyl |
| THF | tetrahydrofuran |
| THFB | tetrahydrofuran borane complex |

# Contents

**Declaration** ... **iii**
**Abstract** ... **vii**
**Lay Summary** ... **ix**
**Acknowledgements** ... **xi**
**Abbreviations** ... **xiii**
**Chapter 1 Borane Alcoholysis** ... **3**
1.1 Introduction: Boron Reagents ... 4
1.1.1 Generalities ... 4
1.1.2 The Importance of Boron Compounds ... 5
1.1.3 Protected Boron Reagents ... 7
1.1.3.1 Synthesis of MIDA Boronates ... 8
1.2 Dialkoxyboranes: an Alternative Route to Coupling Reagents ... 10
1.2.1 Hydroboration ... 10
1.2.2 Alkyne Hydroboration: Generalities ... 10
1.2.2.1 Synthesis of Alkenylboronates ... 11
1.2.3 Dialkoxyboranes ... 12
1.3 Phosphine Borane Complexes: as a Source of Borane ... 13
1.3.1 Borane Sources ... 13
1.3.2 Phosphine Borane Complexes ... 14
1.3.2.1 Synthesis of Phosphine Borane Complexes ... 15
1.3.3 Deprotection Methods ... 15
1.3.3.1 Alcoholysis of Phosphine Borane Adducts ... 16
1.4 Aims ... 17
1.5 Results and Discussion ... 19
1.5.1 Initial Mechanistic Studies ... 19
1.5.1.1 Phosphine Borane Complexes Solvolysis ... 19

1.5.1.2 Intermediate Identification ..... 20
1.5.1.3 Irreproducibility ..... 22
1.5.2 Effect of Temperature ..... 23
1.5.3 Effect of Solvolytic Agent ..... 24
1.5.3.1 Primary Alcohols ..... 24
1.5.3.2 Secondary and Tertiary Alcohols ..... 25
1.5.4 Effect of Solvent ..... 26
1.5.4.1 Non-halogenated Solvents ..... 26
1.5.4.2 Halogenated Solvents ..... 30
1.5.5 Mixture of Solvents ..... 32
1.5.5.1 Dioxane/Chloroform Mixtures ..... 33
1.5.5.2 Other Halogen Sources Mixtures ..... 35
1.5.6 Mechanistic Studies ..... 37
1.5.6.1 Bubble Surface Effects ..... 38
1.5.6.2 Radical Initiation ..... 39
1.5.6.3 Boronium ..... 39
1.5.6.4 Proposed Mechanism ..... 40
1.5.7 Other Borane Sources ..... 42
1.5.7.1 Tetrahydrofuran Borane Complex ..... 42
1.5.7.2 Dimethyl Sulfide Borane Complex ..... 43
1.5.8 Effect of Ligand in Borane-Lewis Base Complex ..... 45
1.5.9 Pinacolborane: Alcoholysis Synthetic Application ..... 47
1.5.9.1 HBpin Synthesis from Phosphine Borane $1_{PB}$ ..... 47
1.5.9.2 HBpin Synthesis from DMSB ..... 48
1.5.10 One-pot Synthesis of Alkenylboronic Acid Pinacol Esters ..... 50

1.5.11 Dialkoxyborane: New Hydroborating Agent .....52

**Chapter 2 Borane-catalysed Alkyne Hydroboration .....57**

2.1 Organoboron Derivatives.....58

2.1.1 Introduction .....58

2.1.2 Background .....58

2.2 Hydroboration of Alkynes .....60

2.2.1 Metal-free Hydroborations .....60

2.2.1.1 Borane-catalysed Hydroborations .....64

2.2.1.2 Hydroborations mediated by N-heterocylic Carbenes .....66

2.2.1.3 Acid- and Base-catalysed Hydroborations.....67

2.2.1.4 Hydroboration of Alkynes Mediated by Borenium Cations .....68

2.2.2 Metal-catalysed Hydroborations .....69

2.2.2.1 Zirconium-catalysed Hydroborations.....70

2.2.2.2 Rhodium-catalysed Hydroborations .....71

2.2.2.3 Copper-catalysed Hydroborations .....72

2.3 Aims .....74

2.4 Results and Discussion .....76

2.4.1 Initial Mechanistic Studies .....76

2.4.1.1 Hydroboration of 4-Fluorophenylacetylene with Pinacolborane Catalysed by Dicyclohexylborane .....76

2.4.1.2 Hydroboration of 4-Fluorophenylacetylene with Pinacolborane Catalysed by Dimethyl Sulfide Borane .....79

2.4.2 Stability of Pinacolborane Solution .....80

2.4.3 Irreversibility of Product and Side-product Formation .....82

2.4.4 Productivity of the Intermediate.....84

2.4.5 Boron-catalysed Hydroboration and Transborylation .....88

2.4.6 Kinetic Model for Products .....94

2.4.7 Mechanistic Proposal....96
2.4.7.1 Hydroboration of 4-Fluorophenylacetylene with Pinacolborane Catalysed by 9-Borabicyclo[3.3.1]nonane .... 100
**Chapter 3 Conclusions and Future Work .... 103**
**Chapter 4 Experimental .... 109**
4.1 General Experimental .... 110
4.1.1 Techniques .... 110
4.1.2 Reagents and Solvents .... 110
4.1.3 Chromatography .... 111
4.1.4 Analysis .... 111
4.1.4.1 NMR Spectroscopy .... 111
4.1.4.2 Mass Spectrometry .... 112
4.1.4.3 Melting Points .... 112
4.1.4.4 Computational Studies .... 112
4.2 Reaction Monitoring: Chapter 1 .... 112
4.2.1 Borane Complexes Alcoholysis .... 112
4.2.1.1 Bubble Surface Effects − Modification .... 113
4.2.2 Phosphine Borane Pinacolysis .... 113
4.2.3 Dimethyl Sulfide Borane Complex Pinacolysis .... 114
4.2.4 Boronic Acid and MIDA Condensation .... 114
4.3 Reaction Monitoring: Chapter 2 .... 114
4.3.1 Dicyclohexylborane-Catalysed Alkyne Hydroboration .... 114
4.3.2 DMSB-Catalysed Alkyne Hydroboration .... 115
4.3.3 9BBN-Catalysed Alkyne Hydroboration .... 115
4.3.4 Isotopic Entrainment .... 115
4.3.5 Cross-over Experiment .... 116

4.4 Synthetic Procedures ..... 117
**References ..... 127**
**Chapter 5 Appendix ..... 137**
5.1 Chapter 1 ..... 138
5.2 Chapter 2 ..... 141
5.2.1 Deuteration Efficiency of [$D_3$]-THFB ..... 143
5.2.2 Synthesis Optimisation Summary for [$^{10}$B]-Tris(o-tolyl)-phosphine borane 144
5.2.3 Double addition side-product NMR data ..... 147

# Chapter 1 Borane Alcoholysis

# 1.1 Introduction: Boron Reagents

## 1.1.1 Generalities

Boron is a group 13 element in the second period, located on the left-hand side of carbon in the periodic table. Since atomic boron has three valence electrons ($2s^2$, $3p^1$), neutral boron molecules can generally engage in three $sp^2$ hybridised bonds, resulting in a trigonal planar geometry, and a vacant *p*-orbital on the boron centre orthogonal to the plane (Figure 1.1). This nature dominates the reactivity patterns and physical characteristics of all neutral $sp^2$ boron compounds as electron-deficient species in organic and inorganic chemistry fields.

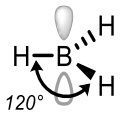


**Figure 1.1** – Borane trigonal planar geometry.

For example, the Lewis acidity of boron-containing compounds have been widely utilised for organic chemistry, such as hydroboration chemistry[1–3], Lewis-acidic boron mediated chemistry[4], boron-enolate chemistry[5] and Suzuki-Miyaura (SM) cross-coupling chemistry[6–8]. To = synthesise these types of boron-containing compounds, a boron-containing chemical bond should be constructed.

In general, the existence of this empty *p*-orbital of the boron atom in boron-containing reagents, cause them to become susceptible towards electron donation from Lewis bases. Consequently, it allows nucleophile additions to them to form a boron-nucleophile bond.

Boron-containing reagents have unique advantages:

- They are inexpensive and readily prepared.
- Have a broad functional-group tolerance, are relatively stable and generally environmentally benign.

- Some are thermally stable and inert to water and oxygen, thus easy to handle (industry).
- Transmetalate with a variety of metal compounds under exceptionally mild reaction conditions, especially versatile with palladium(II) complexes.

The use of organoboron compounds is also valued because the inorganic byproducts of the reaction are nontoxic and can be easily removed by simple workup procedures.

### 1.1.2 The Importance of Boron Compounds

Boron reagents are truly essential in modern synthesis. Due to their versatility, and the fact that they exhibit a unique range of physical, chemical and reactivity characteristics, chemists have acquired the ability to adapt the reagent for the reaction in hand (Figure 1.2). This has allowed their use in the synthesis of a large number of natural products, pharmaceutical targets and lead compounds, as well as being applied in scale-up for clinical trials, process development and even manufacture.[9]

The main application of such species has predominantly become as reagents in transition metal catalysed cross-coupling reactions, now a routine method for discovery chemistry in the pharmaceutical, materials and agrochemical sectors.[10] This has allowed the SM reaction to develop into the most widely-applied transition metal catalysed C−C bond formation reaction to date.

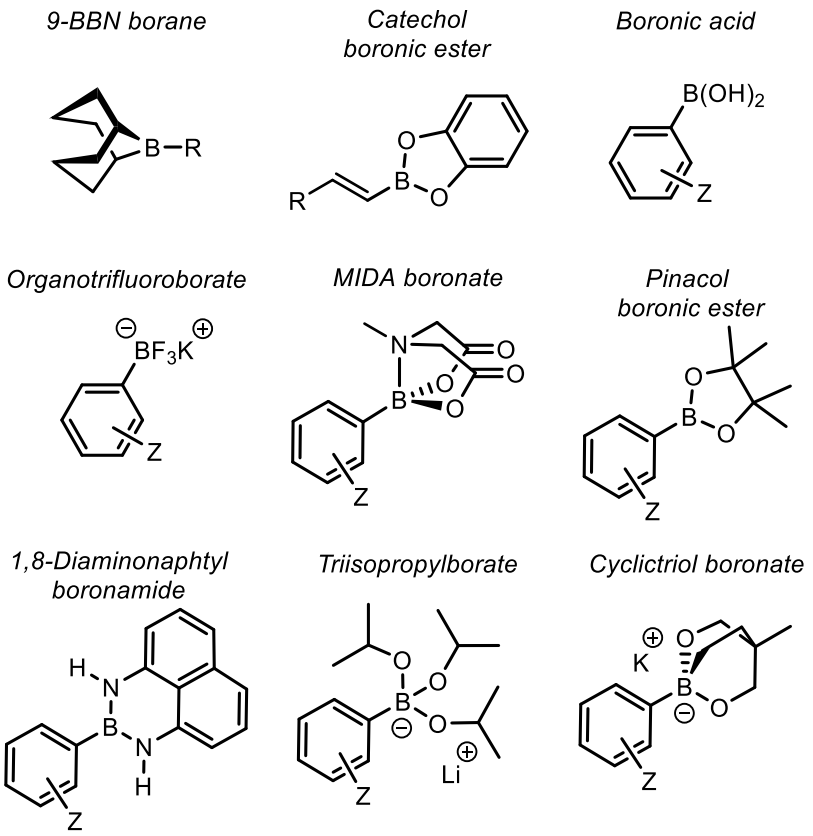


**Figure 1.2** – Some of the most popular boron reagents used directly or indirectly in SM coupling reactions.

The key to the success of the SM coupling reaction resides on the exceptional functional group tolerance of the catalyst system and the mild reaction conditions that are employed. This originates from the relatively stable, innocuous and environmentally benign nature of the boron-containing reagent. Nonetheless, transmetallation of organoboron compounds with the appropriate palladium(II) complex proceeds rapidly and efficiently. These combined features contribute to the practical up-scaling of the reaction and, together with the relatively low cost of the reagent, explain its value to the fine industries. Indeed, SM coupling has become the "gold standard" for biaryl construction, arguably resulting in the ubiquity of this moiety in medicinal chemistry.[11]

### 1.1.3 Protected Boron Reagents

Boron reagents often come in "protected" form.[12] This is to minimise exposure of the reagent to undesired side reactions or storage degradation, such as protodeboronation, oxidation and/or polymerisation. Under specific reaction conditions, the active species can be released *in situ via* solvolysis when required, either in series or in parallel with coupling.

A good example of the use of these reagents are trifluoroborates.[13,14] These are easily prepared as potassium organotrifluoroborates, which are tetrahedral in geometry and not Lewis acidic due to the additional ligand bound to the boron centre as depicted in Figure 1.3. This quaternisation with exceptionally strong B–F bonds, together with their monomeric solid structure (tend to melt and decompose only at very high temperatures), grants them the characteristic to be stable to air and aerobic moisture. Accordingly, this not only broadens their availability, but also makes them more useful for employment in combinatorial chemistry and in multi-step syntheses.

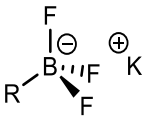


**Figure 1.3** – Tetrahedral geometry from a general organotrifluoroborate.

*N*-methyliminodiacetic acid (MIDA) boronates are another example of protected boron reagents[15]. Used initially to mitigate side reactions from their boronic acid counterparts, these have been evolved to become a powerful and useful strategy for the synthesis of complex organic molecules.[16] There are formally two B–O covalent bonds plus a dative bond that forms from donation of the Lewis basic lone pair on nitrogen to the Lewis-acidic boron atom. This donation hybridises boron from $sp^2$ to $sp^3$, whilst weakening the B–O bonds and forcing the boron into a tetrahedral geometry (Figure 1.4). MIDA boronates have a uniform benchtop stability and remarkable capacity for *in situ* slow release of unstable boronic acids,

including 2-heterocyclic, vinyl and cyclopropyl derivatives. Consequently, this provides air-stable and highly effective substitutes for all three of these challenging boronic acid classes. In the recent years, MIDA boronates have emerged as an increasingly general and automated platform for building block-based synthesis of small molecules.[16]

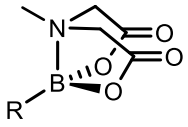


**Figure 1.4** – General MIDA boronate structure.

### 1.1.3.1 Synthesis of MIDA Boronates

The MIDA ligand can be synthesised on very large scale at low cost,[15] is commercially available and is fully biodegradable.[17] Many methods now exist for preparing MIDA boronates from a wide range of different starting materials (Scheme 1.1), including boronic acids,[18–22] haloboranes,[20,23] boronic esters,[24] trialkoxyborate salts,[15,24–27] organohalides,[27] organolithium reagents[27] and Grignard reagents.[24,26]

Some disadvantages on current pathways for the synthesis of MIDA boronates are the requirement of harsh and/or special specific conditions. Many boronic acids can be transformed into their corresponding MIDA boronate by condensation with MIDA under Dean-Stark conditions (Scheme 1.1, reaction a).[19,21,22,28,29] The removal of water by a variety of alternative techniques (e.g. molecular sieves, azeotropic drying with acetonitrile, etc.) can also promote full conversion to the MIDA boronate product. Typically, this condensation process requires heating to at least 40 °C (in some cases up to 130 °C), and the use of dimethyl sulfoxide as co-solvent is required to partially dissolve the MIDA ligand.

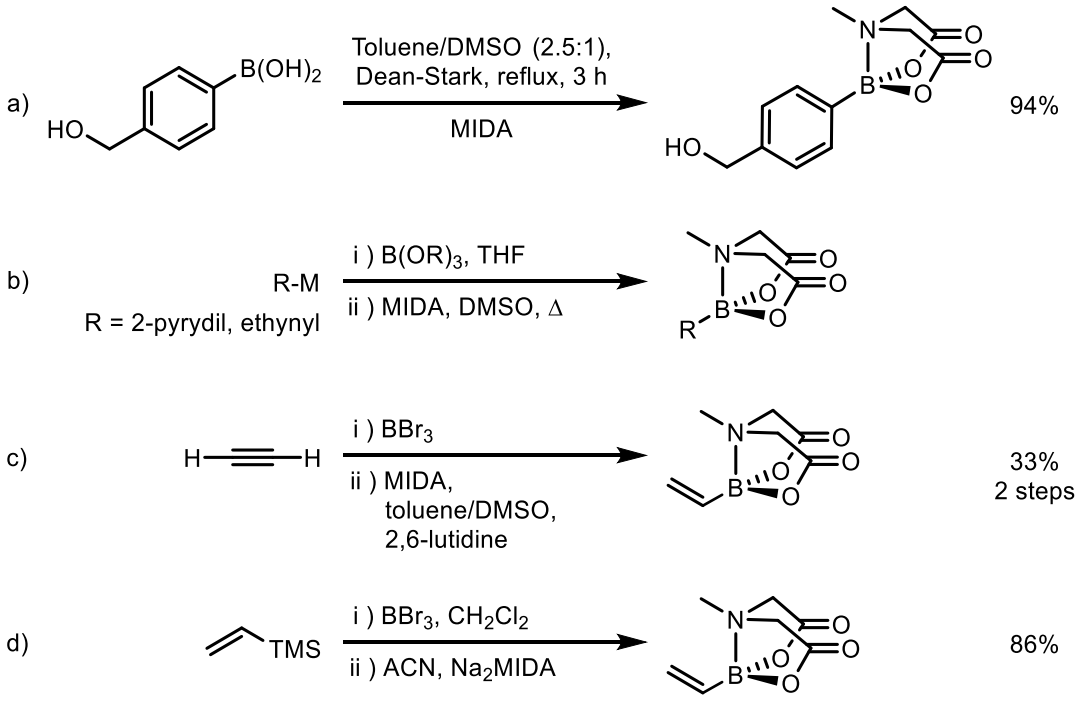


**Scheme 1.1** – Preparation of MIDA boronates for some different substrate classes.

Research has also led to the development of several methods that enable the preparation of MIDA boronates without the intermediacy of a boronic acid. Alkenyl MIDA boronates can be synthesised *via* bromoboration of an alkyne to form the corresponding dibromoborane followed by trapping with MIDA in the presence of 2,6-lutidine (Scheme 1.1, reaction c).[20] More than 24 hours are needed to prepare the dibromoborane precursor (and more than 72 hours to obtain the MIDA boronate); three distillations are required and carefully heating the crude mixture to 65 °C with risk of triggering a polymerisation reaction of slightly overheated.

## 1.2 Dialkoxyboranes: an Alternative Route to Coupling Reagents

### 1.2.1 Hydroboration

Hydroboration constitutes one of the most important and facile methods for the synthesis of organoboranes from unsaturated compounds. The organoboranes serve as valuable intermediates for the synthesis of a wide variety of organic compounds.[30] For that reason, there is a huge interest in exploring their chemistry and in developing new hydroboration reactions of major significance in synthetic organic chemistry.

The facile addition of boron-hydrogen moiety to C−C multiple bonds of unsaturated organic derivatives gives organoboranes (Scheme 1.2). The reaction is very rapid, usually being completed within a few minutes at temperatures below 25 °C.


**Scheme 1.2** – Hydroboration of unhindered C−C double bonds with diborane leading to trialkylboranes.

### 1.2.2 Alkyne Hydroboration: Generalities

Hydroboration of unsaturated carbon bonds by pinacolborane (HBpin) or catecholborane (HBcat) without using harsh reaction conditions is difficult, but with the addition of a suitable metal catalyst they readily add to alkynes.[31,32] Systems have been reported that employ non-precious metal catalysts[33–35] and even metal-free catalysts.[25,36–38]

The hydroboration of terminal alkynes (Scheme 1.3) allows readily access to alkenylboranes and catecholboronic esters,[39,40] a process that provided the reagents employed by Suzuki and Miyaura for their initial discovery and investigation of the SM coupling reaction. In addition, the hydroboration of alkynes is a useful

method for the synthesis of 1-alkenylboronate compounds, which are versatile intermediates in organic synthesis[41] owing to their use as nucleophilic partners in C–C bond forming reactions.[6,42,43]

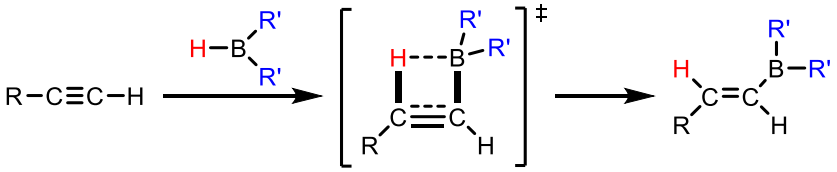

**Scheme 1.3** – General mechanism of hydroboration of alkynes showing the transition state where the boron atom adds regiospecifically to the less substituted carbon atom.

The boronate is much more favourable than dialkylboryl group to Pd-catalysed cross-coupling reactions due to virtual impossibility of side reactions arising from the two alkyl groups on the boron atom. Alkenylboronates can be prepared from alkynes directly as well as indirectly.

### 1.2.2.1 Synthesis of Alkenylboronates

Brown and co-workers reported the indirect procedure according to which the hydroboration of alkynes with dibromoborane-dimethyl sulfide complex ($HBBr_2 \cdot SMe_2$), followed by alcoholysis or hydrolysis-esterification sequence, furnished the corresponding alkenylboronates.[44] In addition, they prepared (*Z*)-1-alkenylboronates through hydroboration of 1-bromo-1-alkyne with $HBBr_2 \cdot SMe_2$, followed by a similar esterification and hydrodebromination with potassium triisopropoxyborohydride.[45] The methodology for the synthesis of alkenylboronates using $HBr_2 \cdot SMe_2$ is general and useful; however, the method with alcoholysis was complicated by the formation of $Me_2S \cdot HBr$, and the route with hydrolysis-esterification required the isolation of alkenylboronic acids.

One-pot procedures for preparing (*E*)-1-alkenylboronic acid pinacol esters were achieved by Hoffmann[46] and Vaultier[47,48] and co-workers. Their methods, however, consisted of three steps, namely, hydroboration of 1-alkyne with dialkylborane, esterification of the dialkylboryl group and transesterification with pinacol.

Hara and co-workers realised the preparation of 2,2-disubstituted 1-alkenylboronates by means of bromoboration of 1-alkyne with $BBr_3$.[49] Thus, esterification of (*Z*)-2-bromo-1-alkenyldibromoborane gave (*Z*)-2-bromo-1-alkenylboronate, which could be cross-coupled with organylzinc chloride in the presence of Pd(0) with retention of stereochemistry to afford 2-organyl-1-alkenylboronates.

There are several more procedures for the synthesis of alkenylboronates *via* alkyne hydroboration; these are reviewed in depth in Chapter 2.

### 1.2.3 Dialkoxyboranes

In general, dialkoxyboranes have been scarcely reported, Heinrich Nöth and co-workers studied the temperature dependant reactions of $Zr(OBu)_4$ and $Zr(OEt)_4$ with tetrahydrofuran borane complex in THF that led to $HB(OR)_2$ and $B(OR)_3$.[50] The reactions that were carried away at lower temperatures (−30 °C to 0 °C) showed better relative intensities for those products in the $^{11}B$ NMR spectra.

A facile method for the generation and application of dialkoxyboranes would be desirable. A metastable $HB(OR)_2$ reagent (not commercially available) could be used in alkyne hydroboration reactions giving versatile alkenylboronate products. For example, the dialkoxyborane-catalysed addition of HBpin to alkynes is a route that has been used to prepare alkenyl MIDA boronates[51], after laborious exchange of the pinacol moiety.[24] Thus alkenylboronates would represent an entropically favoured route to prepare MIDA boronates after transesterification (Scheme 1.4) or other synthetically useful compounds under milder reaction conditions.

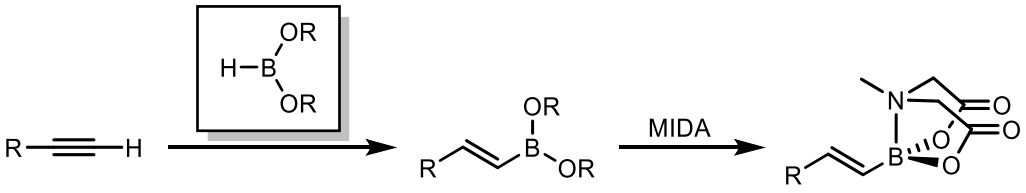


**Scheme 1.4** – Simplified proposed route for application of metastable dialkoxyborane reagent.

## 1.3 Phosphine Borane Complexes: as a Source of Borane

### 1.3.1 Borane Sources

Diborane ($B_2H_6$), the simplest borane, is a useful reagent with many applications but with considerable disadvantages: being pyrophoric, gaseous and not convenient to handle. Borane-Lewis base complexes are often found in literature, from these, tetrahydrofuran borane complex (THFB) and dimethyl sulfide borane complex (DMSB) are the most common ones used as a borane source (Figure 1.5). Both reagents are commercially available as a solution, therefore, are easier to handle than diborane. A minor drawback is their volatility and flammability. DMSB can be obtained in higher molarity than THFB though it has a pungent unpleasant odour.

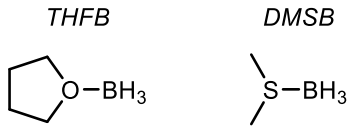


**Figure 1.5** – Tetrahydrofuran borane complex and dimethyl sulfide borane complex as representative borane sources.

Unfortunately, there are significant challenges associated with the use of THFB, it is unstable and prone to disproportionation unless stored in low concentration at low temperatures. THF is a weak Lewis base which coordinates do $BH_3$, forming a complex which can equilibrate to dissociated products. One of these dissociated products is free diborane, which is a highly volatile and pyrophoric gas known to readily ignite when brought in contact with water or air.[52] Another important degradation pathway, that causes the effective molarity of the THFB solution to decrease, corresponds to borane facilitating hydride-mediated ring opening of THF producing dibutoxyborane and ultimately tributoxyborane as unwanted byproducts (Scheme 1.5).

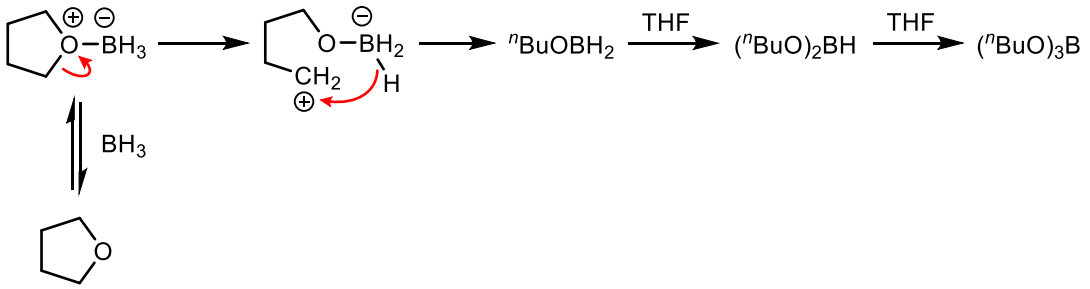


**Scheme 1.5** – Ring opening degradation pathway of tetrahydrofuran borane complex.

At or above room temperature THFB degradation is facile, however, the ring opening is absent or minimal below 5 °C. On the contrary, DMSB does not suffer from this problem due to the neat complex in dimethyl sulfide is very stable. However, DMSB releases a stoichiometric amount of highly volatile and flammable dimethyl sulfide. These limitations discourage the application of borane reactions in large scale processes and create unique problem associated with their storage and large scale transportation.

### 1.3.2 Phosphine Borane Complexes

Phosphine borane complexes, which have a broad application in catalysis, materials and coordination chemistry, were first reported by Burg and Wagner.[53] It was shown in as early as 1965 by Frisch and co-workers that triphenylphosphine ($Ph_3P$) can easily react with borane to furnish triphenylphosphine borane complex ($Ph_3P{\cdot}BH_3$).[54]

This strategy, that has been widely utilised to create a robust and stable complex, consists in quenching the phosphorus lone pair through coordination to borane. The low polarity and polarizability of the P–B and B–H bonds make them rather unreactive. This borane protecting strategy affords air and moisture stable phosphine borane complexes which are easy to handle and have the advantageous characteristic to tolerate aerobic column chromatography.[55–57]

### 1.3.2.1 Synthesis of Phosphine Borane Complexes

Phosphine borane complexes are usually prepared by direct reaction between phosphines and commercially available solutions of borane complexed to labile Lewis bases (Scheme 1.6, method a).[58] The most frequent borane sources used for this purpose are THFB and DMSB, the latter being more stable and with a higher boronating capacity than THFB. The higher Lewis basicity of phosphines compared to tetrahydrofuran or dimethyl sulfide causes the migration of the borane group to furnish the phosphine borane complex quantitatively.

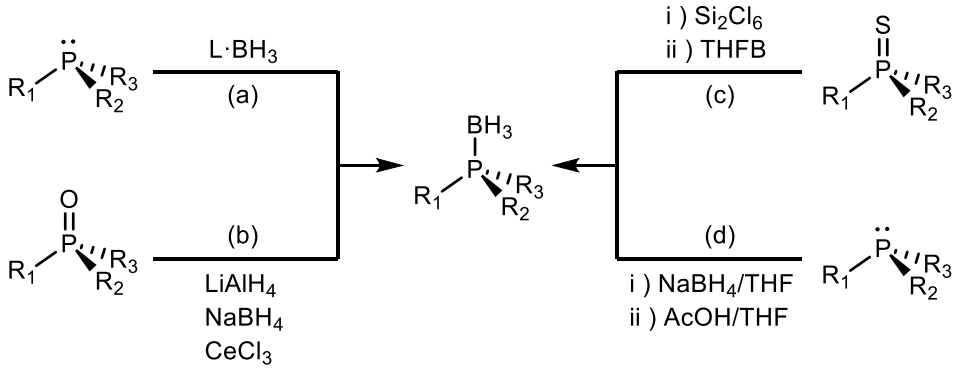


**Scheme 1.6** – Boronation of phosphines.

Imamoto and co-workers developed a one-pot transformation of phosphine oxides into phosphine boranes (Scheme 1.6, method b).[59] Starting from optically pure phosphine oxides yielded only racemic phosphine borane complexes. Corey and co-workers prepared optically pure phosphine boranes by *in situ* desulfurisation-complexation with retention of configuration (Scheme 1.6, method c).[60] Additionally, Zhou and McNulty reported a simple, general, economical and high-yielding synthesis of phosphine borane complexes using sodium borohydride as the borane source (Scheme 1.6, method d).[61]

## 1.3.3 Deprotection Methods

Phosphines would not the suitable if the borane group could not easily be removed. Various reliable methods have been developed. One is the treatment of phosphine boranes with amines or alcohols, these act as borane acceptors. The first use of an

alcohol (ethanol) for deprotection of a phosphine borane was reported by Jugé and co-workers in 2000.[62] However, ethanolysis only received widespread attention after further reports that demonstrated its scope and limitations.

Another general method includes the use of a nucleophilic amine, although phosphine boranes are in general more stable than amine boranes, the presence of large excess of amine is frequently sufficient to displace the equilibrium and deprotect completely the phosphine. Typical amines used for this transformation are diethylamine,[63] tetramethylethylenediamine (TMEDA),[64] pyrrolidines,[65,66] morpholine,[67] and 1,4-diazabicyclo[2.2.2]octane (DABCO).[68,69] The reactions are usually carried out at room temperature or with moderate heating in neat amine with the exception of DABCO, being a solid, it has to be dissolved first (typically in toluene).

Another method of deprotection involves the use of certain acidic conditions. These include the use of $HBF_4$, which after hydrolysis with sodium bicarbonate releases the free phosphine into solution in quantitative yields.[70–72] Following this, other acids have successfully been applied in the deprotection including trifluoroacetic acid,[73,74] and trifluoromethanesulfonic acid.[75,76]

#### 1.3.3.1 Alcoholysis of Phosphine Borane Adducts

Despite it was shown in as early as in the 1960s the analogous hydrolysis of triphenylphosphine borane complex, alcoholysis has received relatively little attention.

Jugé and co-workers found that stirring some phosphine borane complexes in ethanol was enough to cleave the borane group; contrastingly, classical decomplexation with DABCO produced many unidentified byproducts.[62] This method has been extended, with slight modifications, to other alcohols and phosphine boranes.[77,78] Not surprisingly, basic trialkylphosphine boranes are not deprotected following this procedure. Although no detailed studies on the mechanism has been reported, it is thought to involve the formation of tertiary borates and hydrogen gas as depicted in Scheme 1.7.[77–79]

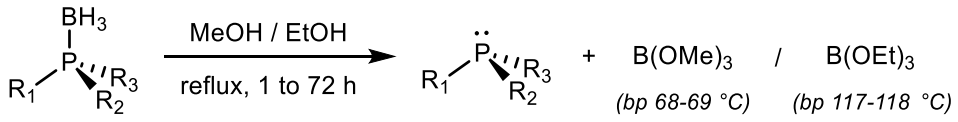


**Scheme 1.7** – General phosphine borane complex alcoholysis deprotection

In the Lloyd-Jones group, preliminary kinetic studies of reaction of $R_3P{\cdot}BH_3$ with simple alcohols, such as ethanol, have been conducted. The results with ethanol (and higher or lower linear alcohols) were very surprising and form the basis of the project presented in this thesis.

## 1.4 Aims

Phosphine borane adducts have limited application as reagents for hydroboration; an alternative manner of how these are currently used would be desirable. A plausible route to this could be the use of stoichiometric hydroboration of alkynes with $HB(OR)_2$ in the presence of a suitable catalyst and adequate conditions, furnishing the corresponding alkenylboronate in high yields.

The advantage sought for this reaction is that the dialkoxyborane, *in situ* generated by the alcoholysis of phosphine borane, could be potentially used directly without isolation. The resulting alkenylboronate product could be converted into the corresponding MIDA boronate (a more useful derivative) *via* transesterification with pinacol. Given the favourable features of this platform, the development of highly versatile organoborane reagents represents an important goal.

Consequently, this project aims to contribute to this growing area of research by exploring, whether the *in situ* deprotection of phosphine borane complex and subsequent use of the metastable borane species in alkyne hydroboration, could be applicable.

Furthermore, to propose a plausible mechanism that represents the pathway by which the dialkoxyborane is likely produced, and either consumed or stabilised,

during the phosphine borane alcoholysis reaction, this by examining how variation at the borane source, alcohol and solvents affect the reaction. It is hoped that this knowledge will aid in the design of new improved synthetic procedures.

## 1.5 Results and Discussion

### 1.5.1 Initial Mechanistic Studies

#### 1.5.1.1 Phosphine Borane Complexes Solvolysis

Initial studies focused on obtaining a reaction model to test the kinetics of the phosphine borane deprotection by alcohols. This model needed to include a set of conditions such as being easy to handle, react on a timescale amenable to measurement, and be representative for synthetically useful procedures. With this in mind, tris(*o*-tolyl)phosphine borane complex $\mathbf{1_{PB}}$ was taken as standard substrate due to its benchtop stability and nucleofugality (leaving group ability). Deprotection by solvolysis can be achieved within a reasonable timescale (suitable for *in situ* NMR spectroscopy monitoring) performing the reaction at a concentration of 0.03 M of $\mathbf{1_{PB}}$ with EtOH (5 M) in toluene at 30 °C (Scheme 1.8). The resulting homogenous reactions were monitored using $^{11}B\{^{1}H\}$ NMR spectroscopy where three peaks can be distinguished having distinct chemical shifts (discussed in more detail in Section 1.5.1.2 on page 20).

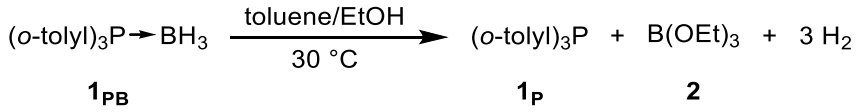


**Scheme 1.8** – Reaction conditions used to investigate the kinetic profile of alcoholysis reactions; $[\mathbf{1_{PB}}]_0$ = 0.03 M and $[EtOH]_0$ = 5 M.

The consumption of the phosphine borane complex showed a high equilibrium constant reaching high conversions of the phosphine product, consistent with studies by Van der Eycken[78] and in disagreement with Nozaki and Hiyama report where the use of molecular sieves (4 Å) are stated as essential for the reaction;[77] this provided a suitable model reaction and a synthetically useful procedure with full conversions.

### 1.5.1.2 Intermediate Identification

A generalised scheme for the theoretical products generated from phosphine borane alcoholysis is shown in Scheme 1.9. The final borate is produced after a three-stage solvolysis, generated after initial nucleophilic displacement by the alcohol.

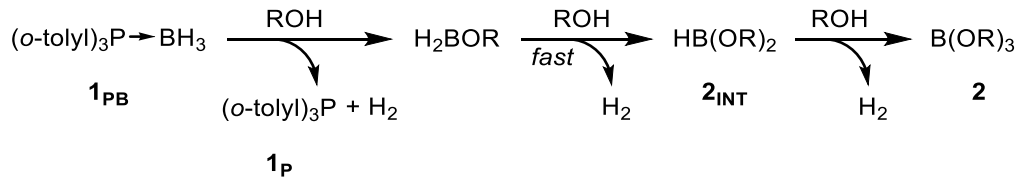


**Scheme 1.9** – Theoretical products formed during alcoholysis of $\mathbf{1}_{PB}$.

Initial mechanistic studies were carried out using ethanol (EtOH) as the solvolytic agent of choice due its practicality, low toxicity and price. $^{11}B\{^{1}H\}$ NMR temporal concentration profiles followed a clean pseudo-first order decay of phosphine borane complex $\mathbf{1_{PB}}$ generating the final borate **2** over time, preceded by the consumption of an intermediate $\mathbf{2_{INT}}$ (Figure 1.6).

Correspondingly, monitoring the reaction using $^{31}P\{^{1}H\}$ NMR showed only two peaks. One corresponding to $\mathbf{1_{PB}}$ being consumed and the second matching the release of free phosphine $\mathbf{1_P}$, this process occurring at the same rate as observed by $^{11}B\{^{1}H\}$ NMR, with the difference being that no other species are shown indicating that the intermediate (and product) detected by $^{11}B\{^{1}H\}$ NMR contains no phosphorus (Figure 1.6).

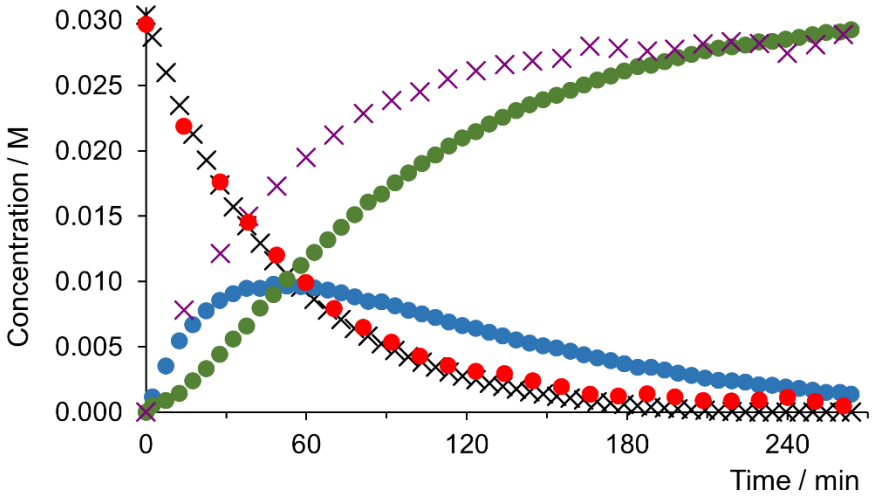


**Figure 1.6** – Temporal concentration profiles for two different ethanolyses of **1$_{PB}$**, monitored by $^{11}B\{^1H\}$ NMR (red circles: **1$_{PB}$**, blue circles: **2$_{INT}$**, green circles: **2**) and by $^{31}P\{^1H\}$ NMR (black crosses: **1$_{PB}$**, purple crosses: **1$_{P}$**). Conditions: $[\mathbf{1_{PB}}]_0$ = 0.03 M, $[EtOH]_0$ = 5 M in toluene at 30 °C.

$^{11}B$ NMR spectroscopy was used to gain further insight into the nature of the intermediate. From the coupling constants and chemical shifts they can be assigned to $HB(OEt)_2$ **2$_{INT}$**, visible as a doublet at 26.4 ppm ($J_{B-H}$ 162.6 Hz); $B(OEt)_3$ **2** as a sharp singlet at 16.9 ppm (confirmed by spiking $B(OEt)_3$ in), and phosphine borane complex **1$_{PB}$**, a broad signal at −31.4 ppm respectively (Figure 1.7). The intermediate can be assigned in accordance to the values generally found for B–H coupling in the $HB(OR)_2$ scaffold: [$HB(OR)_2$: 26–28 ppm, $^1J_{B-H}$ 160–168 Hz].[80] The absence of $H_2BOR$ in the NMR spectrum indicates the second stage of solvolysis is too fast to be followed by standard NMR techniques.

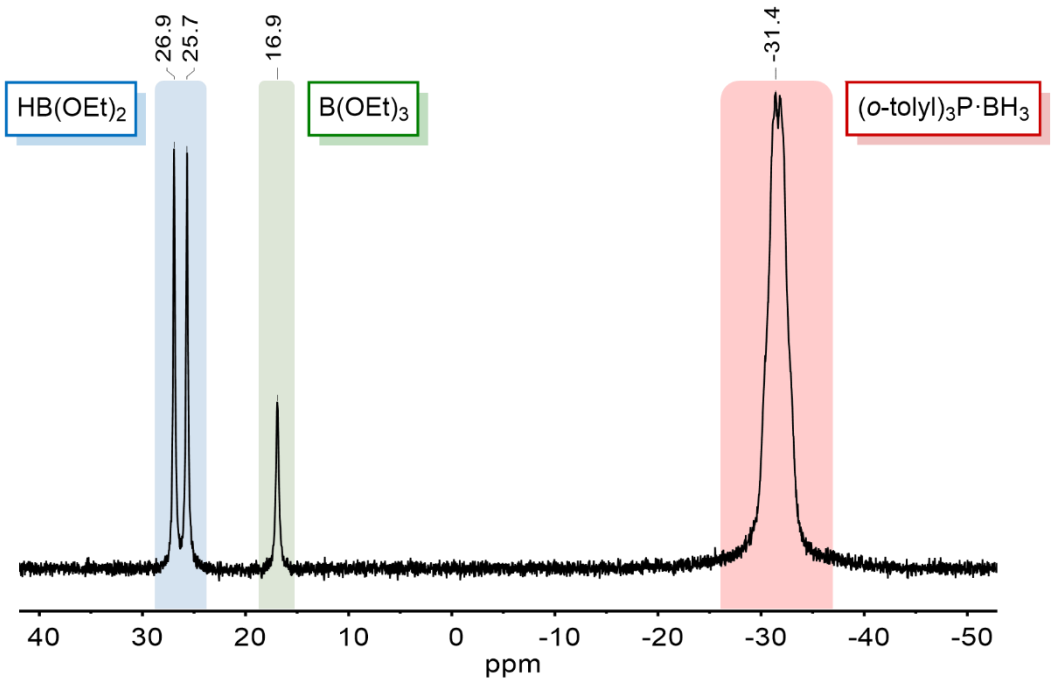


**Figure 1.7** – $^{11}B$ NMR spectrum recorded during the ethanolysis of $\mathbf{1}_{PB}$ showing three unique species; $HB(OEt)_2$ $\mathbf{2}_{INT}$ can be distinguished from its distinctive splitting pattern arising from the expected B–H coupling.

### 1.5.1.3 Irreproducibility

Repetition of experiments using *in situ* $^{11}B\{^1H\}$ NMR demonstrated a high degree of variability regarding the dialkoxyborane intermediate $\mathbf{2}_{INT}$ being accumulated to varying degrees (Figure 1.8 b). This inconsistency in the reaction profile within runs could be due to a critical event initiating rapid solvolysis of the intermediate $HB(OEt)_2$ $\mathbf{2}_{INT}$ to final borate $B(OEt)_3$ **2**.

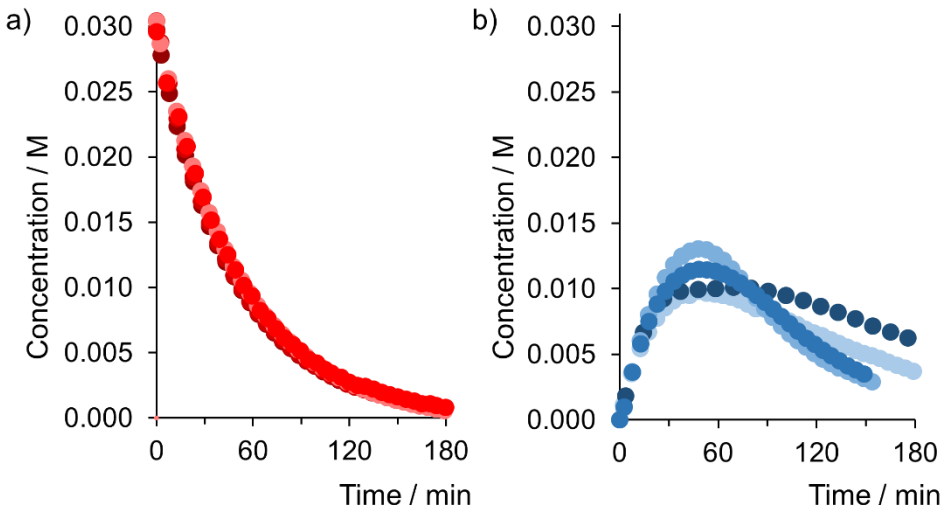


**Figure 1.8** – Temporal concentration profiles for four different ethanolyses of $\mathbf{1_{PB}}$ monitored by $^{11}B\{^{1}H\}$ NMR; **a)** Identical pseudo-first order decay of $\mathbf{1_{PB}}$ (red data); **b)** Irreproducible intermediate $\mathbf{2_{INT}}$ build-up (blue data). Conditions: $[\mathbf{1_{PB}}]_0$ = 0.03 M, $[EtOH]_0$ = 5 M in toluene at 30 °C.

This third stage of solvolysis only (nominally) requires an additional alcohol molecule, which is in high concentration under the solvolytic conditions. However, the direct reaction between EtOH and $HB(OEt)_2$ $\mathbf{2_{INT}}$ is clearly very slow causing the latter to accumulate. The process that converts $HB(OEt)_2$ $\mathbf{2_{INT}}$ into $B(OEt)_3$ **2**, which causes this irreproducibility in this particular system, is investigated further on.

Despite this, the pseudo-first order consumption of $\mathbf{1_{PB}}$ was found to be reproducible, supporting that the irreproducibility issues arise from the consumption of the intermediate (Figure 1.8 a).

## 1.5.2 Effect of Temperature

The rate of the reaction is dependent on temperature. Performing the model alcoholysis reaction at a variety of temperatures provides rate constants (Figure **1.9** a) that, after being manipulated according to the Eyring equation, provide activation parameters. Reactions were performed between 15 and 40 °C inclusive; the corresponding Eyring plot is shown in Figure 1.9 b. For the reaction between $\mathbf{1_{PB}}$ and EtOH, the activation parameters ($\Delta H^{\ddagger}$ = +19.7 kcal $mol^{-1}$, $\Delta S^{\ddagger}$ = −9.0 cal

$K^{-1}$ $mol^{-1}$), in particular the negative entropy of activation, suggests an associative transition state compatible with an $SN_2$-like mechanism.

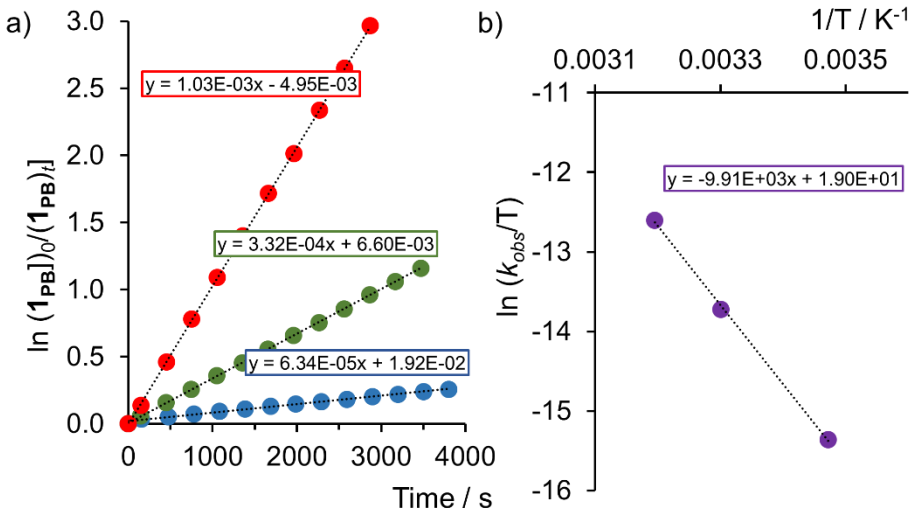


**Figure 1.9** – **a)** Pseudo-first order rate constants ($k_{obs}$) calculated from the decay of **1PB** at 15 °C (blue data), 30 °C (green data) and 40 °C (red data); **b)** Eyring plot for reaction of **1PB** with ethanol; straight lines are least squares minimisation to the data, all Pearson $R^2$ values greater than 0.994. Conditions: $[\mathbf{1_{PB}}]_0$ = 0.03 M, $[EtOH]_0$ = 5 M in toluene at 15, 30 and 40 °C.

## 1.5.3 Effect of Solvolytic Agent

To test the effect of the nature of the alcohol on the rate of deprotection and degree of intermediate accumulation, a series of kinetic reactions were performed using the same conditions detailed in 1.5.1.1 on page 19, varying the solvolytic agent used.

### 1.5.3.1 Primary Alcohols

Kinetics of borane deprotection were performed using saturated straight chain alcohols of the general formula $C_nH_{2n+1}OH$ (n = 1–4). From the data (Figure 1.10), a trend can be visualised between the length of the aliphatic chain on the primary alcohol and the stability gained by the intermediate. The maximum concentration of $HB(OR)_2$ throughout the reaction increased as the carbon chain grew longer: MeOH < EtOH < $^n$PrOH < $^n$BuOH, where the amount of $HB(O^nBu)_2$ is almost 10 times greater than $HB(OMe)_2$.

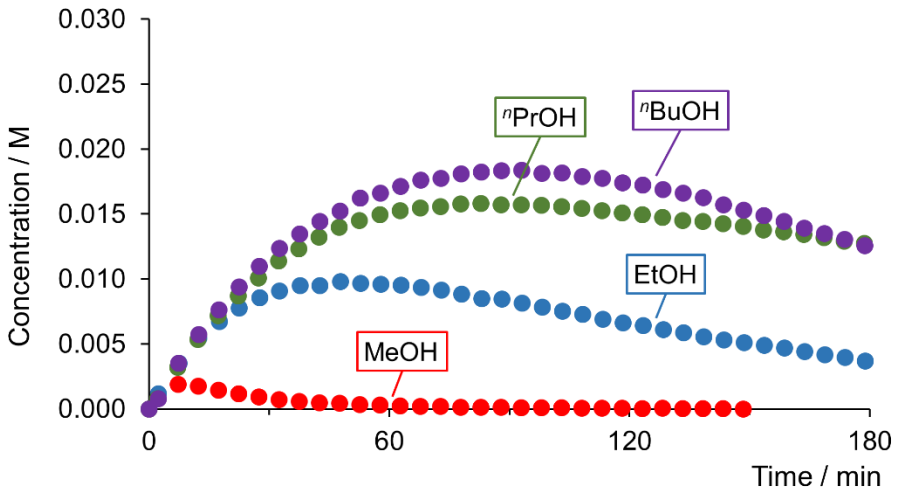


**Figure 1.10** – Temporal concentration profiles for alcoholyses of **1PB** monitored by $^{11}B\{^{1}H\}$ NMR showing different degree of the corresponding intermediate accumulation as the alcohol is varied. Conditions: $[\mathbf{1_{PB}}]_0$ = 0.03 M, $[ROH]_0$ = 5 M in toluene at 30 °C.

### 1.5.3.2 Secondary and Tertiary Alcohols

To probe the effect of increased steric bulk of the alcohol, the deprotection kinetics were measured when saturated secondary and tertiary alcohols were used under analogous conditions. Surprisingly, the maximum concentration of the intermediate previously achieved with $^{n}$BuOH can now be surpassed by using any of the tested branched alcohols as the solvolytic agent (Figure 1.11). This increment is considerable as it causes the intermediate to accumulate almost quantitatively at the expense of a decreased reaction rate, in accordance with an $SN_2$-like mechanism where there is a dependence of rate upon the substrate: the higher the steric hindrance of the nucleophile, the slower the rate of reaction.

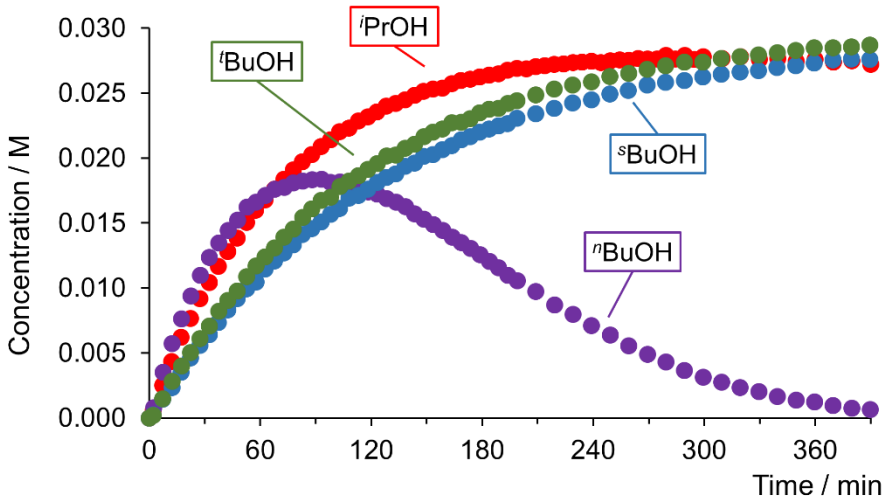


**Figure 1.11** – Temporal concentration profiles for alcoholyses of **1PB** monitored by $^{11}B\{^{1}H\}$ NMR showing a significant build-up of the corresponding intermediate when branched alcohols are used ($^{n}$BuOH kinetic profile displayed for comparison). Conditions: [**1PB**]$_0$ = 0.03 M, [ROH]$_0$ = 5 M in toluene at 30 °C.

This sterically protected intermediate favours its accumulation and hinders the last nucleophilic attack to such degree that the final borate gets almost entirely supressed. This is reflected in the time needed for the intermediate to reach its maximum concentration, from approximately 90 minutes to more than 6 hours, then again, achieving high and more useful concentrations.

## 1.5.4 Effect of Solvent

Choosing the appropriate media, where a chemical reaction takes place in, is critical. To probe whether the solvent has an effect on solubility, stability and reaction rates, a range of solvents were tested by carrying out a number of experiments using the same conditions detailed in 1.5.1.1 on page 19, varying only the solvent used.

### 1.5.4.1 Non-halogenated Solvents

First, non-halogenated solvents were studied, and kinetics recorded. In all cases, pseudo-first order decays in **1PB** were observed. Rate constants ($k_{obs}$) were determined in each solvent; values are displayed in Table 1.1.

| Entry | Solvent | $k_{obs}/s^{-1}$ | $k_{rel}$ |
|---|---|---|---|
| 1 | toluene | $3.56 \times 10^{-4}$ | 1.00 |
| 2 | benzene | $3.04 \times 10^{-4}$ | 0.85 |
| 3 | benzonitrile | $3.50 \times 10^{-4}$ | 0.98 |
| 4 | 1,4-dioxane | $3.74 \times 10^{-3}$ | 10.51 |
| 5 | tetrahydrofuran | $2.68 \times 10^{-3}$ | 7.53 |
| 6 | diethyl ether | $9.03 \times 10^{-4}$ | 2.54 |
| 7 | N,N-dimethylformamide | $1.33 \times 10^{-3}$ | 3.74 |

**Table 1.1** – Pseudo-first order constants ($k_{obs}$) of ethanolyses of $\mathbf{1_{PB}}$ at 30 °C in different non-halogenated solvents ($[\mathbf{1_{PB}}]_0$ = 0.03 M, [EtOH] = 5 M).

Aromatic solvents: benzene and benzonitrile were tested as analogues for toluene, as they are common aromatic non-halogenated solvents used in chemistry with different polarity. Consumption of $\mathbf{1_{PB}}$ was found to be reproducible within solvents showing the same pseudo-first order decay (Figure **1.12** a). The intermediate $\mathbf{2_{INT}}$ builds up at approximately the same rate whereas its consumption is shortened when benzene was used.

Contrary to this, total absence of intermediate was found with benzonitrile where borate $B(OEt)_3$ **2** concentration grows at the same rate as $\mathbf{1_{PB}}$ is being consumed (Figure 1.12 b). Overall, there is no evident mechanistic advantage or disadvantage (other than different solvent toxicity and price) by using benzene instead of toluene as solvent of choice.

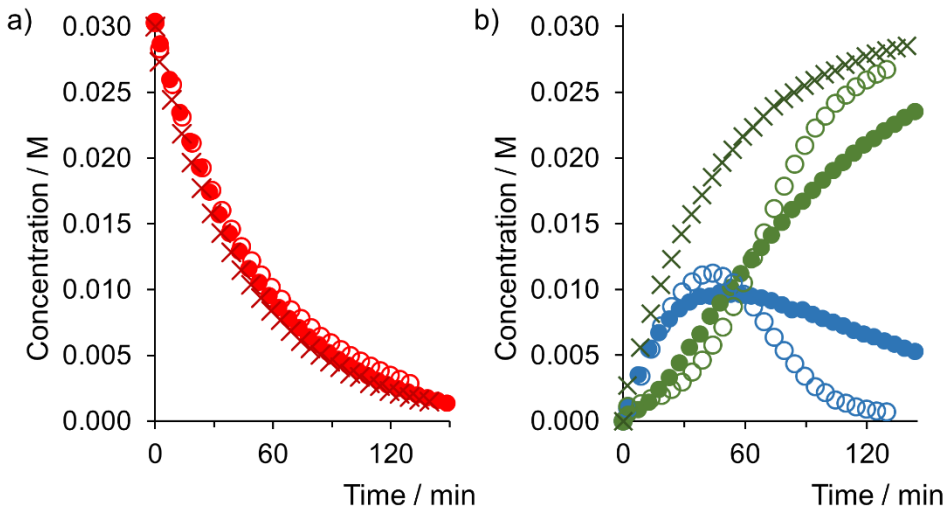


**Figure 1.12** – Temporal concentration profiles for different ethanolyses of $\mathbf{1_{PB}}$ monitored by $^{11}B\{^{1}H\}$ NMR. **a)** Equal pseudo-first order decay of $\mathbf{1_{PB}}$ (red data); **b)** $\mathbf{2_{INT}}$ (blue data) and **2** (green data) being produced at different rates (filled circles: toluene, outlined circles: benzene, crosses: benzonitrile).

Ethereal solvents, 1,4-dioxane (referred to just as dioxane from now on), tetrahydrofuran (THF) and diethyl ether ($Et_2O$), had a similar effect on the kinetic profile obtained for the alcoholysis of $\mathbf{1_{PB}}$. In every case, the deprotection rate constants were remarkably faster than the model reaction (toluene), causing almost a 10 fold increase in the case of both dioxane and THF whose kinetic profiles are essentially identical (Figure 1.13 a). In contrast to $Et_2O$, the use of either dioxane or THF increased the concentration reached by $\mathbf{2_{INT}}$ approximately to 90% of $[\mathbf{1_{PB}}]_0$ before it started to quickly decay to give rise to the final borate **2** (Figure 1.13 b). Together with polarity, the presence of an electronegative atom like oxygen might play an important role in the intermediate stabilisation as seen by the different kinetic profiles obtained. As it is shown, a less polar solvent like $Et_2O$ decreased the intermediate concentration compared to the more polar dioxane or THF even though they all contain oxygen.

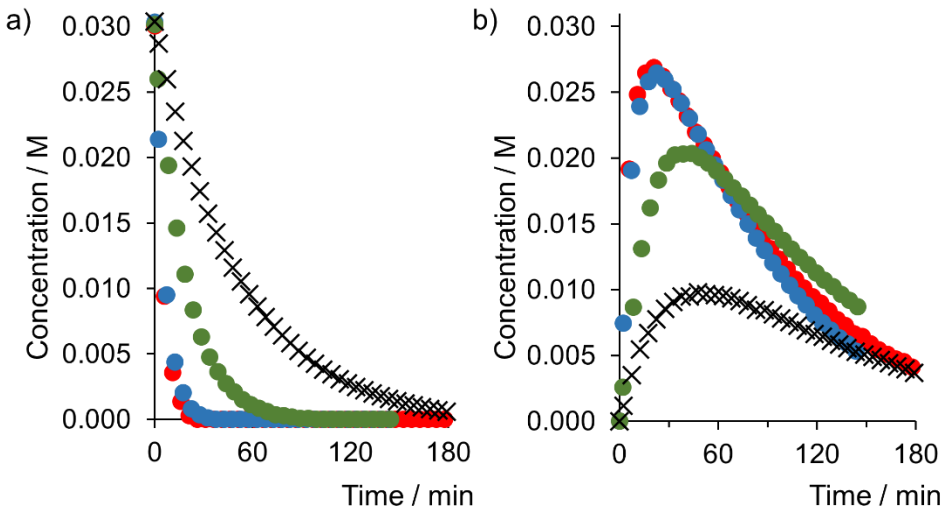


**Figure 1.13** – Temporal concentration profiles for different ethanolyses of $\mathbf{1_{PB}}$ monitored by $^{11}B\{^{1}H\}$ NMR. **a)** Pseudo-first order decay of $\mathbf{1_{PB}}$; **b)** Faster and higher intermediate concentration reached by using ethereal solvents (red circles: dioxane, blue circles: THF, green circles: $Et_2O$, black crosses: toluene [shown for comparison]).

Dipolar aprotic solvents: dimethyl sulfoxide (DMSO), acetonitrile (ACN) and N,N-dimethylformamide (DMF) were also considered and tested, only to be found that only the later could generate an evident homogeneous reaction while DMSO and ACN dissolved $\mathbf{1_{PB}}$ only partially, impeding an accurate comparison between experiments under these conditions. Deprotection in DMF occurred 4 times faster than in standard conditions (toluene). It was comparable to those obtained in ethereal solvents with the difference that intermediate accumulation was significantly supressed. Moreover, a fourth unknown species arose and remained constant throughout the course of the reaction (Figure 1.14).

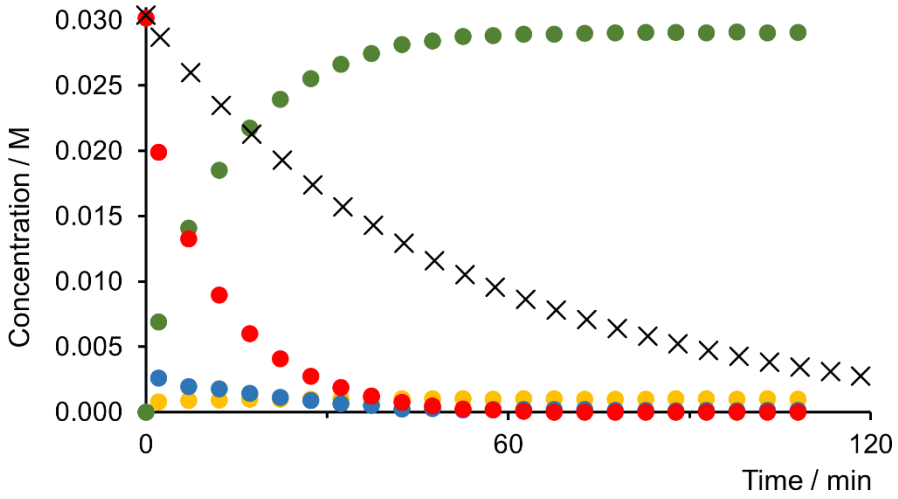


**Figure 1.14** – Temporal concentration profile for ethanolysis of **1PB** in DMF, monitored by $^{11}B\{^{1}H\}$ NMR (red circles: **1PB**, blue circles: **2INT**, green circles: **2**), yellow circles: unidentified species, black crosses: **1PB** in toluene [shown for comparison]).

Hexane proved to be unable to dissolve **1PB**, consequently making unable to carry out the reaction under the same standard conditions and to be followed by the same NMR technique.

### 1.5.4.2 Halogenated Solvents

Second, halogenated solvents were used to study the kinetic profile and effect in the alcoholysis reaction. Consistently, pseudo-first order decays in **1PB** were also observed. Rate constants ($k_{obs}$) were determined in each solvent; values are displayed in Table 1.2.

| Entry | Solvent | $k_{obs}/s^{-1}$ | $k_{rel}$ |
|---|---|---|---|
| 1 | chloroform | $1.11 \times 10^{-4}$ | 1.00 |
| 2 | dichloromethane | $1.29 \times 10^{-4}$ | 1.16 |
| 3 | chlorobenzene | $2.48 \times 10^{-4}$ | 2.23 |

**Table 1.2** – Pseudo-first order constants ($k_{obs}$) of ethanolyses of **1PB** at 30 °C in different halogenated solvents ($[\mathbf{1_{PB}}]_0$ = 0.03 M, [EtOH] = 5 M).

Following the systematic scope of solvents, chloroform ($CHCl_3$) was chosen to be tested next and the results obtained were remarkably different. At first glance, the kinetic profile appears to be rather similar to that obtained in toluene, but with a distinctive difference, in that the time taken to consume $\mathbf{1_{PB}}$ was significantly longer (approximately 13 hours). Thereupon, $\mathbf{2_{INT}}$ remained present throughout the course of the reaction reaching a moderately high concentration prolonging the final borate **2** formation for more than 24 hours (Figure 1.15).

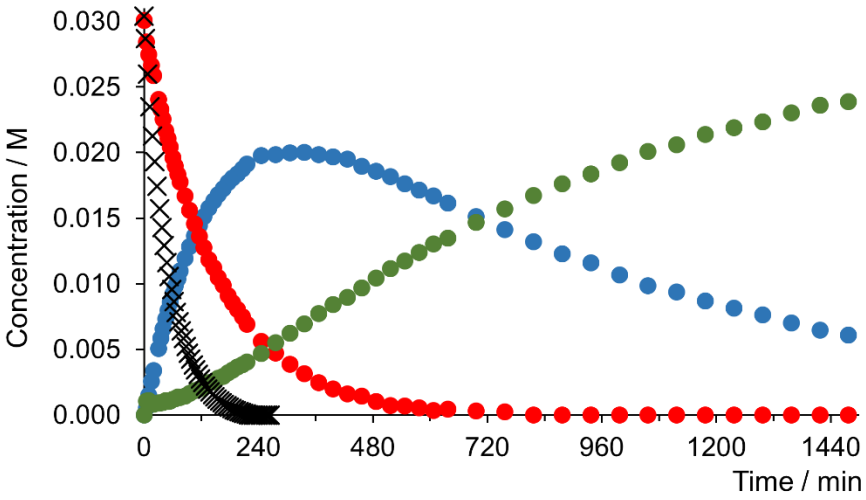


**Figure 1.15** – Temporal concentration profile for ethanolysis of $\mathbf{1_{PB}}$ in $CHCl_3$, monitored by $^{11}B\{^1H\}$ NMR (red circles: $\mathbf{1_{PB}}$, blue circles: $\mathbf{2_{INT}}$, green circles: **2**, black crosses: $\mathbf{1_{PB}}$ in toluene [shown for comparison]).

Moreover, the formation of the intermediate proved to be reproducible within runs regardless whether the solvent was deuterated or not. The observed reproducibility could not be achieved with any of the previously tested solvents (see Appendix for temporal concentration profile).

To test if this slow rate effect was exclusively of $CHCl_3$ or something intrinsically to its nature (e.g. polarity, non-aromaticity), dichloromethane ($CH_2Cl_2$), and chlorobenzene were also used in the alcoholysis of $\mathbf{1_{PB}}$ and their kinetic profiles recorded. The non-aromatic $CH_2Cl_2$ displayed a similar kinetic profile and rate constant to that of $CHCl_3$ while chlorobenzene was to some degree off this trend, showing a slightly faster initial rate, but $\mathbf{2_{INT}}$ stalled at the same concentration as

the rest of the chlorinated solvents (Figure 1.16). Generally, the delayed consumption of $\mathbf{2_{INT}}$ by these halogenated solvents was equally retarded, thus being accumulated in all cases.

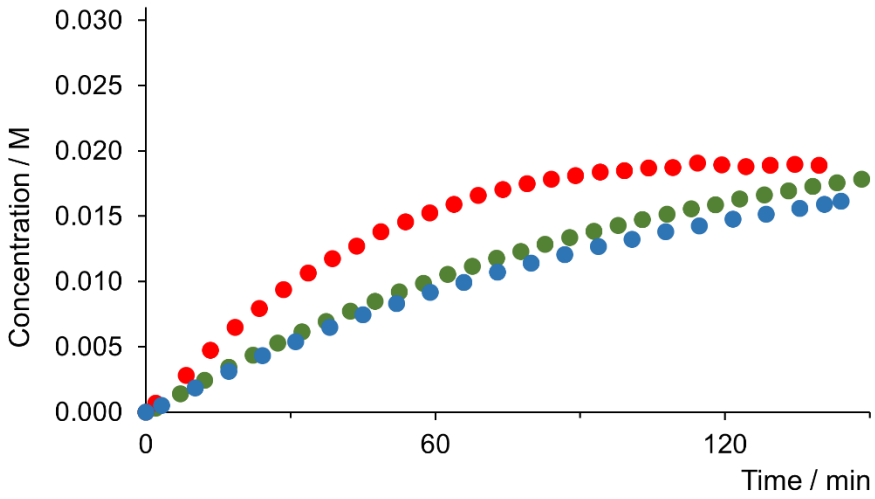


**Figure 1.16** – Temporal concentration profiles for different ethanolyses of $\mathbf{1_{PB}}$ monitored by $^{11}B\{^1H\}$ NMR; only $\mathbf{2_{INT}}$ is plotted. Retarded $\mathbf{2_{INT}}$ build-up regardless of which halogenated solvent was used (blue circles: $CHCl_3$, green circles: $CH_2Cl_2$, red circles: chlorobenzene).

## 1.5.5 Mixture of Solvents

A correlation between rates ($k_{obs}$) and solvents parameters such as dielectric constants showed no clear trend. This was not totally surprising because ethanol is in such a large quantity that is also acting not only as reagent in the alcoholysis but also as a co-solvent in the reaction

Overall, ethereal solvents sped up the reaction and promoted the intermediate concentration to rise up significantly, giving a short window for when the intermediate might be utilised (e.g. as a hydroborating agent) due to its accelerated depletion in this particular system. Contrastingly, the use of chlorinated solvents improved reproducibility of the reaction. At the same time, the stability of the intermediate was considerably enhanced at the expense of the reaction becoming sluggish. The prolonged time needed for the intermediate to reach a suitable concentration made the reaction unpractical and not synthetically useful.

With this in mind, and without trying to hinder the reaction by using more bulky alcohols (as showed in 1.5.3.2 on page 25), a mixture of solvents at different ratios were tested in the solvolysis reaction using the same conditions as stated in 1.5.1.1 on page 19.

### 1.5.5.1 Dioxane/Chloroform Mixtures

Chloroform and dioxane were chosen as initial solvents to test if the two advantages previously seen could be merged together bypassing the drawbacks (short lived intermediate and prolonged reaction time). This was done by running the standard alcoholysis reaction in solvent mixtures of dioxane and $CHCl_3$ in ratios going from 1:1 to 100,000:1 inclusive.

The intermediate formation rate was linearly improved as the ratio between dioxane/$CHCl_3$ increased from 1:1 to 10:1, further increments of such ratio showed no significant effect as they all had already matched the previously observed rate for when dioxane is used solely (Figure 1.17). Remarkably, not only the fast formation of $\mathbf{2_{INT}}$ was achieved from dioxane present in this mixture, but also the stabilisation previously seen from chlorinated solvents. Thus, providing an ideal synergetic interaction that rendered an optimal solvent mixture for obtaining the desired intermediate in high concentration in a fast and operationally simple manner.

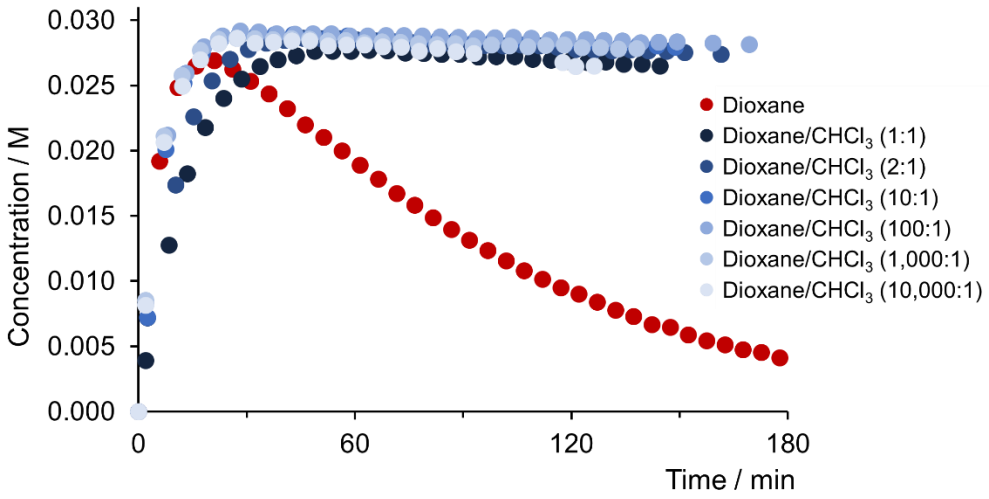


**Figure 1.17** – Temporal concentration profiles for different ethanolyses of $\mathbf{1_{PB}}$ in different solvent ratios monitored by $^{11}B\{^1H\}$ NMR; only $\mathbf{2_{INT}}$ is plotted. Synergetic interaction of solvents providing a fast intermediate $\mathbf{2_{INT}}$ build-up and high stabilisation (kinetic profile in dioxane shown for comparison).

Further dilutions on the range of 80,000:1 to 100,000:1 caused the stabilisation of the intermediate effect to be lost (as $CHCl_3$ is in such low concentrations), after this point, the kinetic profile obtained is similar to that in which only dioxane is used as solvent. Moreover, when repetition of experiments at this borderline dilution level (~80,000:1) were performed, $\mathbf{2_{INT}}$ reached maximum concentration momentarily (Figure 1.18, filled circles). This transient stabilisation lasted for several minutes varying each time the alcoholysis reaction was performed, then $\mathbf{2_{INT}}$ was consumed away to give rise to the final borate $B(OEt)_3$. Notably, this lack of reproducibility did not affect the consumption of $\mathbf{1_{PB}}$, meaning the rate at which EtOH is deprotecting the phosphine remains constant while the effect from $CHCl_3$ is exclusively affecting the intermediate $\mathbf{2_{INT}}$.

The observed irreproducibility can be explained as there is a small error in each experiment (arising from the measured $CHCl_3$ volume) that varies the solvents ratio slightly. It can be inferred that $CHCl_3$ is acting as an inhibitor of some sort of catalytic species which may be present in considerably low concentrations; from run to run, therefore, the time until when the $CHCl_3$ can inhibit the catalyst too will differ. The lack of reproducibility is independent of the chloroform used, either

deuterated or not, and varies from run to run (see Appendix for temporal concentration profiles).

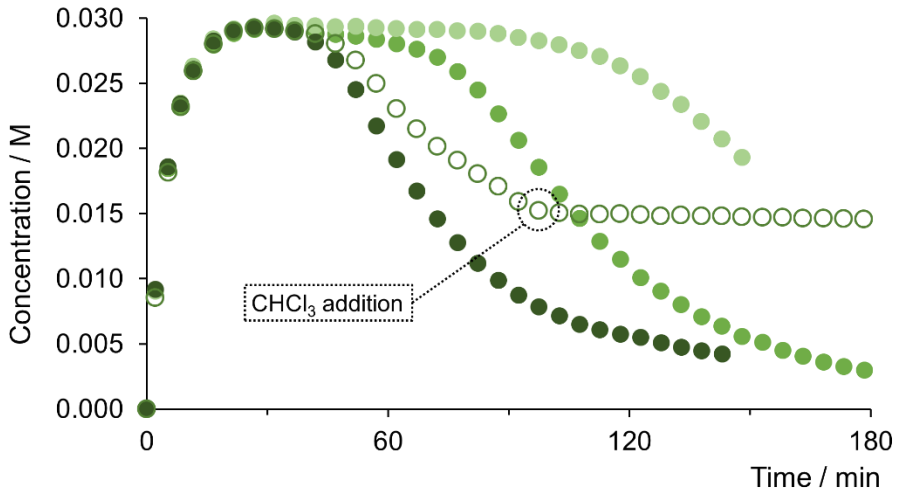


**Figure 1.18** – Temporal concentration profiles for different ethanolyses of $\mathbf{1_{PB}}$ in dioxane/$CHCl_3$ (80,000:1) monitored by $^{11}B\{^1H\}$ NMR; only $\mathbf{2_{INT}}$ is plotted. Different transient stabilisation of $\mathbf{2_{INT}}$ observed in each run (filled circles); $\mathbf{2_{INT}}$ consumption being interrupted after additional $CHCl_3$ (0.19 mmol) was added into the reaction mixture (outlined circles).

To further prove whether $CHCl_3$ was acting as an inhibitor or not, an experiment was set up where the reaction was left to run until the intermediate was being depleted but not totally consumed yet, at which point chloroform (0.19 mmol) was added; as expected, $\mathbf{2_{INT}}$ regained its stabilisation (Figure 1.18, outlined circles). These results clearly showed that there might be an interaction between an unknown catalytic species causing the reaction to proceed forward and $CHCl_3$ preventing this to happen. Additional experiments were performed to try to establish the nature of the catalytic species, see section 1.5.6 on page 37.

### 1.5.5.2 Other Halogen Sources Mixtures

To test if the effect seen on the stabilisation of the intermediate is an intrinsic property of $CHCl_3$ or if could be achieved by other means, different experiments were performed varying the halogen source. Dioxane was chosen to be used in conjunction with the tested halogenated solvents or compounds.

No appreciable difference was observed from the kinetic profiles when bromoform ($CHBr_3$) was used instead of $CHCl_3$ for the solvent mixture (Figure 1.19 a), meaning they are interchangeable and the stabilisation effect is not exclusive to chlorinated molecules.

Diluted hydrochloric acid (HCl), ammonium chloride ($NH_4Cl$) and tetrabutylammonium chloride (TBAC) were tested (as dioxane solutions) as sources of chloride ions in the reaction mixture. This in order to probe if the same effect could be achieved by ionic compounds. Addition of HCl (0.5 µM) into the reaction mixture was enough to reach the same high accumulation of $\mathbf{2_{INT}}$ with the only difference being that its consumption was slightly increased compared to that obtained with either $CHCl_3$ or $CHBr_3$. TBAC showed a similar effect but $\mathbf{2_{INT}}$ only reached approximately 70% of the concentration obtained in dioxane/$CHCl_3$ (100:1); water was being unintentionally added into the system due the hygroscopic nature of TBAC, since dialkoxyboranes are moisture sensitive, this favoured a rapid hydrolysis of borane to give the final borate **2** in the presence of EtOH. Consequently, a rapid competition between this process and the catalyst inhibition by the chloride source might be occurring at the initial state of the reaction giving rise to the observed profile. Finally, an almost identical kinetic profile was obtained, to that of dioxane, when $NH_4Cl$ was used, as the salt proved to be completely insoluble in the reaction conditions (Figure 1.19 b).

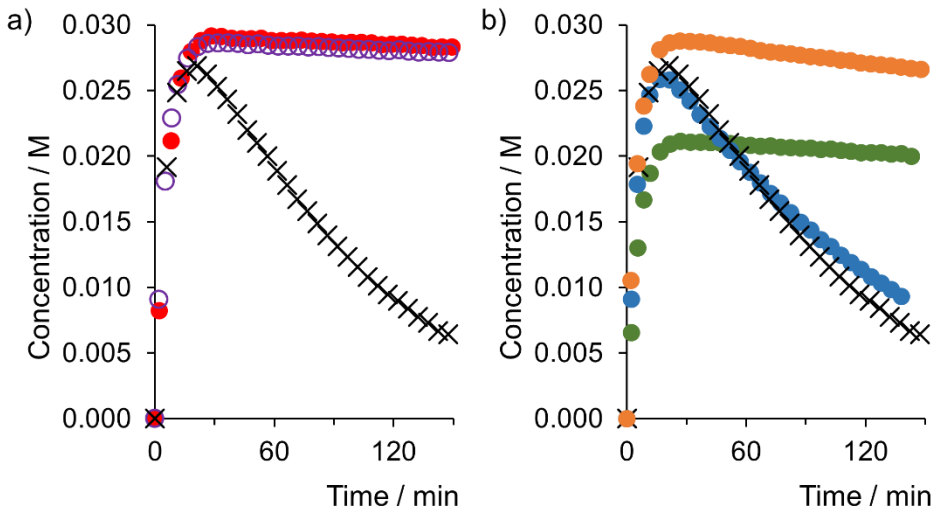


**Figure 1.19** – Temporal concentration profiles for different ethanolyses of $\mathbf{1_{PB}}$ monitored by $^{11}B\{^{1}H\}$ NMR showing differences in intermediate $\mathbf{2_{INT}}$ build-up (black crosses: dioxane, shown for comparison). **a)** Red circles: dioxane/$CHCl_3$ (100:1), outlined purple circles: dioxane/$CHBr_3$ (100:1); **b)** Orange circles: dioxane/HCl, blue circles: dioxane/$NH_4Cl$, green circles: TBAC.

## 1.5.6 Mechanistic Studies

Despite the different effect the solvent, alcohol or additives have on the intermediate, the pseudo-first order consumption of $\mathbf{1_{PB}}$ was found to be reproducible, also matching the initial intermediate production, suggesting that the reproducibly issues arise from the consumption of the intermediate.

An experiment using 2,2,2-trichloroethanol in place of EtOH gave an approximate 2 fold reduction in the rate constant. This suggests the alcohol is acting as a nucleophile, rather than a Brønsted acid, as trichloroethanol is less nucleophilic and more acidic ($pK_a$ = 12.2 vs 16.0 in aqueous solutions) than EtOH. This effect can be greatly enhanced by using perfluoro-tert-butanol where there was practically no reaction despite the large excess of alcohol used (Figure 1.20).

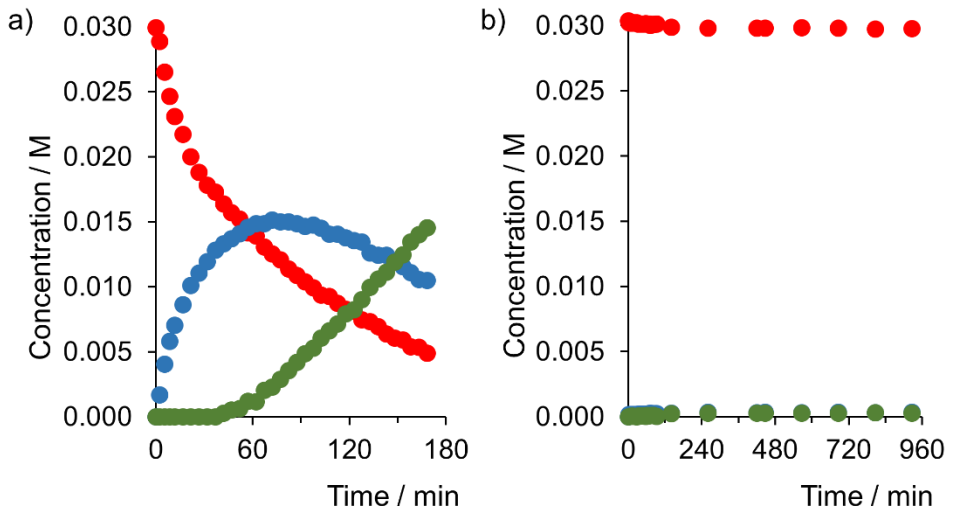


**Figure 1.20** – Temporal concentration profiles for different ethanolyses of $\mathbf{1_{PB}}$ monitored by $^{11}B\{^{1}H\}$ NMR (red circles: $\mathbf{1_{PB}}$, blue circles: $\mathbf{2_{INT}}$, green circles: **2**). **a)** Kinetic profile obtained from alcoholysis using trichloroethanol; **b)** No reaction recorded when perfluoro-tert-butanol was used as the solvolytic agent.

A series of specific experiments were performed to probe for particular mechanistic pathways that might have been taking place.

### 1.5.6.1 Bubble Surface Effects

To probe whether surface effects (promoting dihydrogen evolution) play an influential role in this process or not, studies were carried out under a system where air and nitrogen were bubbled through over the course of the reaction. A set up was created that allowed the gas to flow from the bottom of the NMR tube to the surface (with a pressure release outlet) at a constant controlled rate.

Inconclusive results were obtained from these experiments, as bubbling $N_2$ after the reaction had started (between 20 and 60 minutes inclusive) seemed to slow down the rate of consumption of intermediate, while bubbling either $N_2$ or $O_2$ since the beginning of the reaction greatly supressed its formation and sped up the rate of formation of the final borate (see Appendix for experimental results).

### 1.5.6.2 Radical Initiation

Benzoyl peroxide (BPO) can produce radical species under mild conditions and promote radical reactions. BPO was used as an additive in the standard alcoholysis reaction in concentrations from 5 mol% to 10 mol% inclusive.

No change from the standard conditions results were observed, as the pseudo-first order consumption of $\mathbf{1_{PB}}$ was found to be the same between experiments while the concentration and consumption of $\mathbf{2_{INT}}$ showed the same irreproducible results from previously discussed experiments. Given these results, it can be inferred that it is unlikely that a radical process is taking place in the alcoholysis reaction (see Appendix for temporal concentration profiles).

### 1.5.6.3 Boronium

Another mechanistic possibility could be an ionic catalysed reaction where a boronium cationic species, present in low concentrations, is driving the reaction forward. This potential catalyst could be inhibited by a halogenated species such as $CHCl_3$ or HCl in the appropriate conditions and concentration.

Boronium cation $[THF{\cdot}BH_2{\cdot}NH_3][BAr^F{}_4]$ was tested to see its effect on a standard reaction performed in dioxane. The main difference was the maximum intermediate concentration reached when the boronium cation was added. $\mathbf{2_{INT}}$ reached 76.7% of $[\mathbf{1_{PB}}]_0$ when 1 mol% of the boronium was used and only 62% of $[\mathbf{1_{PB}}]_0$ when 10 mol% was used instead, that is respectively 13.3 and 28% less than the standard reaction in dioxane (Figure 1.21).

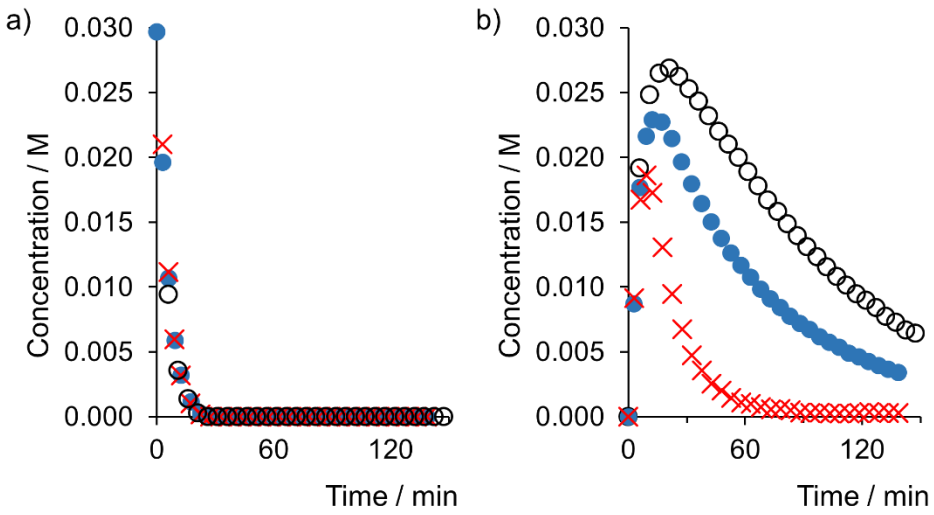


**Figure 1.21** – Temporal concentration profiles for different ethanolyses of **1**$_{PB}$ monitored by $^{11}B\{^{1}H\}$ NMR (red crosses: 1 mol% of boronium cation, blue circles: 10 mol% of boronium cation, outlined black circles: dioxane). **a)** Matching pseudo-first order decay of **1**$_{PB}$; **b)** Maximum concentration of **2**$_{INT}$ diminished with faster consumption rates as boronium percentage increased.

While these experiments did not confirm the reaction mechanism is going through a boronium catalysed pathway, it showed the addition of $[THF{\cdot}BH_2{\cdot}NH_3][BAr^F{}_4]$ sped up the reaction by shortening the lifetime of the intermediate.

### 1.5.6.4 Proposed Mechanism

From the evidence gathered so far, a plausible mechanism was proposed; a detailed stepwise mechanism of phosphine borane alcoholysis is shown in Scheme 1.10. The initial nucleophilic attack and subsequent displacement of the phosphine ligand is a slow process causing the gradual and reproducible consumption of the phosphine borane. The product of this first attack, $H_2BOEt$, results in the exposure of the vacant *p*-orbital on boron that can accept a pair of electrons from a Lewis base causing an almost immediate attack by a second molecule of EtOH; this process occurs in such a fast fashion that it cannot be monitored by standard *in situ* NMR spectroscopy technique. A third consecutive attack by EtOH gives rise to intermediate $HB(OEt)_2$, **2**$_{INT}$. The accumulation can be explained as the last hydride loss occurs *via* a strained four-membered ring that is unfavoured to some degree: $H_2$ elimination is faster the greater the protonic character of the OH hydrogen and

the greater the hydridic character of the BH hydrogen (Scheme 1.11, upper pathway); the increased steric bulk from more ethoxy groups also plays a role interfering with the spatial arrangement needed for the $H_2$ elimination. This rationale can also explain the previously observed trend when secondary and tertiary alcohols were used as nucleophiles (Section 1.5.3), agreeing with the usual interpretation that the acidity of the hydroxylic hydrogen in these alcohols decreases in this order: primary > secondary > tertiary.

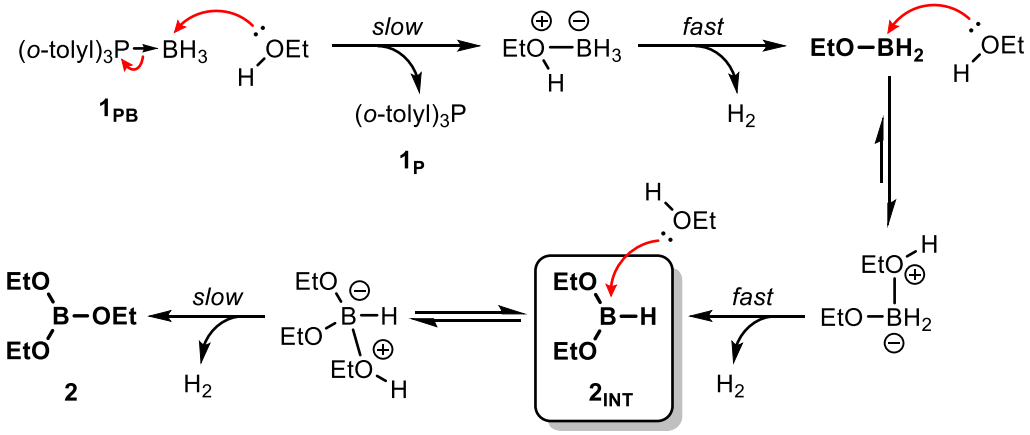


**Scheme 1.10** – Proposed mechanism for ethanolysis of (*o*-tolyl)$_3$P·BH$_3$ (**1$_{PB}$**) in ethanol (5 M in toluene) at 30 °C. Intermediate highlighted inside the shadowed box (**2$_{INT}$**).

Unfortunately, no definitive cause of the irreproducibility in the kinetic stability of the intermediate was established but it was most likely to be an inconsistent generation of an ionic active species. A boronium-like species could catalyse the last nucleophilic attack, after losing its coordinating ligand, the boronium would be capable of speeding up the process where **2$_{INT}$** gives rise to the final borate **2** driven by the ability of the boronium to facilitate the hydride transfer[81]. This process is further promoted by the stability conferred from a six-membered ring intermediate (Scheme 1.11, lower pathway).

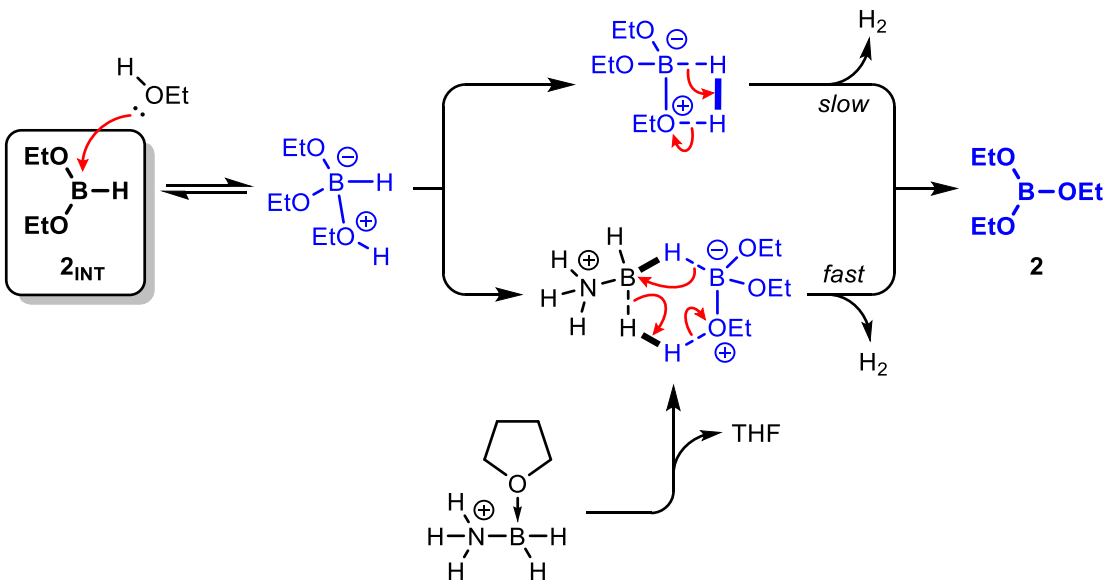


**Scheme 1.11** – Proposed mechanism showing two different pathways $\mathbf{2_{INT}}$ can take: a slow pathway involving a strained four-membered ring (upper pathway), and a faster pathway involving a favoured six-membered ring (lower pathway) when a boronium-like species is present.

## 1.5.7 Other Borane Sources

In order to explore and expand the synthetic capabilities of the alcoholysis reaction, different sources of borane were investigated. Tetrahydrofuran borane complex (THFB) and dimethyl sulfide borane complex (DMSB) were chosen as borane-Lewis base complexes, as these reagents are readily available as solution and easy to handle. Series of reactions involving the deprotection of $\mathbf{1_{PB}}$ in solvolytic conditions using EtOH were performed as stated in 1.5.1.1 on page 19 but varying the source of borane.

### 1.5.7.1 Tetrahydrofuran Borane Complex

First, THFB was chosen as a promising $BH_3$ source as it lacks the pungent odour DMSB has. Higher concentrations of $CHCl_3$ were needed to stabilise the intermediate as previously tested ratios of dioxane/$CHCl_3$ (100:1) failed to achieve the same observed build-up concentrations discussed in 1.5.5.1 on page 33.

The best dioxane/$CHCl_3$ ratio to stabilise the intermediate to a certain extent was found to be 1:1, nevertheless, the decay of $\mathbf{2_{INT}}$ was still appreciable. In stark contrast, using dioxane accelerated this decay by 14 fold while using just $CHCl_3$ as solvent, $\mathbf{2_{INT}}$ was consumed only twice as fast as in the mixture (Figure 1.22). In all cases, THFB complex was immediately consumed after the first spectrum had been taken, the first steps of the reaction being too fast to be monitored by standard NMR techniques; additionally, a limited amount of $\mathbf{2_{INT}}$ was produced (only 33% of $[\mathbf{1_{PB}}]_0$). This was caused by self-degradation, involving THF ring opening that caused accumulation of degradation products like $HB(^nBuO)_2$ and $B(^nBuO)_3$ that reduced the concentration of $THF{\cdot}BH_3$ available to react with EtOH.[82]

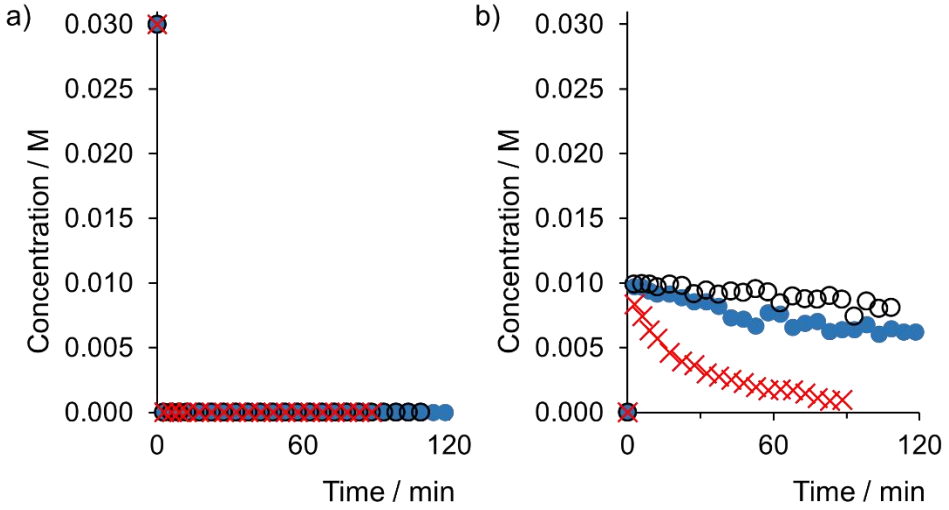


**Figure 1.22** – Temporal concentration profiles for different ethanolyses of THFB monitored by $^{11}B\{^1H\}$ NMR (red crosses: dioxane, blue circles: $CHCl_3$, outlined black circles: dioxane/$CHCl_3$ (100:1)). **a)** Immediate consumption of THFB; **b)** $\mathbf{2_{INT}}$ being formed instantly but reaching a maximum concentration of only 33% of $[\mathbf{1_{PB}}]_0$ due to reagent deterioration.

The use of THFB for synthetic purposes was discarded due its stability issues (must be stored at 0 °C), concentration does not exceed 2 M in $BH_3$ and that it can produce the desired intermediate in only low concentrations.

### 1.5.7.2 Dimethyl Sulfide Borane Complex

Neat DMSB complex solution possess indefinite stability at room temperature, it can be obtained in a pure 1:1 adduct form (~10 M in $BH_3$) and by following general

precautions associated with its handling, represents a viable alternative as $BH_3$ source which can be used in a variety of solvents.

When using DMSB as substrate for the ethanolysis reaction, fast consumption of the complex was also observed independently of the tested solvents and alcohols. Differences in the kinetic profiles were based on the intermediate stabilisation achieved by different solvents or by changing how bulky the nucleophilic alcohol was. Firstly, by using toluene as solvent (standard initial conditions), a quick build-up of $\mathbf{2_{INT}}$ was obtained reaching 80% of $[DMSB]_0$ before it quickly decayed in a pseudo-first order fashion as shown in Figure 1.23. Then, by changing the alcohol used for $^{n}$BuOH, the reaction could be stalled by hindering the last nucleophilic attack on the intermediate, causing its accumulation almost quantitatively (Figure **1.23**), effect previously observed in section 1.5.3.2 on page 25.

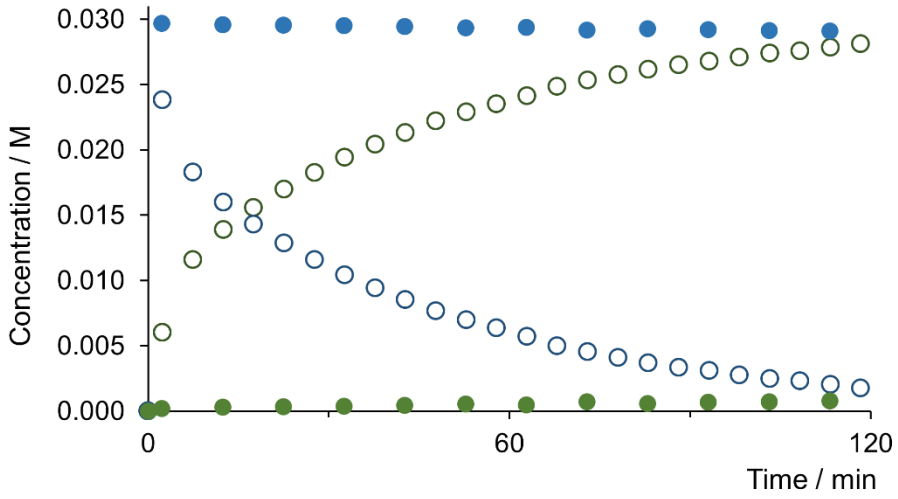


**Figure 1.23** – Temporal concentration profiles for different ethanolyses of DMSB monitored by $^{11}B\{^{1}H\}$ NMR (blue: $\mathbf{2_{INT}}$, green: **2**, outlined circles: EtOH, filled circles: $^{n}$BuOH).

Secondly, changing the solvent to dioxane allowed to reach a quantitative concentration of $\mathbf{2_{INT}}$, reinforcing how important the choice of solvent is for its stabilisation. Regardless of the concentration reached, a decay of $\mathbf{2_{INT}}$ is still observed if no halogenated solvent is used in the reaction mixture, being more significant during the first 30 minutes of the reaction. Additionally,

irreproducibility of the kinetic profile was also observed, as there are no halogenated molecules serving as inhibitors for the suspected catalyst that causes this variation to occur as seen on Figure 1.24.

As expected from the use of dioxane/$CHCl_3$ (100:1), stabilisation and quantitative formation of $\mathbf{2_{INT}}$ was observed (Figure 1.24), proving the solvent mixture at the defined ratio is competent to stabilise the intermediate $\mathbf{2_{INT}}$ regardless of the borane source.

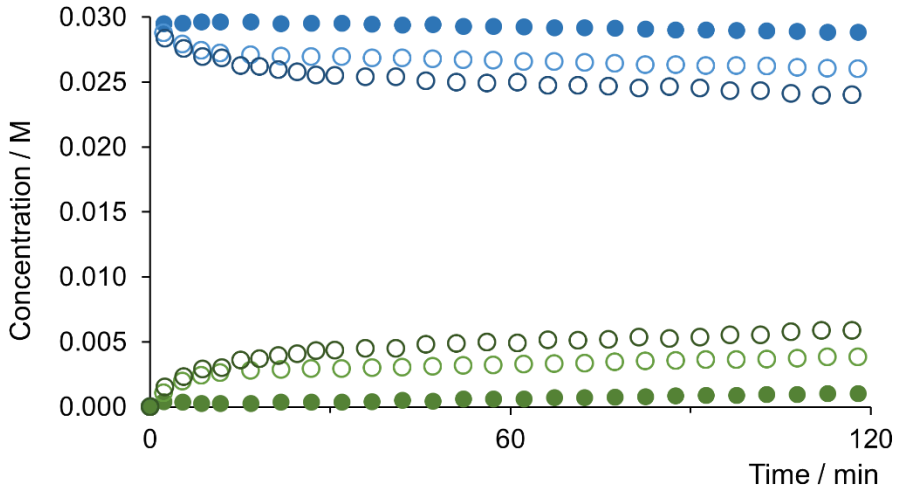


**Figure 1.24** – Temporal concentration profiles for different ethanolyses of DMSB monitored by $^{11}B\{^1H\}$ NMR (blue: $\mathbf{2_{INT}}$, green: **2**, outlined circles: dioxane, filled circles: dioxane/$CHCl_3$ (100:1)).

## 1.5.8 Effect of Ligand in Borane-Lewis Base Complex

From the aforementioned experiments, it can be inferred that the ligand used in the borane-Lewis base complexes is playing an important role that determines how fast the intermediate can be obtained from the alcoholysis reaction.

When the ethanolysis of DMSB was carried out in the presence of 1 equivalent (equiv.) of free phosphine (*o*-tolyl)$_3$P ($\mathbf{1_P}$) dissolved in the reaction mixture (EtOH 5 M in dioxane), $\mathbf{2_{INT}}$ was consumed 17 times faster than the reaction under the same conditions without added phosphine (see Appendix for temporal concentration profile). This could be explained if a background Lewis base

displacement reaction was also taking place; **1P** has stronger Lewis basicity than $Me_2S$ and provides a more thermodynamically stable adduct with $BH_3$ than the latter.[83] $Me_2S$ being displaced from its borane adduct ($Me_2S{\cdot}BH_3$) by **1P** while ethanolysis of $BH_3$ is taking place at the same time resulted in an overall accelerated deprotection, though slightly slower than the one starting from the (*o*-tolyl)$_3$P·$BH_3$ (**1PB**) adduct, which is almost twice as fast.

To further prove a displacement reaction was taking place in the background, two individual experiments were carried out; **1PB** and DMSB complexes were used as borane sources in solvolytic conditions (EtOH 5 M in dioxane), addition of 1 equiv. of their counterpart ligand ($Me_2S$ and **1P** correspondingly), slowed and sped up the consumption of **2INT** respectively, as showed by the labels in Figure 1.25. After addition of the opposite ligand, both reactions, that is the alcoholysis and the ligand displacement, reached equilibrium and from this point onwards the consumption rate of **2INT** was equal between the two reactions.

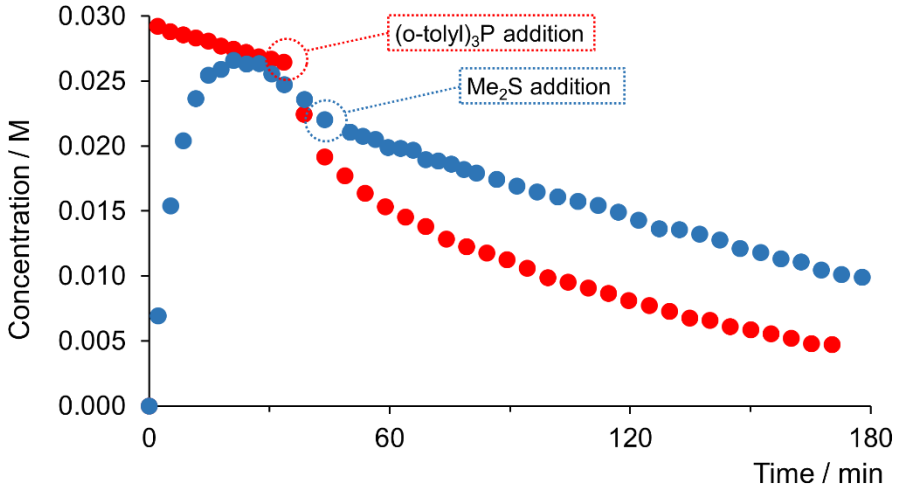


**Figure 1.25** – Temporal concentration profiles for two different ethanolyses of a source of $BH_3$ in dioxane monitored by $^{11}B\{^1H\}$ NMR showing **2INT** being consumed and the effect of adding free ligand to the ongoing reaction (blue: **1PB** used as substrate and $Me_2S$ added, red: DMSB used as substrate and **1P** added).

## 1.5.9 Pinacolborane: Alcoholysis Synthetic Application

From a synthetic point of view, the alcoholysis of borane could afford compounds with high relevance, pinacolborane (HBpin) being one of them. Using pinacol as the nucleophile in the alcoholysis reaction, a series of experiments were conducted to optimise its synthesis, considering the insights gained on stability (due to solvent interactions and bulkiness of the alcohol) and the impact of the Lewis base used to complexate $BH_3$.

With the aim of probing the synthesised HBpin and the effectiveness of its production, a one-pot dicyclohexylborane-catalysed alkyne hydroboration was contemplated as a representative reaction for its use.

### 1.5.9.1 HBpin Synthesis from Phosphine Borane $1_{PB}$

First, as the easiest and safest source of borane, $\mathbf{1_{PB}}$ was utilised as reagent to synthesise HBpin. *In situ* $^{11}B$ NMR spectroscopy was used to monitor and analyse the reactions.

A reaction with $\mathbf{1_{PB}}$ was set up using pinacol (pin) in excess (~9 equiv.), dioxane/$CHCl_3$ (100:1) was chosen as the standard solvent mixture as gave the best intermediate $(RO)_2BH$ stability results, being no different in this case. After a second intramolecular nucleophilic attack of the pinacol to the boron atom, HBpin was formed and sluggishly accumulated overtime, reaching approximately 50% conversion after 19 hours (Figure 1.26). Also seen from the NMR spectra, $B_2pin_3$ was formed as an unwanted side-product, this could be avoided by not using pinacol in large excess, but the reaction would be so slow it will not be practical.

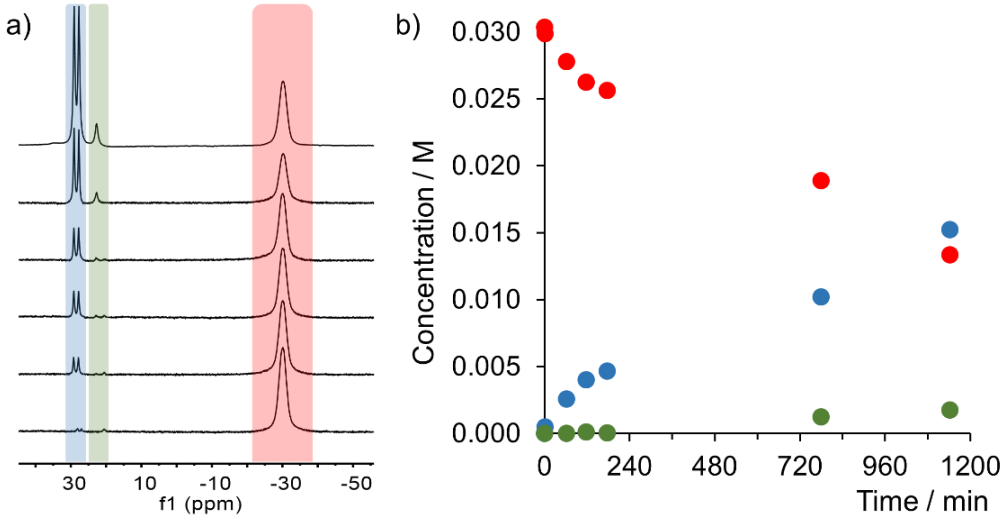


**Figure 1.26** – **a)** $^{11}$B NMR spectra recorded during the alcoholysis of **1$_{PB}$** showing a growing doublet corresponding to HBpin; **b)** Temporal concentration profile for alcoholysis of **1$_{PB}$** monitored by $^{11}$B NMR reaching only 50% conversion after 19 hours (red data: **1$_{PB}$**, blue data: HPpin, green data: $B_2pin_3$). Conditions: [**1$_{PB}$**]$_0$ = 0.03 M, [pin]$_0$ = 0.28 M in dioxane/$CHCl_3$ (100:1) at 23 °C.

### 1.5.9.2 HBpin Synthesis from DMSB

Provided that phosphine complex **1$_{PB}$** was not suitable due to reaction timescale constraints, DMSB was chosen as a source of borane. Due to its low molecular weight and good solubility, accurate, homogeneous and concentrated solutions can be obtained which facilitate an appropriate environment where the reaction can take place in an acceptable time. Dioxane/$CHCl_3$ mixtures were used as solvent of choice.

A stoichiometric reaction between DMSB and pinacol at 30 °C in dioxane furnished HBpin almost quantitatively. Initially, the substrate was swiftly consumed furnishing the product and reaching 50% conversion under the first two hours; after three hours of continuous monitoring, the reaction was left to continue at room temperature and monitored intermittently until reached completion. Despite being slowed down due to temperature change, the reaction progressed reaching 87% conversion after 19 hours (37% more than when **1$_{PB}$** was used) and continued reacting for 49 h more until DMSB was fully depleted. Contrastingly, when pinacol is used in excess (~9 equiv.) in the same solvent system and

temperature, aside from greatly enhancing the speed of the reaction, side-product $B_2pin_3$ is produced in considerable amount throughout the course of the reaction, consequently, the procedure becomes synthetically impractical (see Appendix for temporal concentration profiles).

Ethanolysis of DMSB followed by transesterification with pinacol was envisaged as a quicker alternative to produce HBpin. DMSB was left to react with 2 equiv. of EtOH, when the synthesised $\mathbf{2_{INT}}$ reached maximum concentration, pinacol was then added and the expected HBpin was obtained due to being entropically favoured (Figure 1.27). Along with HBpin, a slight increase of $B_2pin_3$ (side-product) was also observed. This could have been minimised by timing the addition of pinacol more carefully as it was added when some of DMSB had yet not reacted.

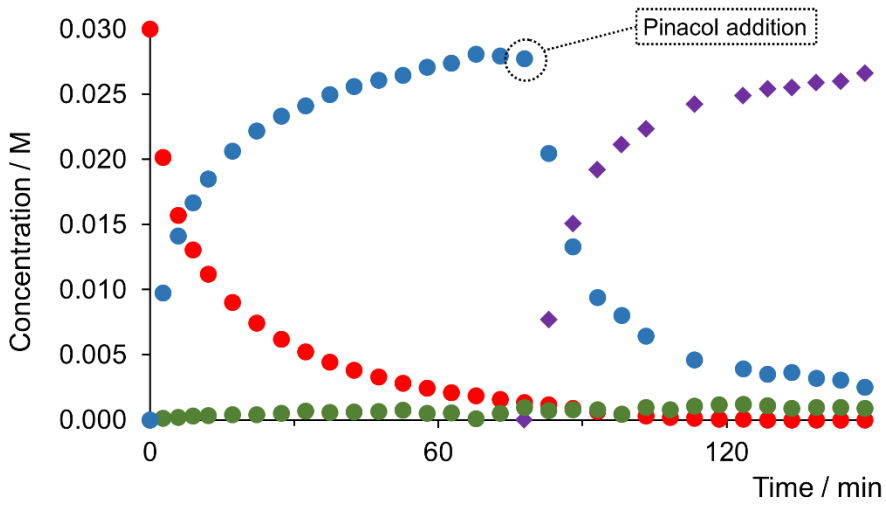


**Figure 1.27** – Temporal concentration profile for ethanolysis of DMSB at 30 °C monitored by $^{11}B\{^1H\}$ NMR and addition of pinacol giving rise to HBpin via transesterification with intermediate $\mathbf{2_{INT}}$ (red circles: DMSB, blue circles: $\mathbf{2_{INT}}$, purple diamonds: HBpin, green circles: **2** and $B_2pin_3$ overlapped).

Despite being a faster way to synthesise HBpin, the abovementioned procedure was discarded to be employed in the borane-catalysed alkyne hydroboration, as it not only requires additional steps for its synthesis and continuous monitoring, but also leftover quantities of EtOH are detrimental for the hydroboration as it would degrade the catalyst (dicyclohexylborane) turning it inactive.

### 1.5.10 One-pot Synthesis of Alkenylboronic Acid Pinacol Esters

In order to develop a one-pot transition-metal free catalysed hydroboration, a reaction needed to include the synthesis of the hydroborating agent (pinacolborane: HBpin) from the previously discussed pinacolysis of DMSB. Additionally, is also necessary for the required catalyst (dicyclohexylborane: $HBCy_2$) to be synthesised in the same vessel, ideally, without further purification.

The synthesis of both HBpin and $HBCy_2$ was monitored by *in situ* $^{11}B\{^1H\}$ NMR spectroscopy. The total amount needed of DMSB to furnish both reagent and catalyst was considered. After adding pinacol to a diluted DMSB solution, HBpin formation was observed and continuously monitored for over 14 hours, after this point HBpin concentration remained constant (meaning all pinacol had been consumed); then cyclohexene (Cy) was added which reacted with the excess DMSB to produce sufficient $HBCy_2$ to catalyse the subsequent hydroboration reaction (Figure 1.28).

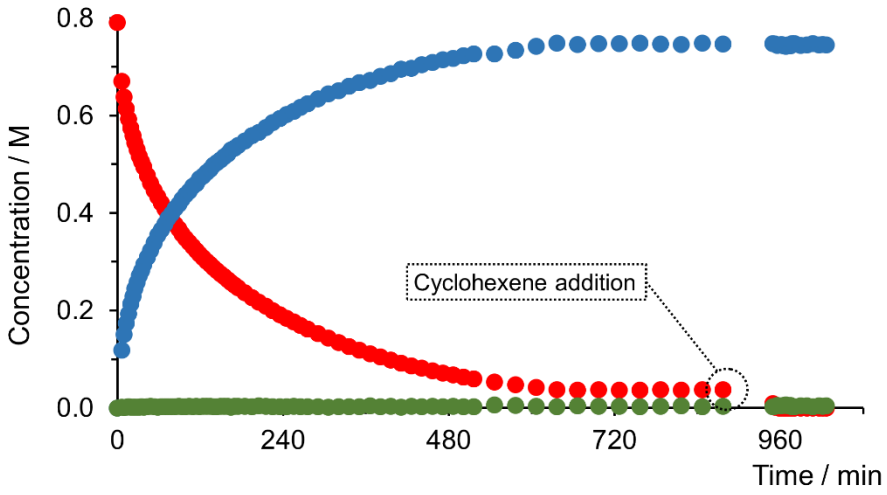


**Figure 1.28** – Temporal concentration profile for pinacolysis of DMSB at 30 °C monitored by $^{11}B\{^1H\}$ NMR showing the formation of HBpin and subsequently addition of cyclohexene to produce $HBCy_2$ (red: DMSB, blue: HBpin, green: $B_2pin_3$); note the prolonged reaction time was due to NMR scale dilution.

Next, a series of reactions were performed where reaction times and reagent quantities were optimised. Results are summarised in the table below. Initially, the reaction involved 1.055 equiv. of DMSB in respect to pinacol (1 equiv.) for 3 hours, due to the stoichiometry of the reaction, 0.055 equiv. of DMSB were left unreacted (Scheme 1.12 a). Residual DMSB was quenched with cyclohexene (1:2 ratio) for a defined time that furnished $HBCy_2$ and free $SMe_2$ (Scheme 1.12 b). Lastly, 4-fluorophenylacetylene **3** (F-PhAcetylene) was added as substrate and left to react with HBpin in the presence of $HBCy_2$ (catalyst) for 24 hours, ultimately producing the alkenylboronic acid pinacol ester ***E*-4$_{pin}$** in a one-pot procedure (Scheme **1.12** c).

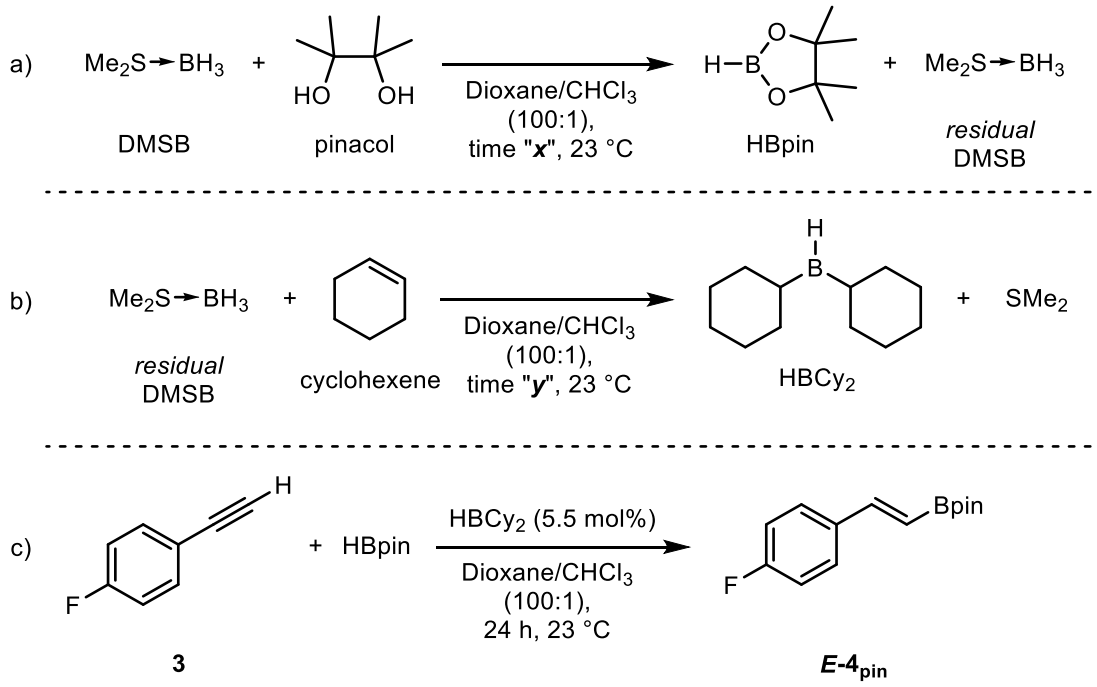


**Scheme 1.12** – One-pot synthesis of alkenylboronic acid pinacol ester ***E*-4$_{pin}$** dioxane/$CHCl_3$ (100:1) at 23 °C presented as a series of individual reactions for clarity purpose. **a)** Synthesis of hydroborating agent HBpin; **b)** Synthesis of catalyst $HBCy_2$; **c)** Boron-catalysed hydroboration of alkyne ***3***.

| Entry | DMSB (equiv.) | Cyclohexene (equiv.) | Pinacol (equiv.) | Alkyne **3** | Time "*x*" | Time "*y*" | NMR Yield (%) |
|---|---|---|---|---|---|---|---|
| 1 | 1.055 | 0.12 | 1 | 1 | 3 | 0 | 20 |
| 2 | 1.055 | 0.24 | 1 | 1 | 3 | 2.5 | 43 |
| 3 | 1.055 | 0.32 | 1 | 1 | 17 | 0.5 | 64 |
| 4 | 1.555 | 0.26 | 1.5 | 1 | 7 | 0.25 | 71 |
| 5 | 1.555 | 1.555 | 1.5 | 1 | 18 | 1 | 77 |

**Table 1.3** – Optimisation of the reaction conditions for the one-pot synthesis of alkenylboronic acid pinacol ester ***E*-4$_{pin}$**.

Time left between addition of cyclohexene and alkyne **3** proved to be crucial as immediate addition of alkyne after cyclohexene addition left not enough time for the DMSB to be quenched and synthesised enough catalyst and, therefore the yield supressed (Table 1.3 entry 1). Additionally, a prolonged HBpin synthesis reaction (Table 1.3 entry 3) and excess of this same reagent (Table 1.3 entry 5), proved to be advantageous for increasing the product yield. The addition of freshly synthesised $HBCy_2$ in a separate vessel can also be used (instead of its *in situ* synthesis) if DMSB is used in stoichiometric quantity without affecting the yield of the reaction.

## 1.5.11 Dialkoxyborane: New Hydroborating Agent

A hydroboration of an alkyne with the metastable intermediate $HB(OR)_2$ (**2$_{INT}$**), then ligand exchange with N-methyliminodiacetic acid (MIDA), was envisioned as a plausible route to generate MIDA boronate esters, R'B(MIDA), under very mild conditions (Scheme 1.13), substrates that have proved their synthetic value in recent years.

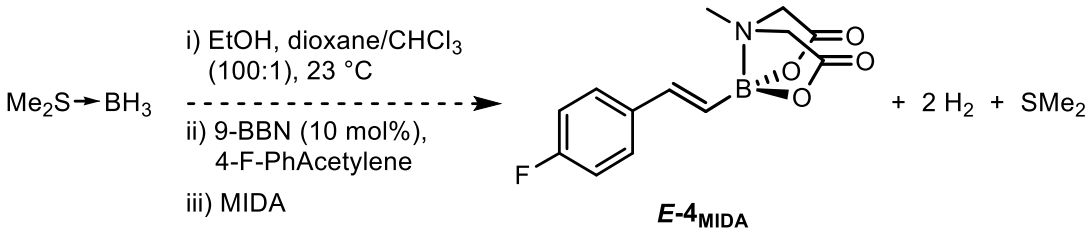


**Scheme 1.13** – Proposed multistep synthetic route for the synthesis of MIDA boronate ester ***E*-4$_{MIDA}$**, involving the generation of **2$_{INT}$** *in situ* (step i), addition of catalyst and substrate **3** (step ii) and lastly, ligand exchange (step iii).

9-Borabicyclo[3.3.1]nonane (9-BBN) was chosen as alternative catalyst due to $HBCy_2$ proved to be not effective towards catalysing the alkyne hydroboration when **2$_{INT}$** was used as hydroborating agent. Preliminary reactions with **2$_{INT}$** as hydroborating agent were performed, NMR yields of 22 and 15% of ***E*-4$_{(OEt)2}$** were obtained after 24 hours when 10 and 20 mol% of 9-BBN were used respectively (Scheme 1.14). A few unidentified species were observed by $^{19}F$ NMR analysis in small quantities. On the contrary, the unreacted starting material always represented the major compound in the crude reaction mixture, up to 67% of the total yield. Addition of MIDA ligand to the reaction catalysed by 10 mol% of 9-BBN decreased the NMR yield from 22 to 15% with no appreciable appearance of the desired R'B(MIDA) product ***E*-4$_{MIDA}$**.

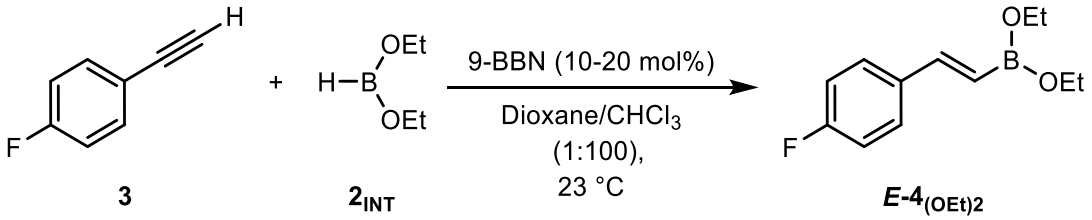


**Scheme 1.14** – Reaction conditions for synthesis of ***E*-4$_{(OEt)2}$** by 9-BBN catalysed hydroboration of **3**.

Due to unsuccessful MIDA ligand exchange from above-mentioned results, an analogous substrate of **3** was synthesised from its corresponding boronic acid. Compound **5$_{(OEt)2}$** was used to test whether a simple transesterification would take place by subjecting the substrate to a solution containing free MIDA in slight

excess (1.1 equiv.) (Scheme 1.15), ruling out low failure of obtaining product $\mathbf{5_{MIDA}}$ due to low concentration of substrate present in the mixture or inhibitory effects from being in a more complex reaction environment.

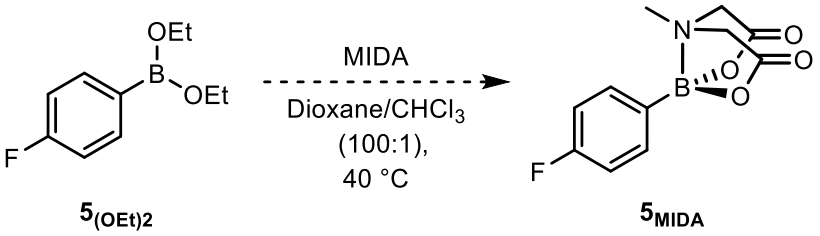


$\mathbf{5_{(OEt)2}}$ $\mathbf{5_{MIDA}}$

**Scheme 1.15** – Reaction conditions for MIDA ligand exchange from diethoxy phenyl boronate $\mathbf{5_{(OEt)2}}$.

Ligand exchange proved to be unsuccessful from substrate $\mathbf{5_{(OEt)2}}$ as no observable change on species was detected over time. Different individual reactions were set up in toluene to try to improve solubility, no product was observed at 23 or 50 °C; the addition of DMF to one of these reactions completely solubilised the ligand but protodeboronated the substrate making it unsuitable for the desired reaction.

Another approach to obtain alkenyl MIDA boronate $\boldsymbol{E}\mathbf{\text{-}4_{MIDA}}$ ester was from its corresponding alkenyl boronic acid $\boldsymbol{E}\mathbf{\text{-}4_{(OH)2}}$ *via* condensation with 1.2 equiv. of MIDA (Scheme 1.16). A reaction was set up and monitored by *in situ* $^{19}$F NMR spectroscopy reaching 92% conversion in ~23 hours as shown in Figure 1.29.

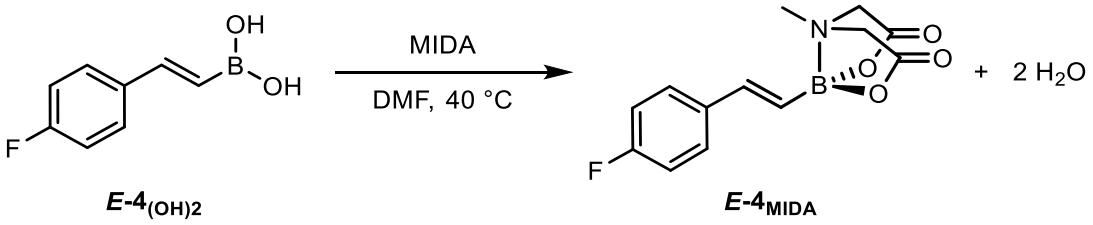


$\boldsymbol{E}\mathbf{\text{-}4_{(OH)2}}$ $\boldsymbol{E}\mathbf{\text{-}4_{MIDA}}$

**Scheme 1.16** – Simple reaction conditions for obtaining alkenyl MIDA boronate ester $\boldsymbol{E}\mathbf{\text{-}4_{MIDA}}$ from its corresponding alkenyl boronic acid $\boldsymbol{E}\mathbf{\text{-}4_{(OH)2}}$.

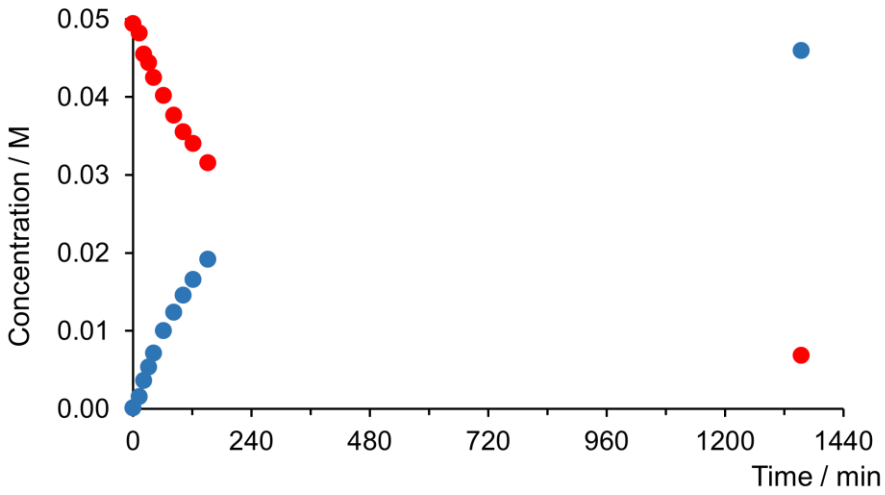


**Figure 1.29** – Temporal concentration profile for condensation reaction between alkenyl boronic acid ***E*-4$_{(OH)2}$** and MIDA monitored by $^{19}$F NMR (red: ***E*-4$_{(OH)2}$**, blue: ***E*-4$_{MIDA}$**). Conditions: [***E*-4$_{(OH)2}$**]$_0$ = 0.05 M, [MIDA]$_0$ = 0.06 M in DMF at 40 °C.

Despite being able to obtain the desired product (not isolated), this alternate procedure provided no real advantage from the commonly used route to synthesise ***E*-4$_{MIDA}$**. First, alkenyl pinacol boronic ester needs to be obtained by hydroboration of 4-fluorophenylacetylene **3** with HBpin, followed by deprotection with sodium periodate ($NaIO_4$) and HCl, a step that is preferably avoided as this reaction yielded low amounts of the corresponding boronic acid and harsher conditions are often required to increase the yield.

# Chapter 2 Borane-catalysed Alkyne Hydroboration

## 2.1 Organoboron Derivatives

### 2.1.1 Introduction

Organoboron derivatives have become truly essential within the past few decades. Their use has spread out not only in organic chemistry but also in medicinal chemistry to a point where it has greatly affected the way organic chemists envisage the construction of C−C bonds, this due to the unique reactivity of the C−B bond present in these types of molecules.

Brown and co-workers discovered the addition of diborane ($B_2H_6$) to alkenes in ethereal solvents to form trialkylboranes[1] and the synthesis of an alkylborane from an alkene using $NaBH_4/AlCl_3$, $NaBH_4/BF_3$ or diborane itself.[84] Since then, an ongoing interest in this reaction led to development of functional group transformations and C−C bond forming reactions that utilised mono-, di-, trialkyl and alkenylboranes. This contribution of organoboron chemistry to organic chemistry was recognised with two Nobel Prizes awarded in 1979 to Herbert C. Brown and in 2010 to Akira Suzuki; both well known for their influence in the development of new synthetic tools for the introduction of boron atoms into organic molecules that make several unique functional group transformations possible.

### 2.1.2 Background

Diborane is the simplest borane reagent and is a strong Lewis acid; it forms a stable complex with $BH_3$ with any Lewis base (being dimethyl sulfide and tetrahydrofuran the most common ones). On the contrary, of all the hydroboration reagents in both catalysed and uncatalysed hydroboration reactions, catecholborane and pinacolborane are amongst the most commonly dialkoxyboranes employed, both achieving widespread use in organoboron chemistry. Some other commonly used hydroborating agents are shown in Figure 2.1.

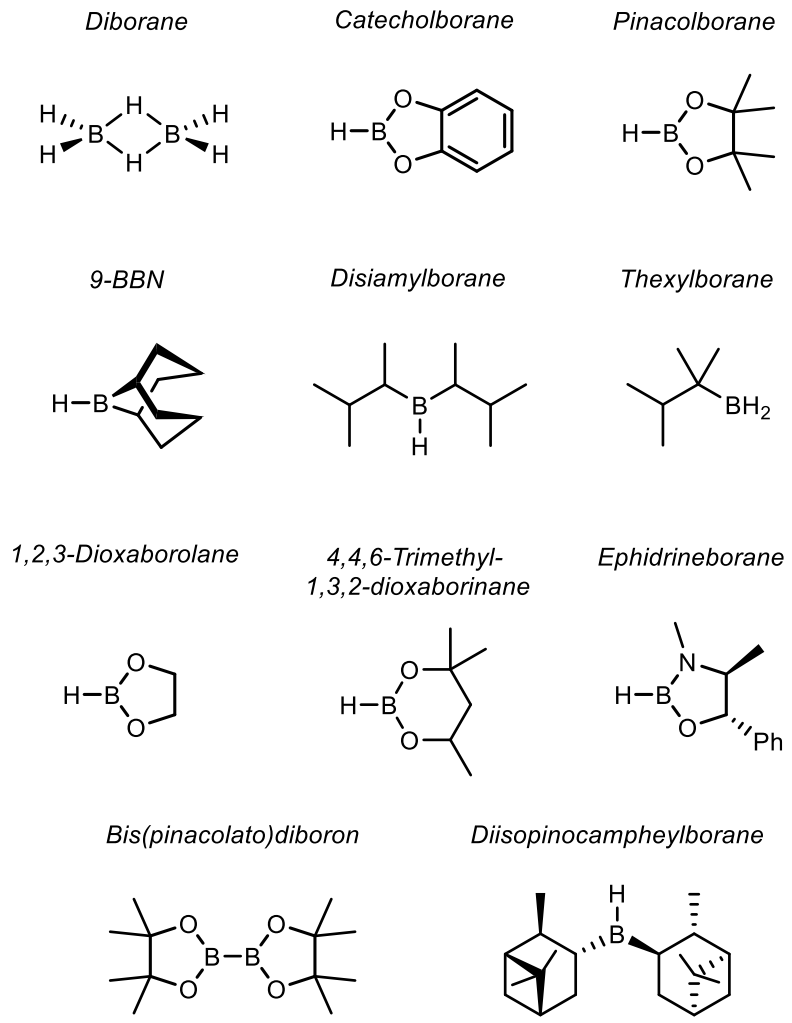


**Figure 2.1** – Most commonly used hydroborating reagents.

Generally speaking, there are some predictable characteristics when borane reacts with alkenes and alkynes.[85] Addition of H and B to the π-bond of an alkene or alkyne occurs rapidly and quantitatively in most cases, that furnish an alkylborane or an alkenylborane, respectively. The reaction proceeds by *cis*-addition of H and B *via* a four-centre transition state. The boron adds regioselectively to give the major product with boron at the less sterically hindered position (anti-Markovnikov addition), in the case of bicyclic and polycyclic alkenes, the boron adds stereoselectively to the less sterically hindered face. Hydroboration proceeds without skeletal rearrangement at normal temperatures.

Experiments have shown that there is no intermediate of the hydroboration, so in order to explain the regioselectivity observed in this reaction, transition states must be examined. As shown in Scheme 2.1, π-electrons of the alkyne can attack the borane (being electrophilic) thus leaving either the substituted or the terminal carbon of the alkyne electron deficient. The transition state in path a is favoured due to the stabilising effect of the alkyl substituent, having lower energy. Contrastingly, path b has an important steric interaction between the $BH_2$ moiety of the borane and the single alkyl group leading to a higher transition state. Ultimately, path a is favoured over path b providing the *cis*-addition product with >90% selectivity.[86]

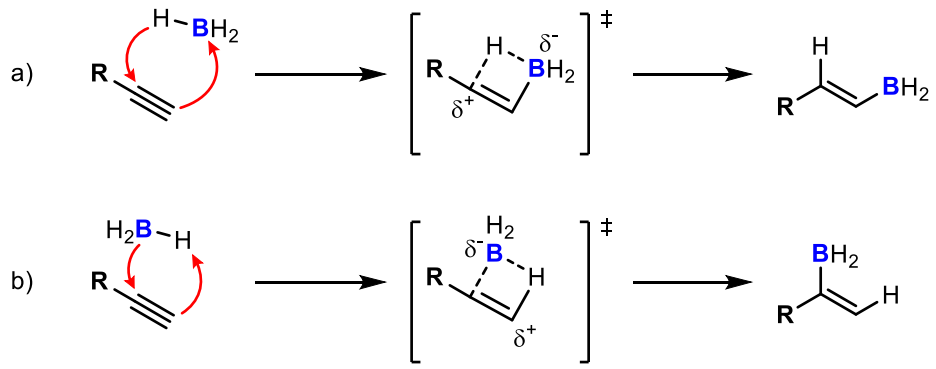


**Scheme 2.1** – Regioselectivity of the uncatalysed hydroboration.

Contrariwise, an ever increasing number of mechanisms of newly developed catalysed hydroboration reactions have been reported.

## 2.2 Hydroboration of Alkynes

### 2.2.1 Metal-free Hydroborations

The uncatalysed *cis*-hydroboration of terminal alkynes is a straightforward, well-understood reaction that has been thoroughly reviewed.[87,88] The aforementioned characteristics, when borane reacts with alkynes, are however altered when unhindered borane reagents are used. This commonly leads to a

mixture of mono- and diborylated products as well as regioisomers as unhindered boranes generally add to alkynes twice. Another factor that can also affect the regioselectivity is the nature of the solvent as well as the substituents on the C–C triple bond.[89]

Woods and co-workers reported the first hydroboration of alkynes in 1966.[90] 4,4,6-trimethyl-1,3,2-dioxaborinane was used for the *trans*-hydroboration of alkynes where heating to 210 °C and 3 days were needed to obtain decent yields (Scheme 2.2).

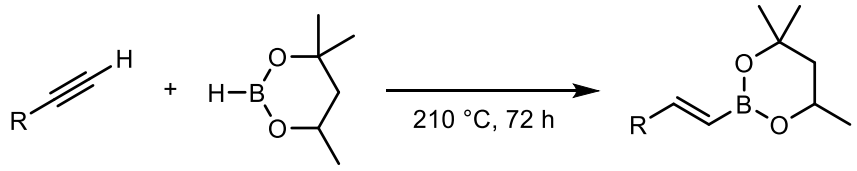


**Scheme 2.2** – *trans*-Hydroboration of terminal alkyne with 4,4,6-trimethyl-1,3,2-dioxaborinane.

Brown and Gupta introduced catecholborane (HBcat) in 1972. Prepared from a simple reaction between catechol and THF·$BH_3$ (THFB), it was shown that HBcat efficiently promotes the mono-hydroboration of alkynes at 70 °C (Scheme 2.3).[91,92] Alkenylcatecholboronates were obtained in near quantitative yields with high regioselectivities, internal alkynes usually taking longer than terminal alkynes to reach full conversion.

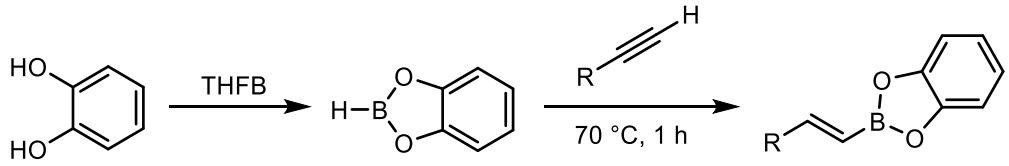


**Scheme 2.3** – Alkyne hydroboration with catecholborane.

Regardless its extensive use in hydroboration reactions, HBcat is nonetheless air and moisture sensitive and difficult to purify.[93] Additionally, HBcat is also prone to decomposition leading to uncontrolled hydroboration products,[94,95] and when a

transition metal is used to catalyse the reaction, the reaction media is even more complicated.[96] Brown and co-workers also studied the mono-hydroboration of terminal and internal alkynes with different dialkylboranes ($HBR_2$).[97] The steric requirements of the dialkylborane and temperature were particularly important, playing an essential role for an effective mono-hydroboration.

These disadvantages were however overcome by the work of Knochel and co-workers when they reported the use of pinacolborane (HBpin) as an alkyne hydroborating agent in 1992.[36] While HBcat needs high temperatures to react, HBpin is able to hydroborate both internal and terminal alkynes under milder conditions affording good yields (Scheme 2.4). Is worth mentioning that HBpin does not react with alkynes at room temperature, contrary to what Knochel published, at the time, catalytic impurities (e.g. $BH_3$) were present in the prepared samples that were responsible for the reactivity found. Nevertheless, HBpin has a high functional group tolerance, a good regio- and stereoselectivity furnishing (*E*)-boronates, and most importantly, pinacol esters are stable to chromatography and are insensitive to air and moisture.

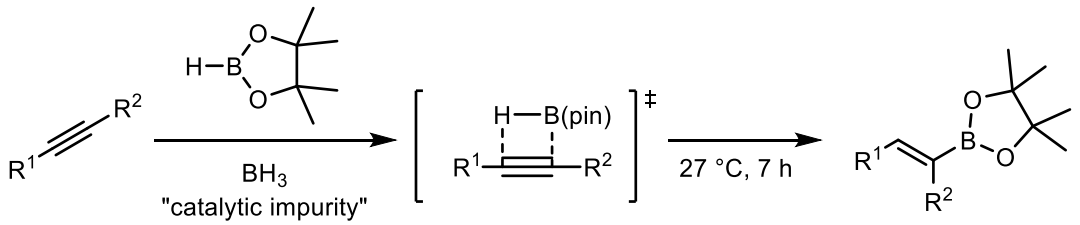


**Scheme 2.4** – General mechanism of uncatalysed hydroboration with pinacolborane.

First reported by Vaultier and co-workers,[47] the use of diisopinocampheylborane ($Ipc_2BH$) as hydroborating agent, has helped to overcome some cases where uncatalysed hydroboration has met mixed successes.[98,99] $Ipc_2BH$ has some attractive features including the inertness to many functional groups (except aldehyde and ketone carbonyls), high regioselectivity resulting from its bulkiness and the ease of dealkylation to the boronic esters under neutral conditions. Miyaura and Suzuki used this latter property to achieve the selective synthesis of

functionalised 1-alkenylboronates in cases where they are not readily available, e.g. alkynes having electron-withdrawing groups attached directly to the triple bond or placed at the propargylic carbon.[100] For the total synthesis of apoptolidin A, Roush and co-workers used $Ipc_2BH$ managing to generate the needed vinylborane *via* a chemoselective hydroboration of a diyne where both HBpin and HBcat proved to be unsuccessful using the same reaction conditions (Scheme 2.5).[101]

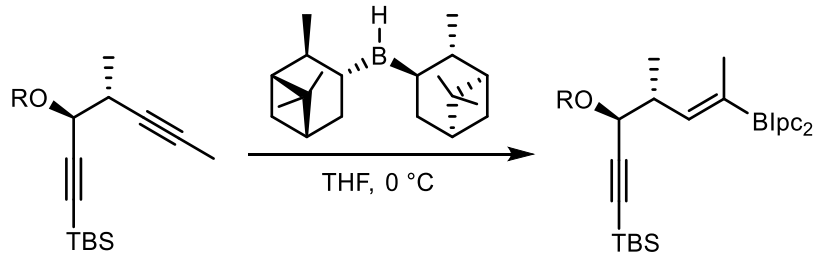


**Scheme 2.5** – Chemoselective hydroboration with diisopinocampheylborane.

Di(isopropylprenyl)borane was introduced by Snieckus and co-workers in 2003. Synthesised *in situ*, this organoborane reagent afforded swift access to alkenylboronic acids with a high diastereoselectivity (Scheme 2.6).[102] The alkenylboronic acid was hydrolysed without isolation followed by further transformations to produce alkenyl boronic acid derivatives. Similarly, this synthetic route proved to be very effective for additional reactions to generate trifluoroborates from the corresponding alkenylboronic acids.[103]

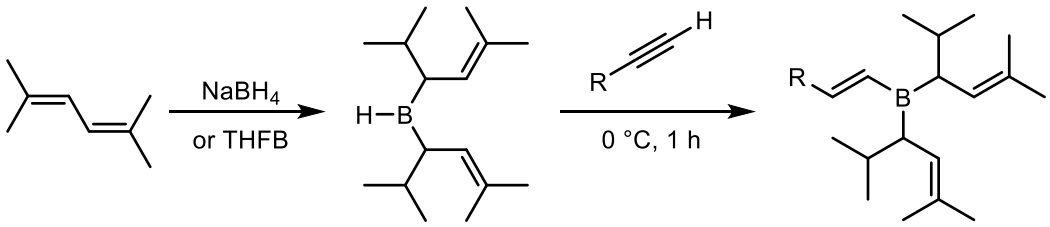


**Scheme 2.6** – Alkyne hydroboration with di(isopropylprenyl)borane.

Chiral boronate esters have been explored in the field of uncatalysed hydroboration of terminal alkynes. Pietruszka and co-workers designed a chiral 1,3,2-dioxaborolane capable of hydroborate terminal alkynes affording chiral

boronate esters, which can direct stereochemistry of subsequent transformations on the vinylboronate, e.g. cyclopropanation (Scheme 2.7).[104]

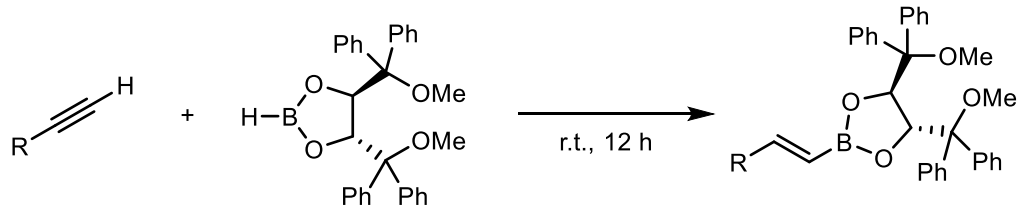


**Scheme 2.7** – Alkyne hydroboration with chiral dioxaborolanes.

### 2.2.1.1 Borane-catalysed Hydroborations

In 1995, Arase and co-workers reported a dicyclohexylborane ($HBCy_2$) catalysed hydroboration of alkynes with HBcat;[105] then in 1997, Hoshi and co-workers used the same catalytic system ($HBCy_2$) to perform hydroboration of 1-halo-1-alkynes with 9-borabicyclo[3.3.1]nonane (9-BBN).[37] It is also shown that carrying the same reactions without catalytic amounts of $HBCy_2$ proceeded sluggishly under usual hydroboration conditions. It was until 2004 when Hoshi and co-workers described that (*E*)-1-alkenylboronic acid pinacol esters could be obtained *via* a boron to boron alkenyl group transfer,[38] the higher reactivity of dialkylboranes over dialkoxyboranes was suggested to explain the catalytic process, though no evidence for the claimed transborylation mechanism was presented. Nevertheless, hydroboration of terminal alkynes with HBpin in the presence of a catalytic amount of $HBCy_2$ at room temperature under neat conditions, led to the desired pinacol ester products (Scheme 2.8).

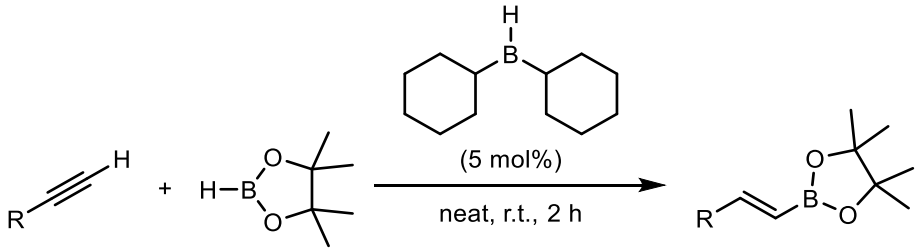


**Scheme 2.8** – Alkyne hydroboration with pinacolborane catalysed by dicyclohexylborane.

Since then, this dicyclohexylborane-catalysed hydroboration has been used in several total syntheses as well as to obtain diverse (*E*)-1-alkenylboronic acid pinacol esters needed for further synthetic modifications, highlighting the importance and ease of this economic synthetic tool.[106–111]

Stephan and Glorius demonstrated in 2016 that Piers' borane ($HB(C_6F_5)_2$), used in catalytic amounts, efficiently converted phenyl acetylene derivatives and terminal alkynes into the corresponding (*E*)-1-alkenyl boronic esters (Scheme 2.9).[112] $HB(C_6F_5)_2$ acts as pre-catalyst generating a 1,1-diborylated species which are the active catalytic species ultimately responsible of the *syn*-1,2-hydroboration of alkynes. Substrates with strongly coordinating functionalities such as dimethylamino moieties and alkynes bearing aldehyde or aliphatic ester groups were not tolerated.

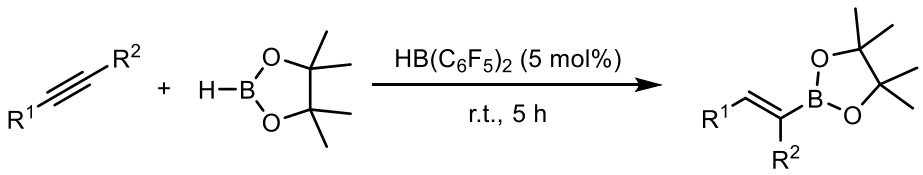


**Scheme 2.9** – Alkyne hydroboration with pinacolborane catalysed by Piers' borane.

In 2017, Melen and co-workers reported a catalytic protocol for the hydroboration of multiple bonds, including alkynes, where tris(2,4,6-trifluorophenyl)-borane (2,4,6-$BAr^{F_9}$) was used as catalyst and HBpin as the hydroborating agent (Scheme **2.10**).[113] This procedure displayed selective hydroboration of the terminal triple bond over the internal unit when a diyne featuring both alkyne groups was used as a substrate. Notably, the use of asymmetric internal alkynes led to a single regioisomer, which sometimes it can represent an issue in some other catalytic systems. Most hydroborations were carried out under 24 hours except in the case of sterically encumbered diphenylacetylene that required 7 days to achieve moderate yields.

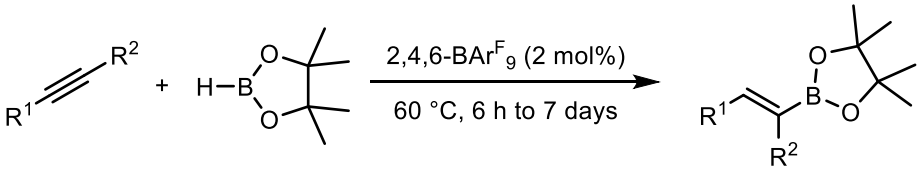


**Scheme 2.10** – Hydroboration of alkynes with pinacolborane catalysed by tris(2,4,6-trifluorophenyl)-borane.

Simple, commercially available borane adducts, $THF{\cdot}BH_3$ (THFB) and $Me_2S{\cdot}BH_3$ (DMSB), have been also reported to catalyse the hydroboration of alkenes and alkynes with HBpin to give the alkyl and alkenyl boronic esters respectively with excellent control of regioselectivity (Scheme 2.11).[114] Slightly higher catalyst loadings, longer reaction times and increased temperatures were needed to achieve good yields. A slight decrease in regiocontrol was observed with benzyl substituted alkynes which worsens when internal alkynes are subjected to hydroboration.

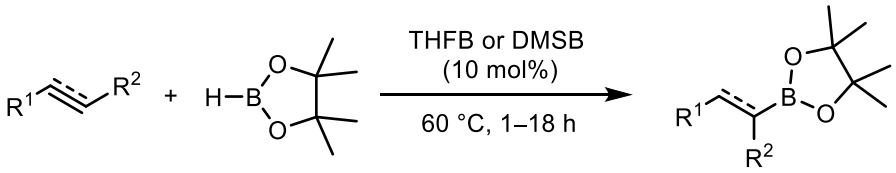


**Scheme 2.11** – Alkene and alkyne hydroboration with pinacolborane catalysed by THFB or DMSB.

### 2.2.1.2 Hydroborations mediated by N-heterocylic Carbenes

A highly regioselective N-heterocyclic carbenes (NHC)-catalysed hydroboration with bis(pinacolato)diboron ($B_2pin_2$) of terminal alkynes was reported by Sun and co-workers in 2013 (Scheme 2.12).[115] The reaction requires a base to activate the NHC precursor and a protic solvent to provide the necessary proton for the addition, and it can be carried out without oxygen/moisture free environment. An example of an internal alkyne was also reported to undergo successful hydroboration though higher temperatures were needed.

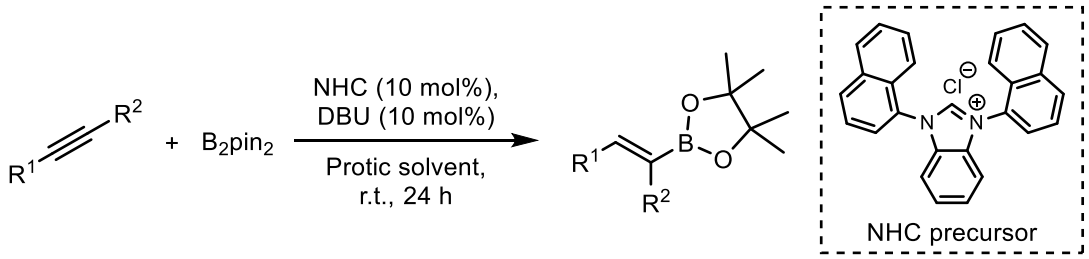


**Scheme 2.12** – Hydroboration of alkynes with bis(pinacolato)diboron catalysed by N-heterocyclic carbene.

### 2.2.1.3 Acid- and Base-catalysed Hydroborations

A carboxylic acid-catalysed hydroboration of alkynes with HBpin was reported in 2014 (Scheme 2.13).[116] Both terminal and internal alkynes afforded the corresponding products in high yields with exclusive regio- and stereoselectivities. A series of organic acids successfully catalysed the reaction although some strong acids, like trifluoroacetic acid decreased the yield. Moreover, strongly Brønsted acidic triflic acid resulted in decomposition without furnishing the desired product. Notably, benzoic acids with an electron-donating group at the *para*-position of the benzene ring showed a remarkably high catalytic activity, being 4-(dimethylamino)benzoic acid the optimum catalyst. The use of nonpolar solvents is preferred for obtaining high yields and other hydroborating agents, 9-BBN and HBcat, are incompatible with this procedure.

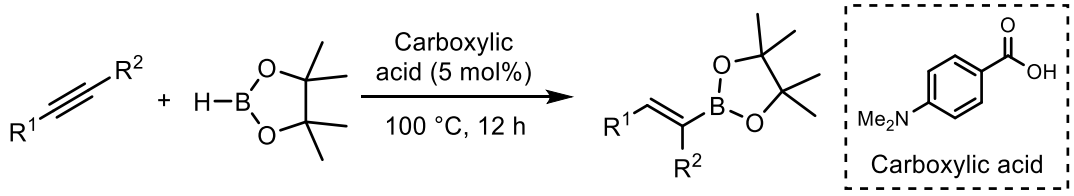


**Scheme 2.13** – 4-(Dimethylamino)benzoic acid-catalysed hydroboration of alkynes with pinacolborane.

In 2016, Yao and Deng published a ligand free hydroboration of terminal alkynes with $B_2pin_3$ where alkynes were directly activated by base, from which Li$O^tBu$ provided the best yields (Scheme 2.14).[117] Arylalkynes gave better yields than alkylakynes regardless of having either electron-withdrawing or electron-donating

groups at the *para*-position. Replacing the cation of the base to NaO$^t$Bu decreased the yield significantly, thus suggesting Li plays an important role in the reaction operating mechanism.

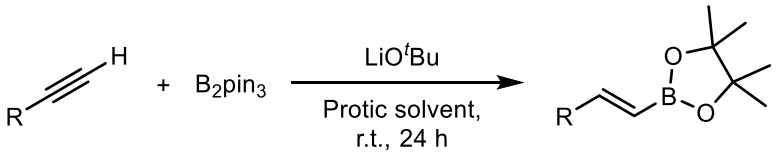


**Scheme 2.14** – Lithium *tert*-butoxide-catalysed hydroboration of alkynes with bis(pinacolato)diboron.

A catalytic hydroboration of alkenes and alkynes initiated by NaOH was reported in 2017 (Scheme 2.15).[118] HBpin and 9-BBN were used to form adducts with nucleophiles, leading to the weakening of the B–H bond which ultimately enhances their hydride character thus facilitating the hydroboration processes. Steric hindrance affects the reaction yields as proved by the low yields obtained when *ortho*-substituted phenylacetylenes were used, additionally, more challenging hydroborations (e.g. diphenylacetylene or methyl-3-phenylpropiolate) only gave a trace amount of the desired products even at high temperatures.

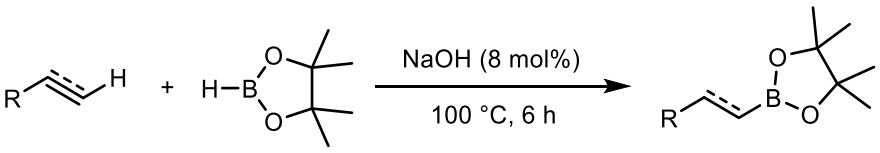


**Scheme 2.15** – Sodium hydroxide-catalysed alkene and alkyne hydroboration with pinacolborane.

### 2.2.1.4 Hydroboration of Alkynes Mediated by Borenium Cations

Curran and co-workers reported in 2013 the hydroboration of silylalkynes by borenium shown in Scheme 2.16. The catalyst can be generated *in situ* by using iodine or triflimide as the activator to afford the mono- or the dihydroboration products, depending on the structure of the substrate.[119]

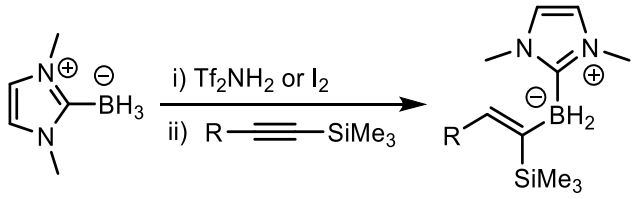


**Scheme 2.16** – Hydroboration of silylalkynes by borenium.

In 2016, Ingleson and co-workers reported a highly selective catalytic *trans*-hydroboration of alkynes with 9-BBN catalysed by borenium cations (Scheme 2.17).[120] The rationale for this procedure is that by using an appropriate borenium cation, the alkyne could be activated then followed by intermolecular hydride transfer from a borane to the less hindered face of the intermediate giving the desired product. Although this protocol affords the desired products, a careful sequence of reagent additions and pre-synthesis of the borenium (sometimes taking up to 48 hours) are required.

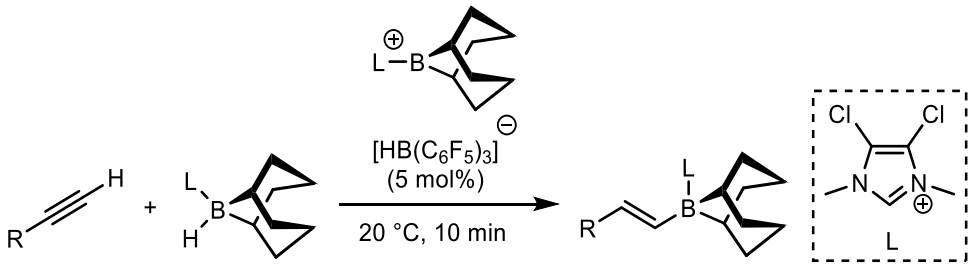


**Scheme 2.17** – Hydroboration of alkynes with 9-borabicyclo(3.3.1)nonane by borenium cations.

## 2.2.2 Metal-catalysed Hydroborations

Knochel's pioneering work was an essential influence that led the way to new developments in the field of alkyne hydroboration and, some years later, the work had expanded at a point where novel reports of transition metal-catalysed hydroboration started to be published.

The wide range of metal complexes that catalyse alkyne hydroboration include zirconium (Zr)[31,121,122], rhodium (Rh)[123–129] and copper (Cu),[130,131,140–

[149,132,150,151,133–139] being these the most generally utilised. Some other less commonly used transition metals are nickel (Ni),[93,123,152] iridium (Ir),[124,153–156] ruthenium (Ru),[157,158] iron (Fe),[159–162] gold[163,164] and earth-abundant metal aluminium (Al).[165–167]

### 2.2.2.1 Zirconium-catalysed Hydroborations

Pereira and Srebnik found that a catalytic amount of Schwartz's reagent ($Cp_2ZrHCl$) could make the reaction proceed at room temperature in the presence of a slight excess of HBpin.[31] In general, the alkenylboronates were obtained with a good *E*-selectivity, except in the case of alkynes with oxygen in their structure, which appear to promote a larger amount of the (*Z*)-alkenylboronate.

This difference in stereoselectivity is thought to occur due to the stabilisation of the pseudo *Z* intermediate through a Zr−O interaction happening after the initial hydrozirconation (Scheme 2.18). Transmetallation and hydride exchange then regenerates the catalyst to afford the alkenylboronate.

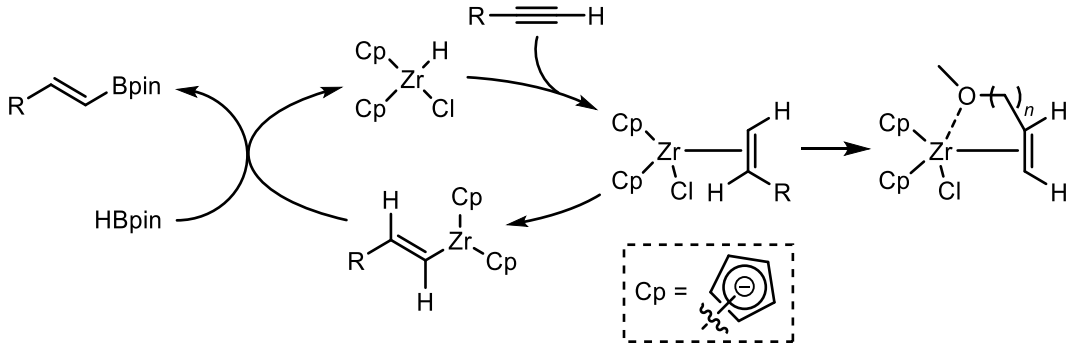


**Scheme 2.18** – General mechanism for the hydroboration of alkynes with pinacolborane catalysed by Schwartz's reagent.

Wang and co-workers improved this protocol by performing the reaction at higher temperatures (60 °C) by adding $NEt_3$.[122] These changes allowed to use oxygen-containing alkynes such as ethers and silylethers while maintaining high yields and good *E*-selectivities (Scheme 2.19).

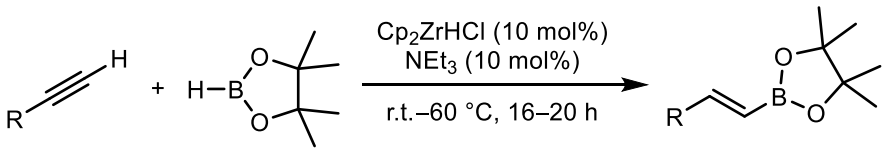


**Scheme 2.19** – Alkyne hydroboration with pinacolborane catalysed by Schwartz's reagent.

### 2.2.2.2 Rhodium-catalysed Hydroborations

Pereira and Srebnik reported the first rhodium-catalysed hydroboration of alkynes.[123] The replacement of one triphenylphosphine ligand from Wilkinson's catalyst with carbon monoxide, $Rh(CO)(PPH_3)_2Cl$, provided excellent yields and good anti-Markovnikov selectivity regardless of the substituent pattern on the alkyne (Scheme 2.20). If Wilkinson's catalyst was used, $Rh(PPH_3)_3Cl$, low stereoselectivities were obtained suggesting that the selectivity in the metal-catalysed hydroborations was clearly influenced by the nature of the ligands.

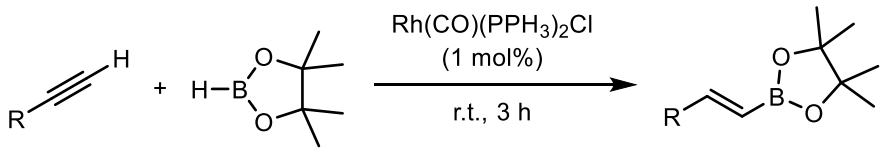


**Scheme 2.20** – Rh-catalysed alkyne hydroboration with pinacolborane.

Miyaura and co-workers did some mechanistic investigation and discovered that a complete reversal of selectivity could be achieved in the presence of a $Rh(I)-P(^iPr)_3$ complex and $NEt_3$. Excess of both the alkyne and $NEt_3$ over the borane reagent are needed to obtain highly pure (*Z*)-alkenylboronate with good yields.[124] Also playing a major role are the steric and electronic effects of $P(^iPr)_3$.

A completely different catalytic cycle was proposed based on deuterium labelling experiments that involves the formation of the vinylidene complex stabilised by the phosphine ligand. As shown in Scheme 2.21, the oxidative addition of a B–H bond to the coordinatively unsaturated metal centre is followed by alkene coordination, insertion and hydride migration onto the coordinated alkene. A subsequent reductive elimination furnishes the B–C bond.

Carbo and Fernandez, based on DFT and quantum mechanical/molecular mechanical ONIOM calculations, proposed a sequence of vinylidene insertion into the Rh−H bond followed by reductive elimination of the C−B bond ( Scheme 2.21, dashed pathway).[125]

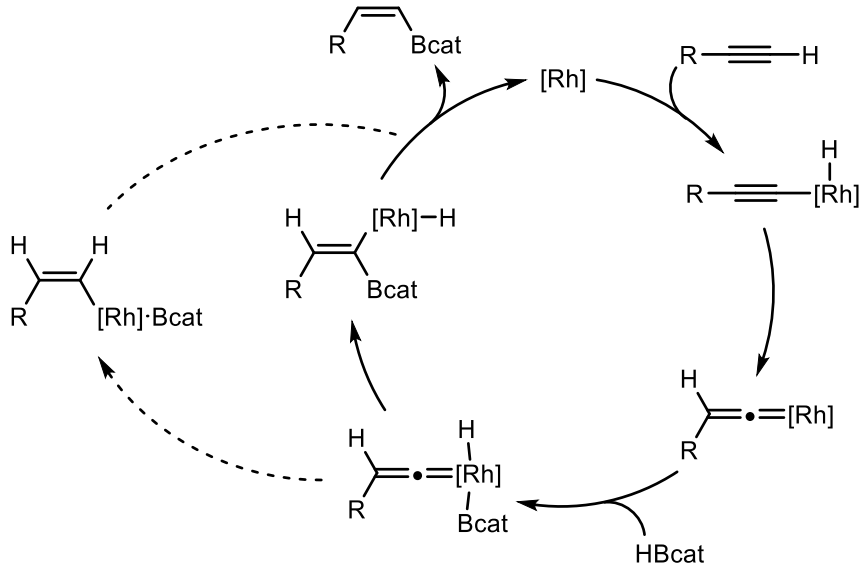


**Scheme 2.21** – Mechanism leading to (*Z*)-alkenylboronate proposed by Miyaura and alternative mechanism proposed by Carbo and Fernandez (dashed pathway).

### 2.2.2.3 Copper-catalysed Hydroborations

Miyaura and co-workers introduced the copper-catalysed hydroboration of alkynes. Reactions were carried out in the presence of CuCl, AcOK and $B_2pin_2$ and provided the 2-alkenylboronate species preferentially.[130] Mechanistic studies suggested the formation of a [Cu(Cl)OAc]K complex, which cleaves the B−B bond of $B_2pin_2$ and leads to a free borylcopper species (Scheme 2.22). The metalloboration followed by the hydrolysis eventually affords the (*Z*)-alkenylboronate.

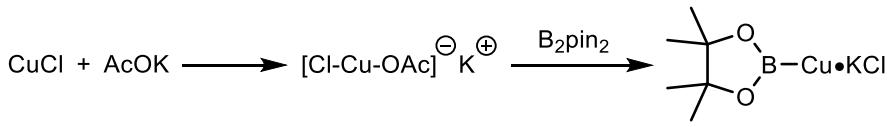


**Scheme 2.22** – Generation of borylation reagent by reaction of bis(pinacolato)diboron with CuCl and AcOK.

A mechanism for the copper-catalysed formation of alkenylboronates substituted by an alkoxycarbonyl group starting from acetylenic esters was proposed by Lipshutz and co-workers.[139] The reaction provides both good yields and good stereoselectivities for (*Z*)-alkenylboronates independently of the substituents on the alkyne (alkyl, aryl, silylether, etc.). The alkyne undergoes a 1,2 addition of CuH forming a carbon-bound copper intermediate rather than an oxygen-bound intermediate, being the latter significantly less stable by 29.5 kcalmol$^{-1}$, according to high-level ab initio calculations. followed by transmetallation with pinacolborane to furnish the desired product (Scheme 2.23).

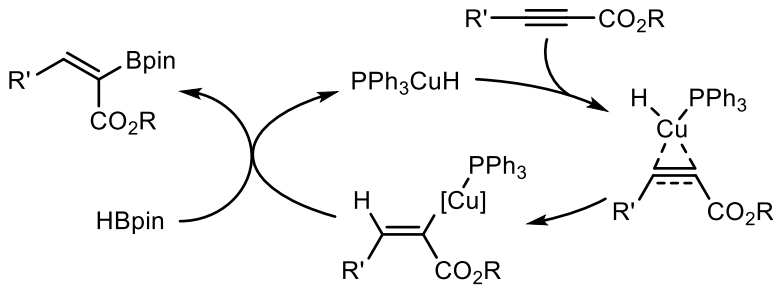


**Scheme 2.23** – Catalytic cycle of the hydroboration of acetylenic ester catalysed by $PPh_3CuH$.

Yun and co-workers reported a copper-catalysed addition of $B_2pin_2$ to α,β-acetylenic esters (Scheme 2.24).[140] The reaction takes advantage from the copper-phosphine catalyst, which allows the stereoselective synthesis of β-borylated-α,β-ethylenic esters. First, the phosphine ligated copper boryl complex adds to the ester and the resulting copper enolate reacts with MeOH to yield the protonated product along with the copper alkoxide. The latter then regenerates the active catalyst by reacting with $B_2pin_2$.

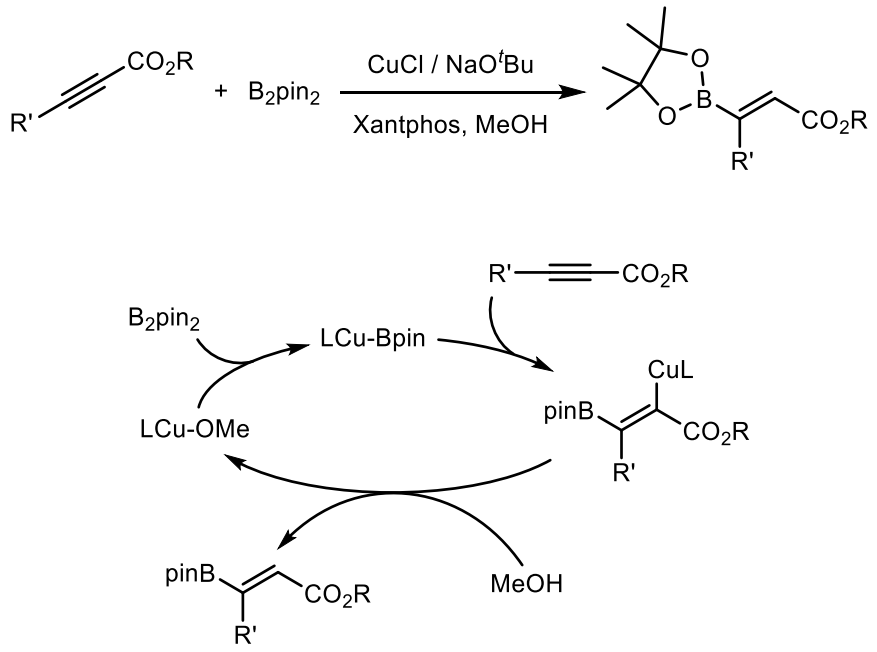


**Scheme 2.24** – Copper-catalysed hydroboration of acetylenic ester with bis(pinacolato)diboron and its mechanism.

## 2.3 Aims

Boronic acid pinacol esters are ubiquitous in Suzuki-Miyaura cross-coupling, offering a more air- and bench-stable alternative to boronic acids. The preparation of alkenyl boronic acid pinacol esters by the hydroboration of alkynes has been exploited using transition metal as catalysts. Diverse complex mechanisms have been proposed for these reactions, and special importance should be given that the mechanism varies, or completely changes, when using different metals, ligands or additives in the reaction mixture.

The synthesis of (*E*)-alkenyl boronic acid pinacol esters by the hydroboration of 1-alkynes with pinacol borane occurs readily in the presence of catalytic dicyclohexylborane. A simplistic mechanism has been proposed by Hoshi and co-workers without experimental evidence, and despite its diverse and extensive application, a thorough investigation has yet not been conducted.

Therefore, the aim of the project consists in establishing a kinetic profile for all components of the transformation of phenylacetylene to its corresponding *cis*-hydroborated product catalysed by dicyclohexylborane. Additionally, to conduct stoichiometric studies employing isotopic labelling to characterise key steps of the borane-catalysed hydroboration reaction.

## 2.4 Results and Discussion

### 2.4.1 Initial Mechanistic Studies

#### 2.4.1.1 Hydroboration of 4-Fluorophenylacetylene with Pinacolborane Catalysed by Dicyclohexylborane

A standard reaction model was used for studying the boron-catalysed alkyne hydroboration reaction mechanism. For these kinetic experiments, a modified procedure of the originally reported reaction by Hoshi in 2004 was employed.[38] Changes include catalyst synthesised *in situ* prior addition of any other reagent, increased concentration in order to obtain a faster reaction to be monitored on a timescale amenable to measurement and dioxane/$CHCl_3$ (100:1) was used as solvent as this mixture was found to help stabilise disubstituted borane species (as discussed previously in Chapter 1 and corroborated from HBpin stability experiments showed in 2.4.2 on page 80). 4-Fluorophenylacetylene **3** was chosen as standard substrate allowing the reaction to be monitored by $^{19}F$ NMR spectroscopy without using deuterated solvents.

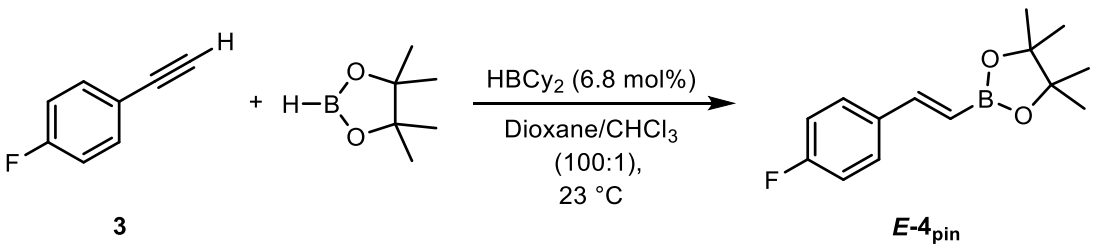


**3** ***E*-4$_{pin}$**

**Scheme 2.25** – Standard reaction conditions used to investigate the kinetic profile of $HBCy_2$-catalysed alkyne hydroboration; [**3**]$_0$ = 0.6 M, [HBpin] = 0.6 M, [$HBCy_2$] = 0.04 M and [1-fluoronaphthalene] = 0.256 M (IS).

The reaction reached completion within 5 h when carried out at 0.6 M in dioxane/$CHCl_3$ (100:1) at 23 °C with 6.8 mol% catalyst loading (Scheme 2.25). Temporal concentrations were calculated relative to the 1-fluoronaphthalene internal standard (IS) signal in the $^{19}F$ NMR spectra.

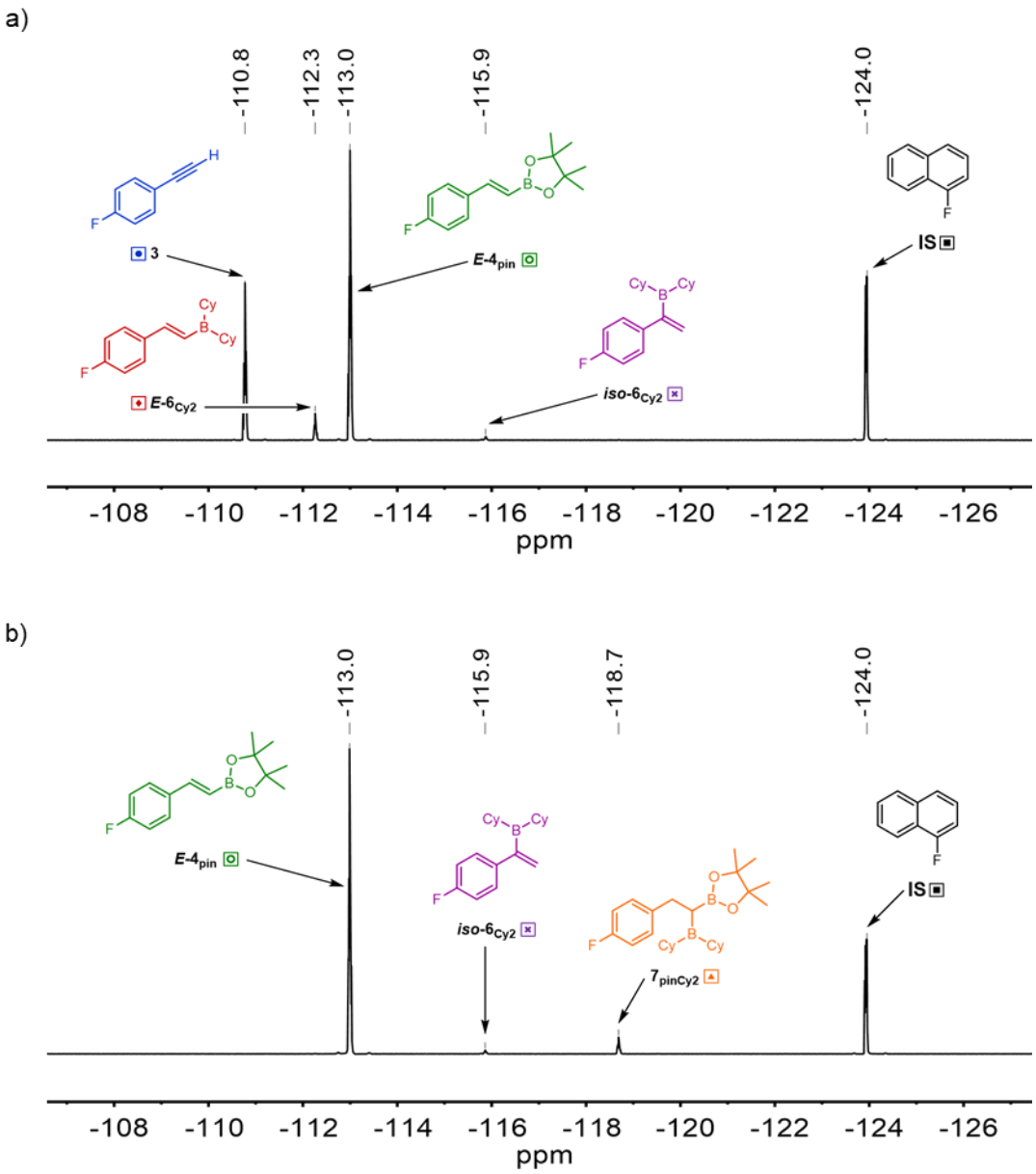


**Figure 2.2** – $^{19}$F NMR spectra recorded during the boron-catalysed hydroboration showing the substrate (**3**) and product (***E*-4$_{pin}$**) in addition to: **a)** The intermediate ***E*-6$_{Cy2}$** present while the reaction is ongoing and the iso-intermediate (***iso*-6$_{Cy2}$**); and **b)** The double addition side-product (**7$_{pinCy2}$**) appearing after the reaction has finished. Peaks are referenced against IS 1-fluoronaphthalene.

Typical spectra from an ongoing reaction are shown above in Figure 2.2 where five clearly resolved peaks, excluding the IS, can be distinguished. These fluorinated species correspond to the substrate (**3**), intermediate (***E*-6$_{Cy2}$**), product (***E*-4$_{pin}$**) and

side-products (***iso*-$\mathbf{6}_{Cy2}$** and **$\mathbf{7}_{pinCy2}$**) of the reaction, all having distinct chemical shifts.

High conversion of the alkenyl boronate product was obtained with minimal formation of side-products that was always limited by the catalyst loading. Higher formation of side-products was observed at higher catalyst loadings thus reflected on the product yield; this contradictious effect is explained in depth later (Section 2.4.3).

From this initial mechanistic study, and as shown in Figure 2.3, a clean consumption of the alkyne **3** was observed and the corresponding increase of product ***E*-$\mathbf{4}_{pin}$**. A transient species was also observed increasing at the beginning of the reaction after a short induction period linked to reactive dissolution of the catalyst suspension. Increasing the catalyst loading raised the formation of this alkenylborane species. The transient intermediate started to fade away just after the substrate had been totally consumed. This species was identified as the intermediate ***E*-$\mathbf{6}_{Cy2}$**, anti-Markovnikov addition of $HBCy_2$ into the triple bond with high regio- and stereochemistry as found by Hoshi,[38] whereas Markovnikov addition of the catalyst into the triple bond gave rise to an inactive iso-intermediate species ***iso*-$\mathbf{6}_{Cy2}$**, that sequestered a small percentage of the active catalyst.

Interestingly, an unwanted species corresponding to a double addition side-product, present in low concentrations, only significantly rises after total consumption of the substrate, showing the high selectivity of $HBCy_2$ towards a triple bond over a double bond. Diboryl **$\mathbf{7}_{pinCy2}$** was consistently generated in quantities directly proportional to the catalyst loading.

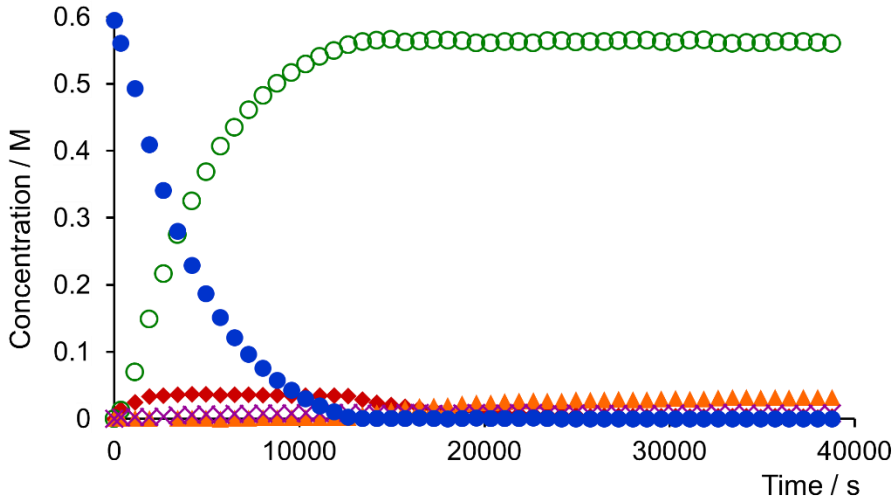


**Figure 2.3** – Temporal concentration profile for hydroboration of **3** by $HBCy_2$, monitored by $^{19}F$ NMR spectroscopy (blue circles: **3**, outlined green circles: ***E*-4$_{pin}$**, red diamonds: ***E*-6$_{Cy2}$**, purple crosses: ***iso*-6$_{Cy2}$**, orange triangles: ***iso*-6$_{Cy2}$**). Conditions: $[\mathbf{3}]_0$ = 0.6 M, [HBpin] = 0.6 M, $[HBCy_2]$ = 0.04 M and [1-fluoronaphthalene] = 0.256 M in dioxane/$CHCl_3$ (100:1) at 23 °C.

### 2.4.1.2 Hydroboration of 4-Fluorophenylacetylene with Pinacolborane Catalysed by Dimethyl Sulfide Borane

In order to assess the effectiveness of $HBCy_2$ as catalyst against a background reaction arising from remaining dimethyl sulfide borane (DMSB), a reaction where the catalyst was replaced with DMSB, was performed (Scheme 2.26).

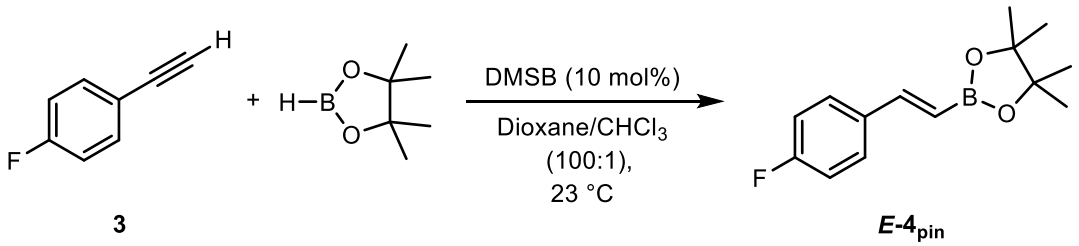


**3** ***E*-4$_{pin}$**

**Scheme 2.26** – Reaction conditions used to investigate the degree of background hydroboration generated by DMSB; $[\mathbf{3}]_0$ = 0.6 M, [HBpin] = 0.6 M, [DMSB] = 0.06 M and [1-fluoronaphthalene] = 0.26 M (IS) in dioxane/$CHCl_3$ (100:1) at 23 °C.

A similar kinetic profile was obtained (Figure 2.4), and even though the hydroboration took place without catalyst, there was a significant difference, the DMSB-catalysed reaction was approximately 14 times slower than the catalysed

by $HBCy_2$. A reaction without $HBCy_2$ or DMSB was carried out and no product was observed after 24 h, proving no hydroboration by HBpin takes place at 23 °C under the tested conditions without the aid of another boron species.

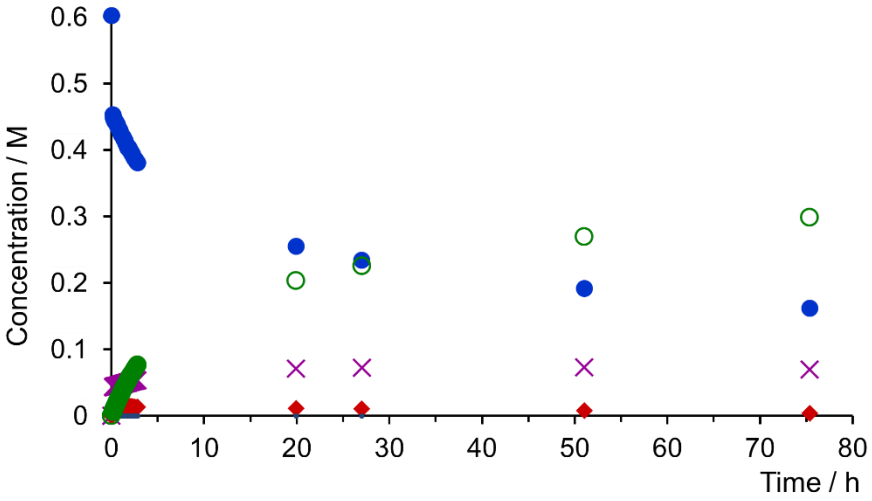


**Figure 2.4** – Temporal concentration profile for hydroboration of **3** catalysed by DMSB, monitored by $^{19}F$ NMR spectroscopy (blue circles: **3**, outlined green circles: ***E*-4$_{pin}$**, red diamonds: ***E*-6$_{Cy2}$**, purple crosses: unidentified side-product). Conditions: [**3**]$_0$ = 0.6 M, [HBpin] = 0.6 M, [DMSB] = 0.06 M and [1-fluoronaphthalene] = 0.26 M in dioxane/$CHCl_3$ (100:1) at 23 °C.

This background reaction was omitted for the purposes of mechanistic studies and kinetic modelling; in every kinetic monitoring of the hydroboration reaction, cyclohexene was used in slight excess to quench any DMSB left thus ensuring any background reactivity from it should be negligible.

## 2.4.2 Stability of Pinacolborane Solution

To probe the stability of pinacolborane in the chosen solvent mixture for the alkyne hydroboration, a series of pinacolborane solutions were prepared and monitored by $^{11}B$ NMR spectroscopy at room temperature over time to follow their decomposition in a semi-quantitative manner. Results are shown in Table 2.1.

| Day | Date | HBpin (%) | | |
|---|---|---|---|---|
| | | Dioxane/$CHCl_3$ (100:1) | Dioxane | $CHCl_3$ |
| 0 | 16/07/2018 | 98.2 | 97.3 | 97.9 |
| 1 | 17/07/2018 | 98.3 | 95.0 | 98.0 |
| 2 | 18/07/2018 | 98.0 | 94.3 | 97.9 |
| 3 | 19/07/2018 | 98.2 | 93.4 | 97.3 |
| 4 | 20/07/2018 | 98.1 | 93.1 | 97.0 |
| 5 | 21/07/2018 | 97.2 | 92.6 | 96.5 |
| 6 | 22/07/2018 | 98.2 | 92.4 | 96.6 |
| 31 | 16/08/2018 | 97.4 | 90.6 | 95.2 |
| 34 | 19/08/2018 | 96.7 | 90.1 | 94.9 |
| 38 | 23/08/2018 | 97.8 | 89.8 | 94.9 |
| 48 | 02/09/2018 | 97.4 | 89.9 | 95.2 |
| 59 | 13/09/2018 | 96.9 | 89.9 | 95.1 |

**Table 2.1** – Percentage of HBpin remaining after monitoring three independent HBpin solutions (0.65 M) in dioxane, $CHCl_3$ and dioxane/$CHCl_3$ (100:1), over 59 days under $N_2$.

Pinacolborane solution made in dioxane presented the highest decomposition with 10.1% loss, followed by the one in $CHCl_3$ with only 4.9%; while this loss of reactant is not significant over almost a two month period, a mixture of both solvents in the chosen ratio (dioxane/$CHCl_3$, 100:1), appreciably helped to stabilise HBpin: only 3.1% loss was observed in this case. As it can be seen qualitatively in Figure 2.5, the degradation of the borane gave rise to a peak that grew over time corresponding to $B_2pin_3$.[168] From these results it can be appreciated the positive effect the combination of solvents have towards the course of the reaction,

providing a stable environment towards the reactants in the case of a prolonged monitoring of the reaction is required or for any particular synthetic purposes.

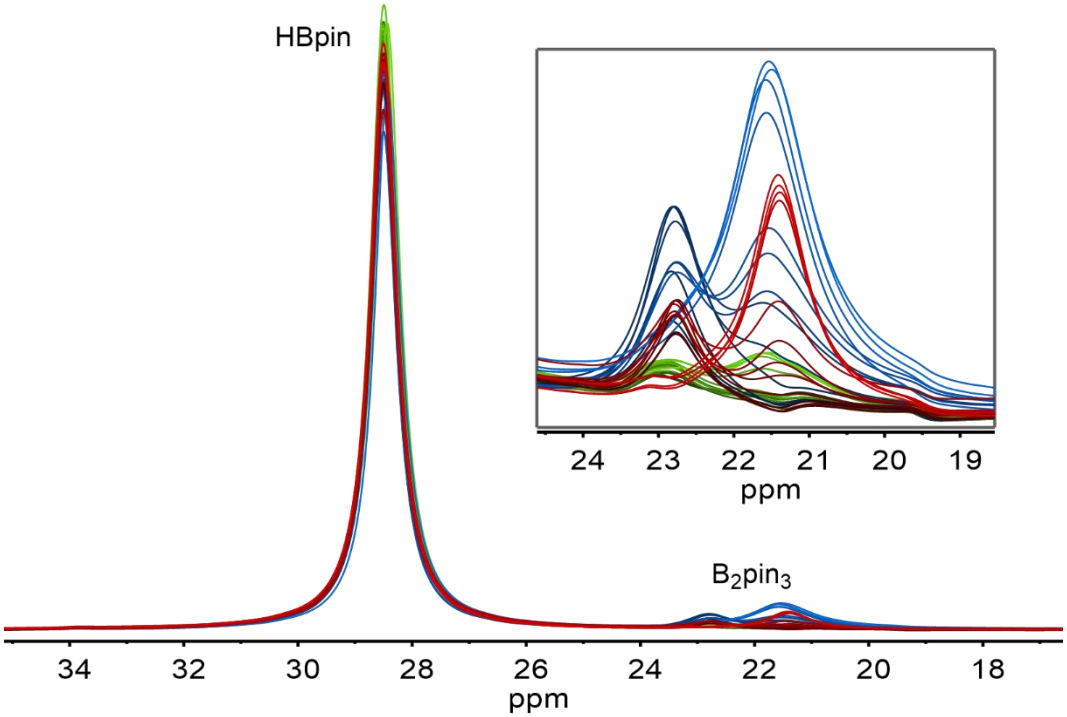


**Figure 2.5** – Stacked spectra showing decomposition of pinacolborane solutions over time (green: dioxane/$CHCl_3$ (100:1), blue: dioxane, red: $CHCl_3$).

## 2.4.3 Irreversibility of Product and Side-product Formation

A cross-over experiment was carried out to verify the transborylation step (intermediate → product) was irreversible, Additionally, it provides evidence to confirm if the last step on the cycle, double addition side-product formation, was also irreversible.

As shown in Scheme 2.27, a catalytic reaction employing [$D_4$]-**3** (1 equiv.) was set up and allowed to reach completion. At this point, additional 1 equiv. of a differently labelled product, [$H_4$]-***E*-4$_{pin}$**, was then added into the reaction along with extra catalyst, resulting in a cross-over of species both giving rise to a mixture of double addition side-products **7**$_{pinCy2}$. The variation on all the differently labelled

species were monitored by $^{19}F$ NMR spectroscopy. Corroboration about the irreversibility of the product formation is given by the same experiment.

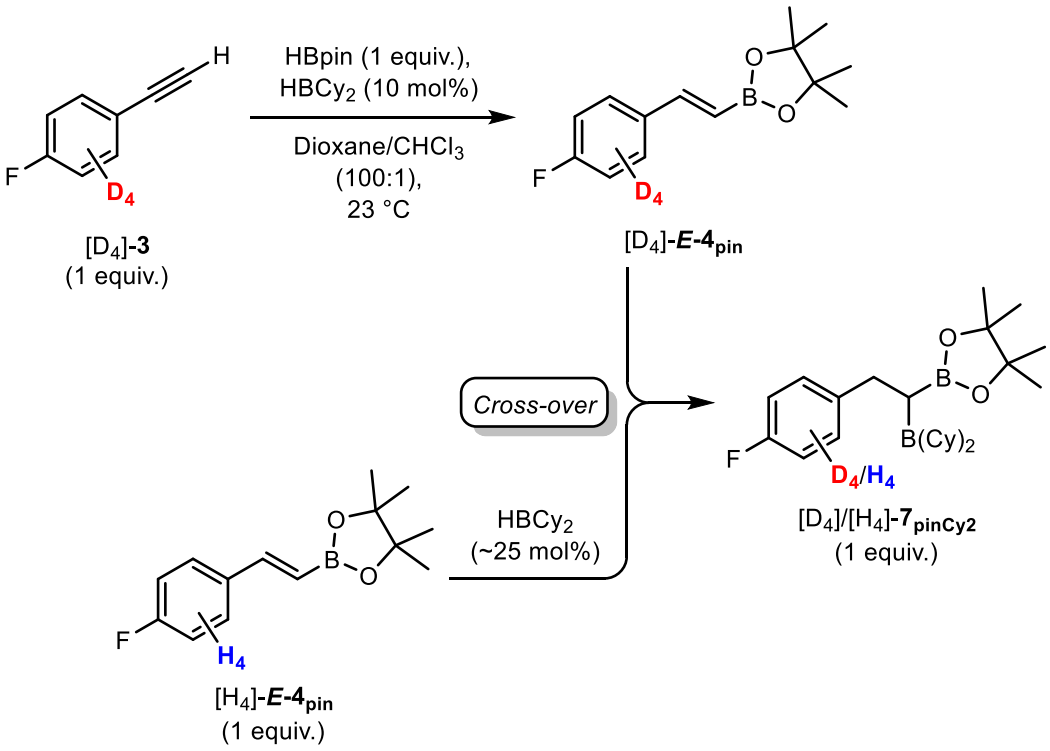


**Scheme 2.27** – Cross-over experiment. Conditions: $[D_4\text{-}3]_0$ = 0.62 M, [HBpin] = 0.79 M, $[HBCy_2]$ = 0.06 M, [1-fluoronaphthalene] = 0.25 M (IS) in dioxane/CHCl3 (100:1) at 23 °C. Further $[H_4\text{-}\boldsymbol{E}\text{-}\mathbf{4_{pin}}]_0$ = 0.23 M and $[HBCy_2]$ = 0.11 M were added along with additional solvent. Note that initial concentrations have changed after being diluted by the second addition of reagents.

Once the reaction using $[D_4]$-**3** has reached completion ("*End point*" in Figure 2.6), $[H_4]$-$\boldsymbol{E}$-$\mathbf{4_{pin}}$ along with $HBCy_2$ were added. No rise in the concentration of the intermediate was observed, neither the $D_4$ nor $H_4$ labelled, corroborating there is no backward reaction once the transborylation has occurred. Notably, there is a consumption of both products, $[D_4]$-**3** and $[H_4]$-**3**, this can only be attributed to the excess $HBCy_2$ added confirming it will add to a double bond present in the product if deprived from any other source of triple bond. Correspondingly, there is a rise in the already present double addition side-product $[D_4]$-$\mathbf{7_{pinCy2}}$ and the analogous appearance of double addition side-product $[H_4]$-$\mathbf{7_{pinCy2}}$. Moreover, neither $[D_4]$-$\boldsymbol{E}$-$\mathbf{6_{Cy2}}$ nor $[H_4]$-$\boldsymbol{E}$-$\mathbf{6_{Cy2}}$ were observed after addition of the extra catalyst,

meaning there is no backward reaction that could give rise to any intermediate, agreeing with previously discussed results.

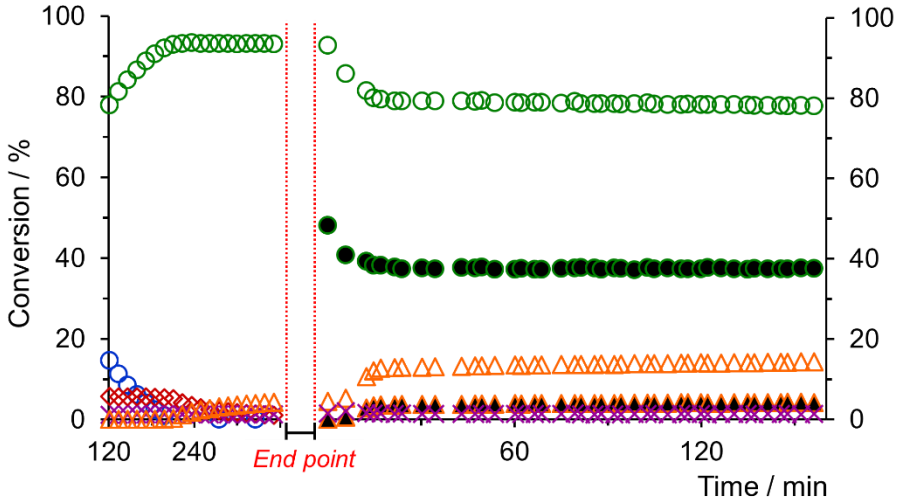


**Figure 2.6** – Partial temporal conversion profile for hydroboration of [D4]-**3** by $HBCy_2$, monitored by $^{19}F$ NMR spectroscopy; "End point" tag marks the beginning of the cross over experiment (blue circles: [D4]-**3**, green circles: [D4]-***E*-4$_{pin}$**, red diamonds: [D4]-***E*-6$_{Cy2}$**, purple crosses: [D4]-***iso*-6$_{Cy2}$**, orange triangles: [D4]-**7$_{pinCy2}$**, black filled circles: [H4]-***E*-4$_{pin}$**, black filled triangles: [H4]-**7$_{pinCy2}$**).

## 2.4.4 Productivity of the Intermediate

The kinetic data presented in 2.4.1.12.4.1 on page 7976 suggests the presence of an intermediate during the reaction but it does not discriminate between this species being peripheral to the productive catalytic cycle (Scheme 2.29, case A) or an integral part of it (cases B–D). In order to distinguish between these four possibilities, an isotopic entrainment experiment was carried out.

Preparation of [D4]-**3**, in which the aromatic ring is perdeuterated results in an upfield shift of 0.5 ppm in the $^{19}F$ NMR signal of [D4]-**3**, relative to **3**, and as well as any other species produced as a result of its reaction. As depicted in Scheme **2.28**, a catalytic reaction employing [H4]-**3** (0.5 equiv.) was allowed to evolve until [H4]-intermediate has reached its maximum concentration. At this point, further 0.5 equiv. of a differently labelled substrate, [D4]-**3**, was then immediately added, resulting in an isotopic perturbation of the system. At the point that [D4]-**3** is added,

there has been 26% net conversion of [$H_4$]-***E*-4$_{pin}$**. However, neither of the products (***E*-4$_{pin}$** or ***E*-6$_{Cy2}$**) yet contain any of the deuterium label: all of this resides in unreacted [$D_4$]-**3**. The key features are the changes in [$D_4$]-population in the substrate **3**, and entrainment into the intermediate ***E*-6$_{Cy2}$**, and product ***E*-4$_{pin}$** as the reaction evolves. This experiment was also useful to obtain additional information as the deuterium incorporation also occurs in the iso-intermediate ***iso*-6$_{Cy2}$** and, after the reaction has finished, in the double addition side-product **7$_{pinCy2}$**; this is discussed further below.

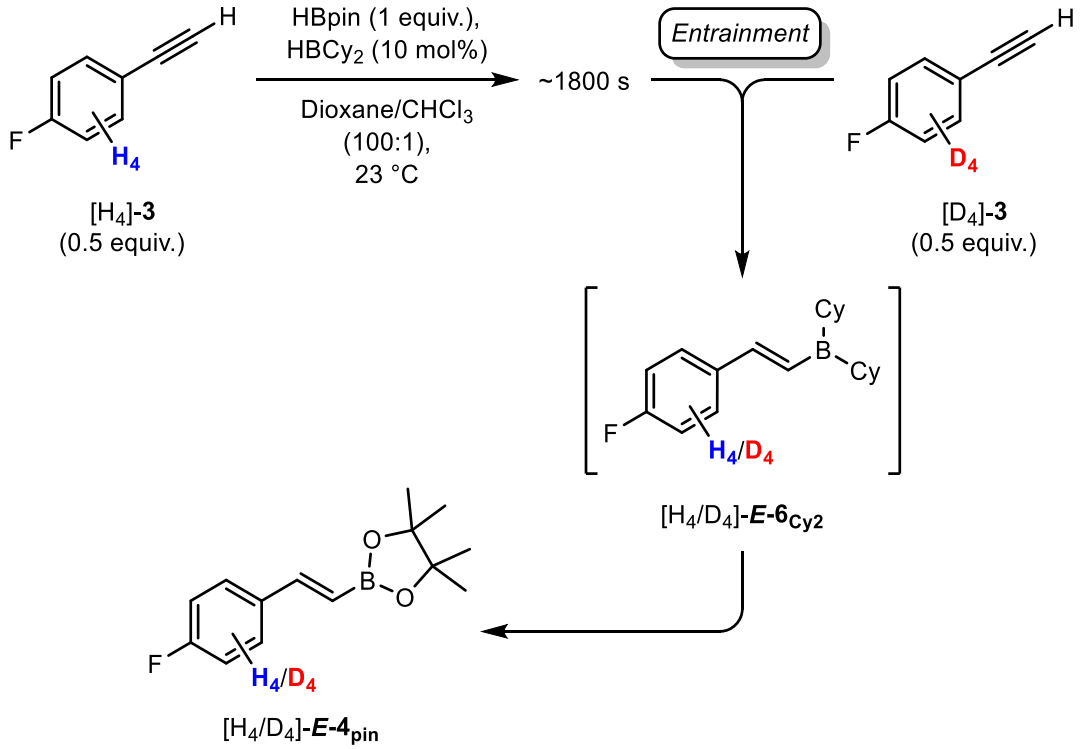


**Scheme 2.28** – Deuterium ($D_4$) entrainment into catalytic cycle. Conditions: [$H_4$-**3**]$_0$ = 0.3 M, [$D_4$-**3**]$_0$ = 0.3 M added at 26% net conversion of $H_4$-**3**, [HBpin] = 0.67 M, [$HBCy_2$] = 0.06 M, [1-fluoronaphthalene] = 0.25 M (IS) in dioxane/$CHCl_3$ (100:1) at 23 °C.

Irrespective of the pathway (Scheme 2.29, cases A–D) the population in the final product must ultimately rise from 0% to 50%, as dictated by the equal proportions of [$H_4$]-**3** and [$D_4$]-**3** added overall. For case A, where the intermediate is off-cycle, the isotope population in ***E*-6$_{Cy2}$** will depend only on that of the final product (***E*-4$_{pin}$**; max 50% $D_4$) and at all stages will be lower or equal to it; moreover, $D_4$

population in ***E*-6$_{Cy2}$** will rise following incorporation in ***E*-4$_{pin}$**. For case B, where the intermediate is on-cycle, but is in equilibrium with the substrate, the $D_4$-population in **3** will be reduced, in the limit from 71% (Equation 2.1) to 63% (Equation 2.2). For cases C and D, where the catalyst addition into the substrate to produce the intermediate is irreversible, the isotope population in **3** is constant (71% $D_4$) and the $D_4$-content in ***E*-6$_{Cy2}$** rises from 0% to a maximum of 71% as it is repopulated from **3**. However, for case C, equilibration of intermediate with product ***E*-4$_{pin}$** will attenuate the rise in $D_4$-population in ***E*-6$_{Cy2}$**, in the limit to 50%. Only for case D will the $D_4$ isotope population in ***E*-6$_{Cy2}$** rise, in advance of product ***E*-4$_{pin}$**, to reach a maximum 71% $D_4$.

$$\left(\frac{50\%\ D_4\text{-added}}{Total_{substrate}\ \text{before entrainment}}\right)\ x\ 100 = 71\% \quad \textbf{Equation 2.1}$$

Where $Total_{substrate}$ before entrainment:

$$Total_{substrate} = 30\%\ H_4\text{-remaining} - 10\%\ H_4\text{-intermediate} + 50\%\ D_4\text{-added}$$

$$Total_{substrate} = 70\%$$

$$\left(\frac{50\%\ D_4\text{-added}}{Total_{substrate}\ \text{after entrainment}}\right)\ x\ 100 = 63\% \quad \textbf{Equation 2.2}$$

Where $Total_{substrate}$ after entrainment (assuming fast equilibration between intermediate and substrate):

$$Total_{substrate} = 20\%\ H_4\text{-produced} + 10\%\ H_4\text{-intermediate} + 50\%\ D_4\text{-added}$$

$$Total_{substrate} = 80\%$$

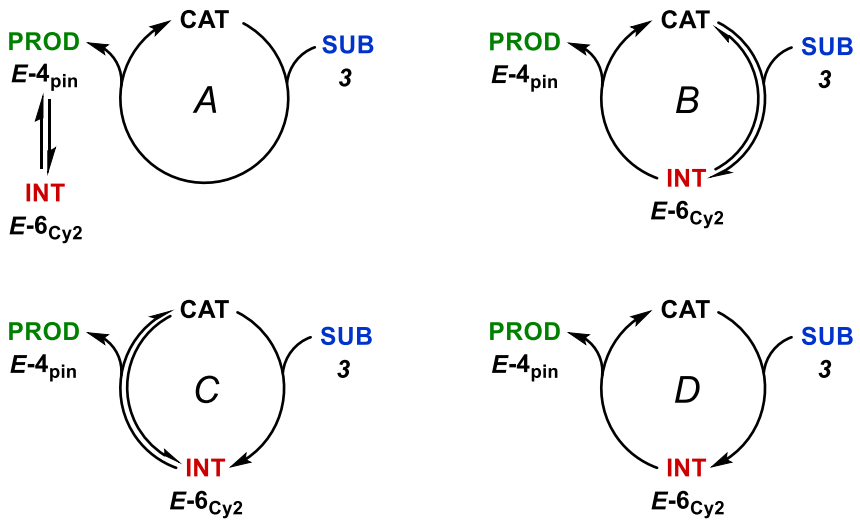


**Scheme 2.29** – Different theoretical scenarios where the intermediate is either off-cycle (case *A*) or on-cycle (cases *B*–*D*), and some of these processes are either reversible or not.

Comparison of the predicted and experimentally determined $D_4$-populations as a function of net conversion (Figure 2.7) confirms that ***E*-4$_{pin}$** arises from two irreversible sequential reactions where ***E*-6$_{Cy2}$** is the productive catalytic intermediate (case D). There are no significant reversible reactions connecting **3** with any intermediates or products (on- or off-cycle), **3** remains 71% throughout the whole experiment. The isotope ratio in transient intermediate ***E*-6$_{Cy2}$** grows, prior all other species except **3**, and quickly reaches the same level of incorporation as **3**.

The product ***E*-4$_{pin}$** accumulates $D_4$ after addition of ***E*-6$_{Cy2}$**, rising to 50% after a short induction period. The accumulation in the product is thus dependant on the growth of $D_4$ in an intermediate that connects it with the substrate **3**.

Additionally, this corroborates the iso-intermediate ***iso*-6$_{Cy2}$** being a locked-species. It is generated in low proportion (1.2% of total product) at a slower rate than ***E*-6$_{Cy2}$**, but in advance of ***E*-4$_{pin}$**. It eventually reaches 52% incorporation due to being irreversibly generated (iso-intermediate not turning over), this number is established by the equal proportions of [$H_4$]-**3** and [$D_4$]-**3** feeding this species.

After the starting material has been consumed, changes in [$D_4$]-populations were still recorded mainly for monitoring changes in double addition side-product. As expected from the kinetic profile previously recorded, its population only becomes relevant after there is no more alkyne left to hydroborate (only 0.5% present throughout the first 95% of the reaction evolution), thus giving rise to $D_4$ incorporation of $\mathbf{7}_{\mathbf{pinCy2}}$ to a maximum of 48%, demonstrating that $\mathbf{7}_{\mathbf{pinCy2}}$ is generated from $\boldsymbol{E}$-$\mathbf{4}_{\mathbf{pin}}$.

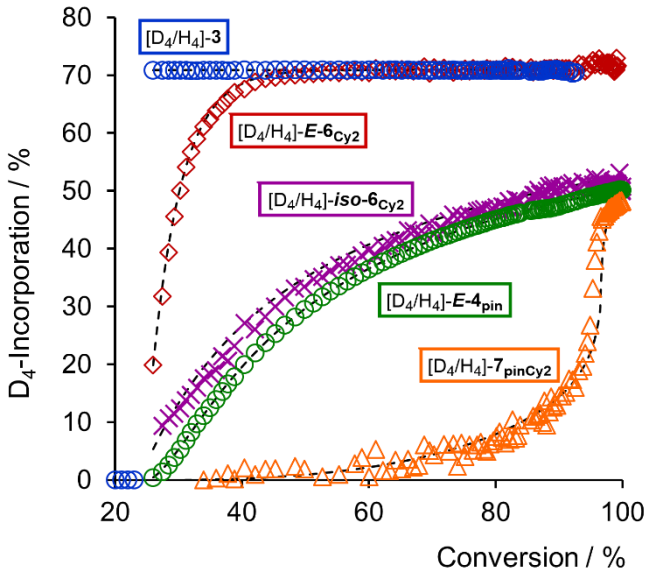


**Figure 2.7** – Entrainment of [$D_4$]-**3** into [$H_4$] catalytic cycle. Experimental data for [$D_4$]-Incorporation (%) plotted as a function of net conversion of [$D_4$/$H_4$]-**3** + [$D_4$/$H_4$]-$\boldsymbol{E}$-$\mathbf{6}_{\mathbf{Cy2}}$ into [$D_4$/$H_4$]-$\boldsymbol{E}$-$\mathbf{4}_{\mathbf{pin}}$, [$D_4$/$H_4$]-$\boldsymbol{iso}$-$\mathbf{6}_{\mathbf{Cy2}}$ and [$D_4$/$H_4$]-$\mathbf{7}_{\mathbf{pinCy2}}$ (%). Kinetic simulated data of $D_4$ incorporation showed as dashed black lines.

## 2.4.5 Boron-catalysed Hydroboration and Transborylation

Slow hydroboration at room temperature occurs without $HBCy_2$ when DMSB is present in the reaction mixture. Following the same mechanism, both species can perform a concerted *syn* addition of B and H across the triple bond, with the boron adding to the less substituted carbon, the difference relies on the intrinsic properties of $HBCy_2$ being a disubstituted borane with two bulky alkyl groups which gives the later a unique regioselectivity that DMSB does not possess.

A reaction without a source of borane (either $HBCy_2$ or DMSB) to catalyse the alkyne hydroboration with HBpin does not proceed at room temperature. In order to probe the catalyst initially adds into the triple bond, being the hydride source, and a real transborylation occurs subsequently furnishing the final product, two experiments were carried out using isotopically labelled reagents ($DBCy_2$ or $H^{10}Bpin$) and a sacrificial volatile alkyne as trapping agent (1-pentyne), thus effectively achieving a single turnover under genuine multi-turnover conditions.

As shown in Scheme 2.30, a stoichiometric reaction between alkyne **3** and $HBCy_2$ was set up and allowed to react to completion. At this point, 1-pentyne was added in excess followed by isotopically labelled $H^{10}Bpin$. The use of an alkyne (1-pentyne) in large quantities ensures the trapping of any unreacted catalyst before the addition of the hydroborating agent, this minimises the attack on the product thus preventing the formation of the double addition side-product. Additionally, an unhindered linear alkyne theoretically reacts faster than **3**, therefore, capturing newly released catalyst from reaction turning over ensuring the isolated product comes effectively from a single turnover of the catalytic cycle. A control reaction was also carried out where non-labelled reagents were used instead.

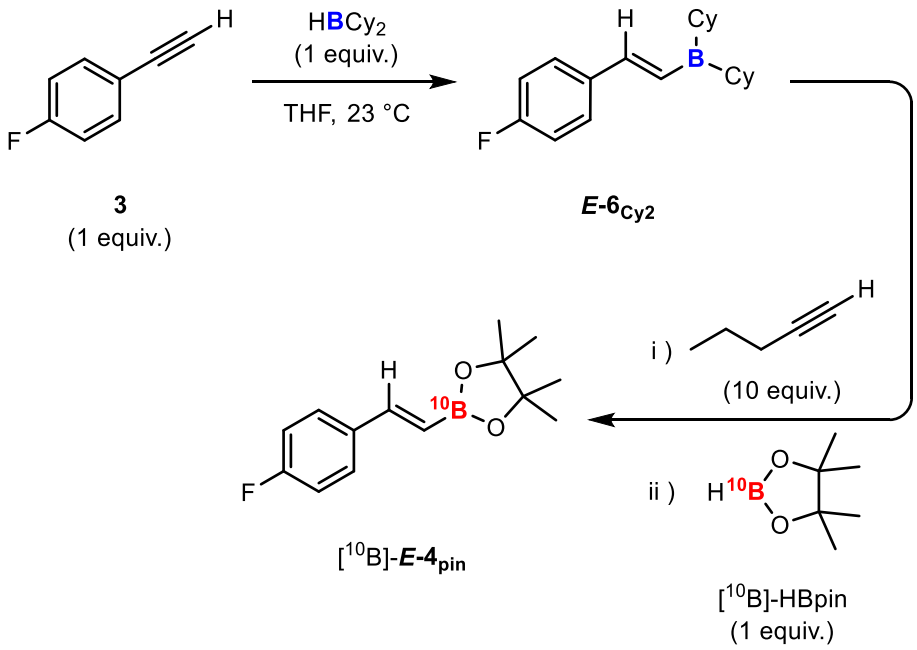


**Scheme 2.30** – Single turnover experiment to probe transborylation. Conditions: [**3**]$_0$ = 0.19 M, [HBCy$_2$] = 0.19 M, [1-pentyne] = 1.90 M, [H$^{10}$Bpin] = 0.20 M in THF at 23 °C.

Incorporation of $^{10}$B in the product was determined and compared against unlabelled product **3** using $^{11}$B NMR and $^{10}$B NMR spectroscopy. Analysis comprised qualitatively comparison of the ratios of a natural abundance boron containing compound ($^{11}$B/$^{10}$B, 4:1) against the labelled and unlabelled products. 4-Fluorophenyltrifluoroborate was used as reference for this purpose. Reaction with labelled H$^{10}$Bpin displayed almost quantitative $^{10}$B incorporation in the product as reflected on the high intensity signal present in the $^{10}$B NMR spectrum and a negligible peak when analysed by $^{11}$B NMR (Figure 2.8 a).

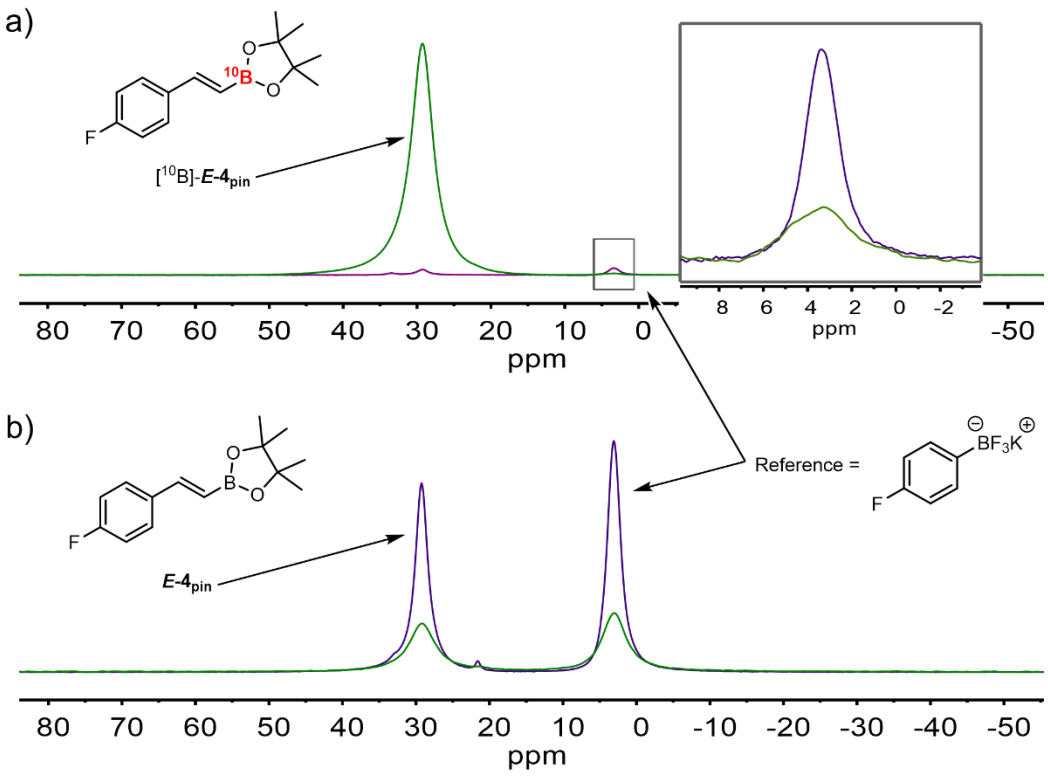


**Figure 2.8** – Superimposed $^{11}B$ NMR (purple) and $^{10}B$ NMR (green) spectra showing $^{11}B/^{10}B$ ratio of 4:1 present in the reference compound used for comaprison; **a)** Isolated labelled product [$^{10}B$]-***E*-4$_{pin}$** showing > 98% of $^{10}B$ incorporation; **b)** Isolated product ***E*-4$_{pin}$** from control reaction displaying typical natural abundance $^{11}B/^{10}B$ isotope ratio of 4:1.

In contrast, control reaction with unlabelled HBpin furnished product ***E*-4$_{pin}$** maintaining the natural abundance $^{11}B/^{10}B$ isotope ratio of 4:1 (Figure 2.8 b). In addition to NMR spectroscopy, electron ionization mass spectrometry was used to corroborate incorporation of $^{10}B$ in the product (see Appendix for details and EI-MS spectra).

Furthermore, [$^{10}B$]-***E*-4$_{pin}$** was analysed by HRMS (EI$^+$) where $C_{14}H_{18}{}^{10}BFO_2{}^+$ $[M]^+$ found was: 247.14250 m/z, requires: 247.14147 m/z (+1.03 ppm). These results prove the operating mechanism from which the product is obtained is an actual transborylation where the $sp^2$ carbon migrates from boron to boron to produce the desired product.

Similarly, a stoichiometric reaction between alkyne **3** and labelled catalyst $DBCy_2$ was set up and allowed to react to completion as depicted on Scheme 2.31. At this point, 1-pentyne was added in excess followed by HBpin. Alkyne (1-pentyne) was used in the same way guaranteeing the isolated product comes effectively from a single turnover of the catalytic cycle. A control reaction was again carried out where non-labelled reagents were used instead.

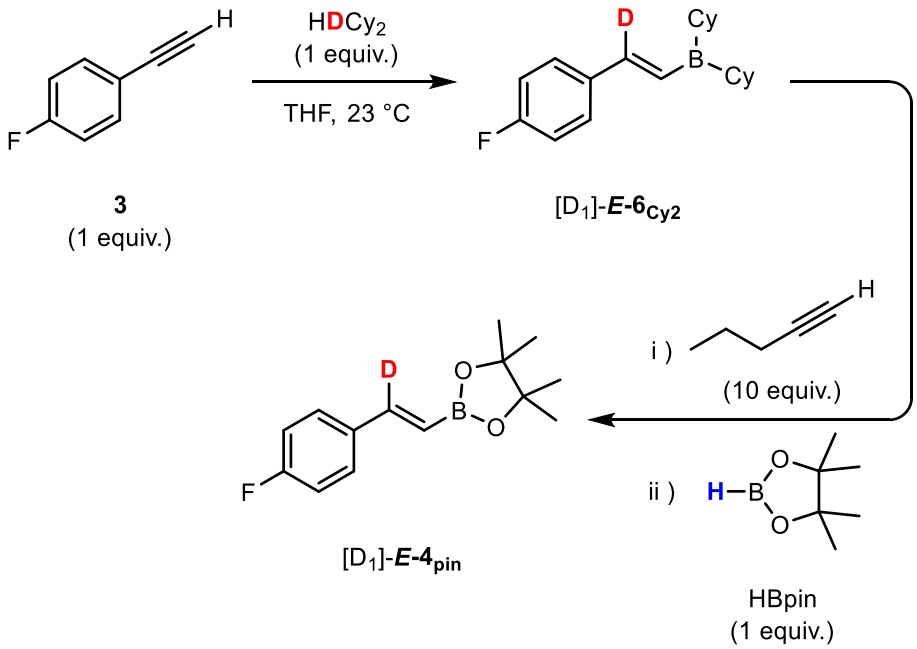


**Scheme 2.31** – Single turnover experiment to probe hydride source. Conditions: $[3]_0$ = 0.18 M, $[DBCy_2]$ = 0.18 M, [1-pentyne] = 1.90 M, [HBpin] = 0.20 M in THF at 23 °C.

Analysis and comparison of $^1H$ NMR spectra of both isolated products (from labelled and unlabelled reactions, Figure 2.9) revealed incorporation of deuterium in the product only when $DBCy_2$ was used. As shown in Figure 2.9 a, the peak corresponding to alkenyl proton $H_a$ is absent due to *syn*-addition of D−B from the catalyst into the triple bond; the recently incorporated deuterium remained in the final product after transborylation with HBpin has occurred. Furthermore, corroborating the incorporation of $^2D$ in the product was the change in the signal arising from proton $H_b$, from a doublet to a small triplet with a low coupling constant (2.3 Hz) as expected from $^1H$–$^2D$ coupling. It is worth mentioning the non-

complete deuterated product obtained, seen from the residual doublet signal, was due to incomplete deuterated THF [$D_3$]-borane complex used for the synthesis of $DBCy_2$ (see Appendix for details on experiment).

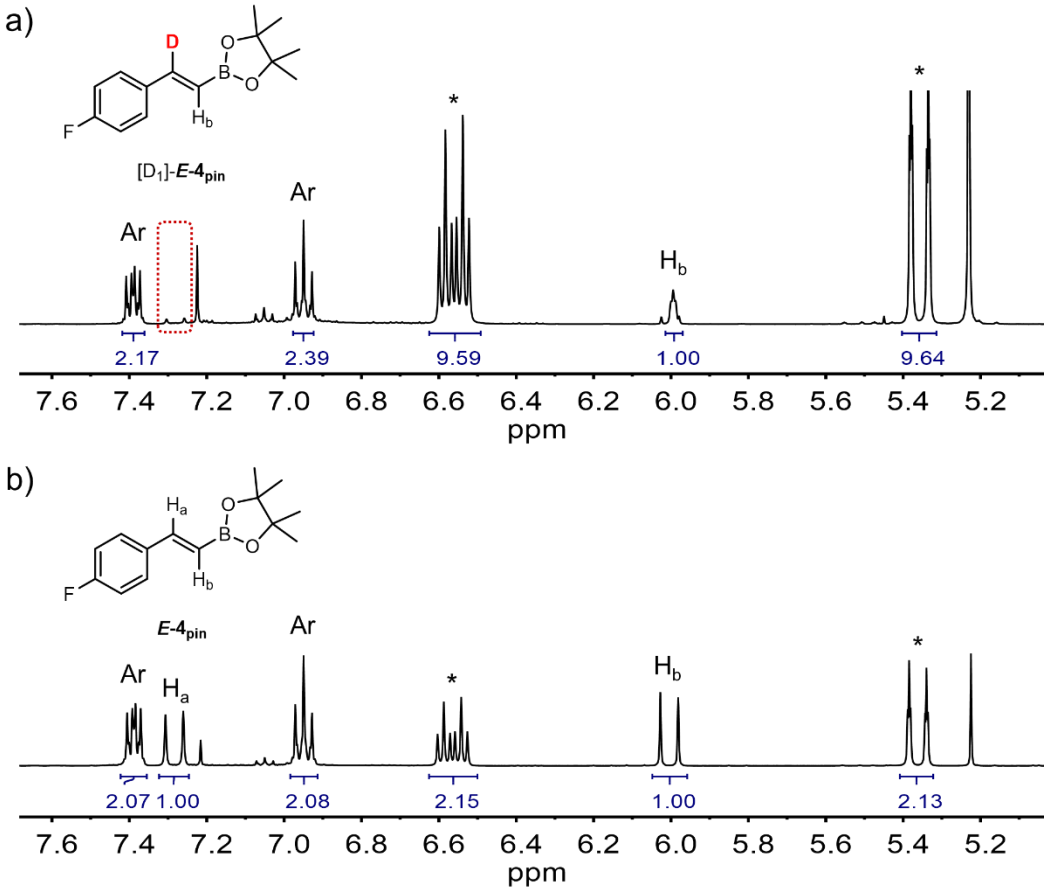


**Figure 2.9** – $^1$H NMR spectra; **a)** Isolated labelled product [$D_1$]-***E*-4$_{pin}$** highlighting the missing signal from deuterium incorporation; **b)** Isolated product ***E*-4$_{pin}$** from control reaction displaying both alkenyl protons and their respective couplings. Remaining 1-pentyne peaks (*) also shown.

Besides NMR spectroscopy, [$D_1$]-***E*-4$_{pin}$** was analysed by HRMS ($EI^+$) where $C_{14}H_{17}DBFO_2^+$ $[M]^+$ found was: 249.14412 m/z, requires: 249.14412 m/z (+0.01 ppm). The obtained results corroborate the productive catalytic cycle where $HBCy_2$ serves both as a hydride source and as a genuine catalyst for the hydroboration of terminal alkynes with pinacolborane.

### 2.4.6 Kinetic Model for Products

Based on the kinetic profile previously obtained and when the species appeared in the course of the reaction, multi-step temporal concentration data was simulated using the model shown in Scheme 2.32 and fitted to experimental data.

A key step that needed to be included was the incorporation of the catalyst into solution as it initially consists of a mostly-insoluble aggregated species (possibly a dimer). Once it starts to quickly react with **3**, the aggregated species breaks apart and goes into solution as the reaction proceeds forward, creating a homogeneous solution once it has been added into the triple bond forming the intermediate ***E*-6$_{Cy2}$** and iso-intermediate ***iso*-6$_{Cy2}$**, both soluble species. While ***iso*-6$_{Cy2}$** is a dead end in the catalytic cycle, being an unreactive species, ***E*-6$_{Cy2}$** turns over to furnish product ***E*-4$_{pin}$** regenerating $HBCy_2$ back into the catalytic cycle.

Another pathway that would suppose a dead end for the catalyst, is the competing hydroboration of ***E*-6$_{Cy2}$** by the catalyst furnishing a diborylated product where both boron atoms come from $HBCy_2$ generating ***E*-6$_{(Cy2)2}$**. This process was found to be negligible as ***E*-6$_{(Cy2)2}$** was not detected under the reaction conditions.

After a transborylation step, where the alkenyl carbon transfers from boron to boron (B−C−B), and once **3** has been totally consumed, $HBCy_2$ then attacks the double bond of the product generating the double addition side-product **7$_{pinCy2}$** which remains in solution sequestering all remaining catalyst.

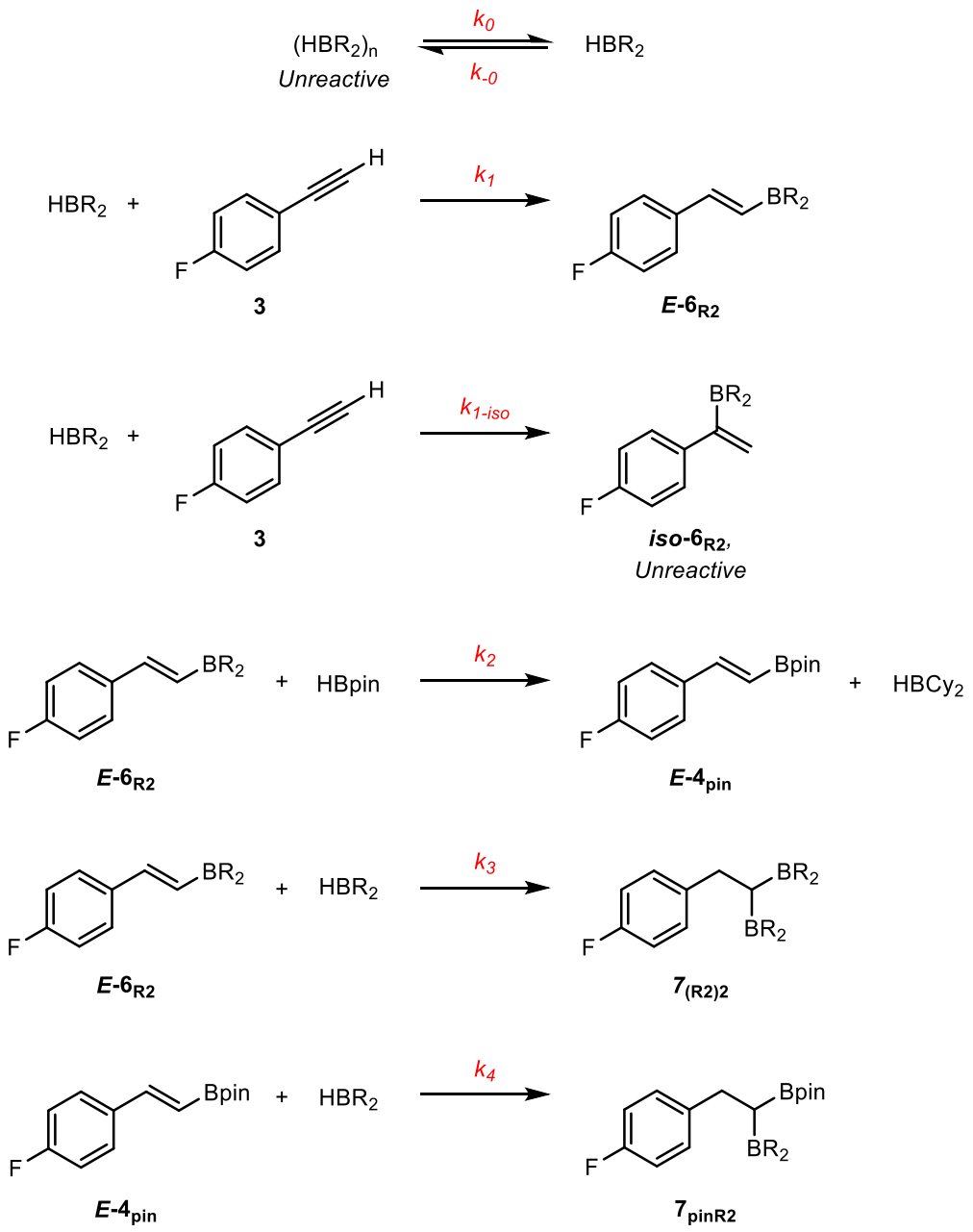


**Scheme 2.32** – Model for boron-catalysed hydroboration of 4-fluorophenylacetylene.

The simulated model was optimised to achieve the best fitting to the experimental data set as shown in Figure 2.10. An exceptional good fitting was observed including the intricate changes in the species present in low concentrations, as is the case of the intermediate and side-products. From this, rate constants were obtained using a 95% confidence integral (Table 2.2).

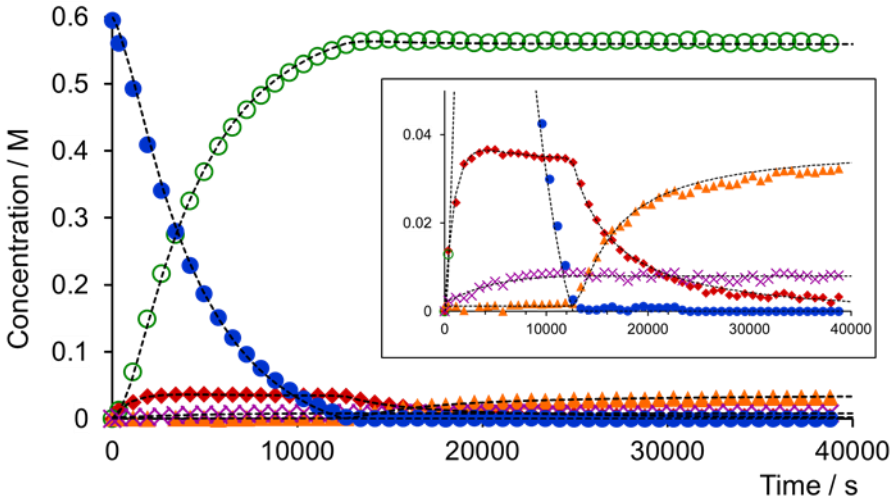


**Figure 2.10** – Simulated model fitted to experimental temporal concentration profile for hydroboration of **3** by $HBCy_2$ monitored by $^{19}F$ NMR. Expansion window shows an amplified view of the intermediate and side-products precise fitting (blue circles: 3, outlined green circles: ***E*-4$_{pin}$**, red diamonds: ***E*-6$_{Cy2}$**, purple crosses: ***iso*-6$_{Cy2}$**, orange triangles: **7$_{pinCy2}$**, black dashed lines: simulated data according to the proposed model).

| Rate | Value | Units |
|---|---|---|
| $k_0$ | $1 \times 10^{-3}$ | $s^{-1}$ |
| $k_1$ | $\geq 3$ | $mol^{-1}\ dm^3\ s^{-1}$ |
| $k_{1\text{-}iso}$ | $k_1 / 89$ | $mol^{-1}\ dm^3\ s^{-1}$ |
| $k_2$ | $6.6 \times 10^{-3}$ | $mol^{-1}\ dm^3\ s^{-1}$ |
| $k_3$ | $\geq k_1 / 2 \times 10^{-3}$ | $mol^{-1}\ dm^3\ s^{-1}$ |
| $k_4$ | $k_1 / 2 \times 10^{-3}$ | $mol^{-1}\ dm^3\ s^{-1}$ |

**Table 2.2** – Rate constants used for the modelling of dicyclohexylborane-catalysed hydroboration of 4-fluorophenylacetylene.

## 2.4.7 Mechanistic Proposal

Taking into account the simplistic catalytic cycle proposed by Hoshi[38], the number of species observed by $^{19}F$ NMR spectroscopy and the analysis of the kinetic profile obtained from the hydroboration of alkyne **3** and its simulation according to the

model displayed above, a thorough catalytic cycle was proposed. This reaction mechanism is further supported by the computed minimum energy pathway (Figure **2.11**).

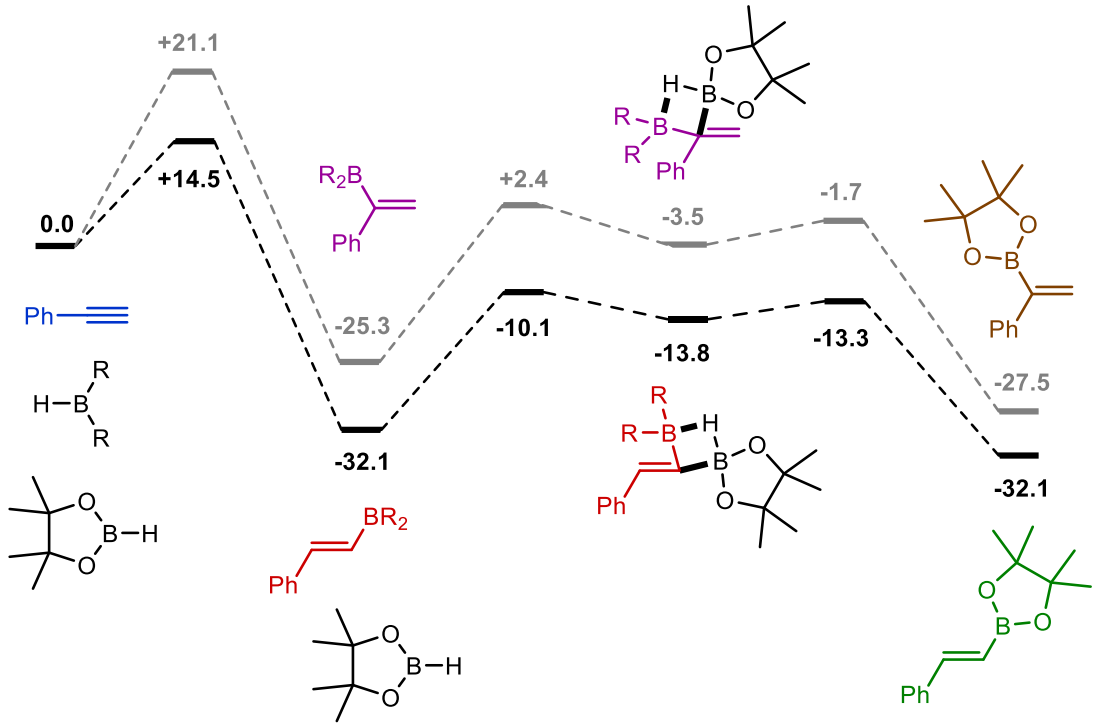


**Figure 2.11** – Computed minimum-energy pathways for transitions states and intermediates in both plausible pathways of the dicyclohexylborane-catalysed hydroboration of phenylacetylene. Free energies (ΔG) are expressed in kcal $mol^{-1}$.

The first step on the cycle commences with the catalyst as initially it sits in its aggregated form then it solubilises as it reacts with the terminal alkyne **3**, from this point onwards, the fate of $HBCy_2$ resides in the regioselectivity of addition into the alkyne, giving way to two possible pathways. A productive pathway that will ultimately generate the desired product ***E*-4$_{pin}$**, and an inhibition pathway that produces an inactive species that sequesters to a certain proportion ($k_{1\text{-}iso}/k_1$) the available catalyst every cycle (Scheme 2.33).

The catalyst $HBCy_2$ hydroborates the alkyne **3** to give (*E*)-isomer intermediate ***E*-6$_{Cy2}$** displaying the right regioselectivity so the attack by HBpin can take place next. This regioselectivity provides an adequate spatial orientation for the

transborylation to occur through a four-membered ring as showed in Scheme **2.33** *(a). Accordingly, the alkenyl group of the intermediate is replaced with the hydride of HBpin furnishing product ***E*-4$_{pin}$** along with regeneration of $HBCy_2$, thus completing a single turnover of the catalytic cycle. The replacement proceeds through a quasi-concerted reaction involving an $sp^2$ carbon migration from boron to boron and the concomitant transfer of hydride *via* a transient bridged intermediate. Furthermore, the decrease of π-electron density from an electron-withdrawing group retards the replacement, this expected effect was observed when the substituent on the aromatic ring (F) was changed with a more electron-withdrawing group ($CF_3$) that made the reaction 0.6 times slower.

Contrastingly, the inhibition pathway occurs when $HBCy_2$ hydroborates the alkyne in Markovnikov fashion to give a regioisomeric product ***iso*-6$_{Cy2}$** in small amounts, this results in an inadequate structural configuration where the attack by HBpin is sterically hindered by the bulkier aromatic ring and HBpin itself, as showed in Scheme 2.33 *(b). Therefore, the iso-intermediate ***iso*-6$_{Cy2}$** acts as a dead end of the catalytic cycle secluding and preventing the regeneration of $HBCy_2$. It is important to realise this path is unfavoured as the direction of addition is governed by polarization of the B−H bond and by combination of steric and electronic effects of substituents at the multiple bond, this is reflected by the $k_1/k_{1\text{-iso}}$ ratio being approximately 100; in other words, just 1 for every 100 times the substrate enters the catalytic cycle, it will be deviated into the non-productive pathway.

Once all the substrate has been consumed, the cycle goes into a final degradative stage, where the catalyst attacks the double bond in the product to form a double addition side-product **7$_{pinCy2}$** (Scheme 2.33). This process is present during the entire course of the catalytic cycle as an almost null background side reaction; the relative affinity of $HBCy_2$ towards the triple bond over the double bond can be quantitively calculated from the appropriate rate constants, being $k_1/k_4$ ratio approximately 120,000. This high value indicates why the significant concentrations of **7$_{pinCy2}$** appear only at the end of the reaction.

The reaction kinetics were found to be pseudo-zero order in alkyne. Thus, the rate is independent of the concentration of the substrate, and first order in both catalyst and hydroborating agent, meaning the rate of reaction is directly proportional to the concentration of both $HBCy_2$ and HBpin.

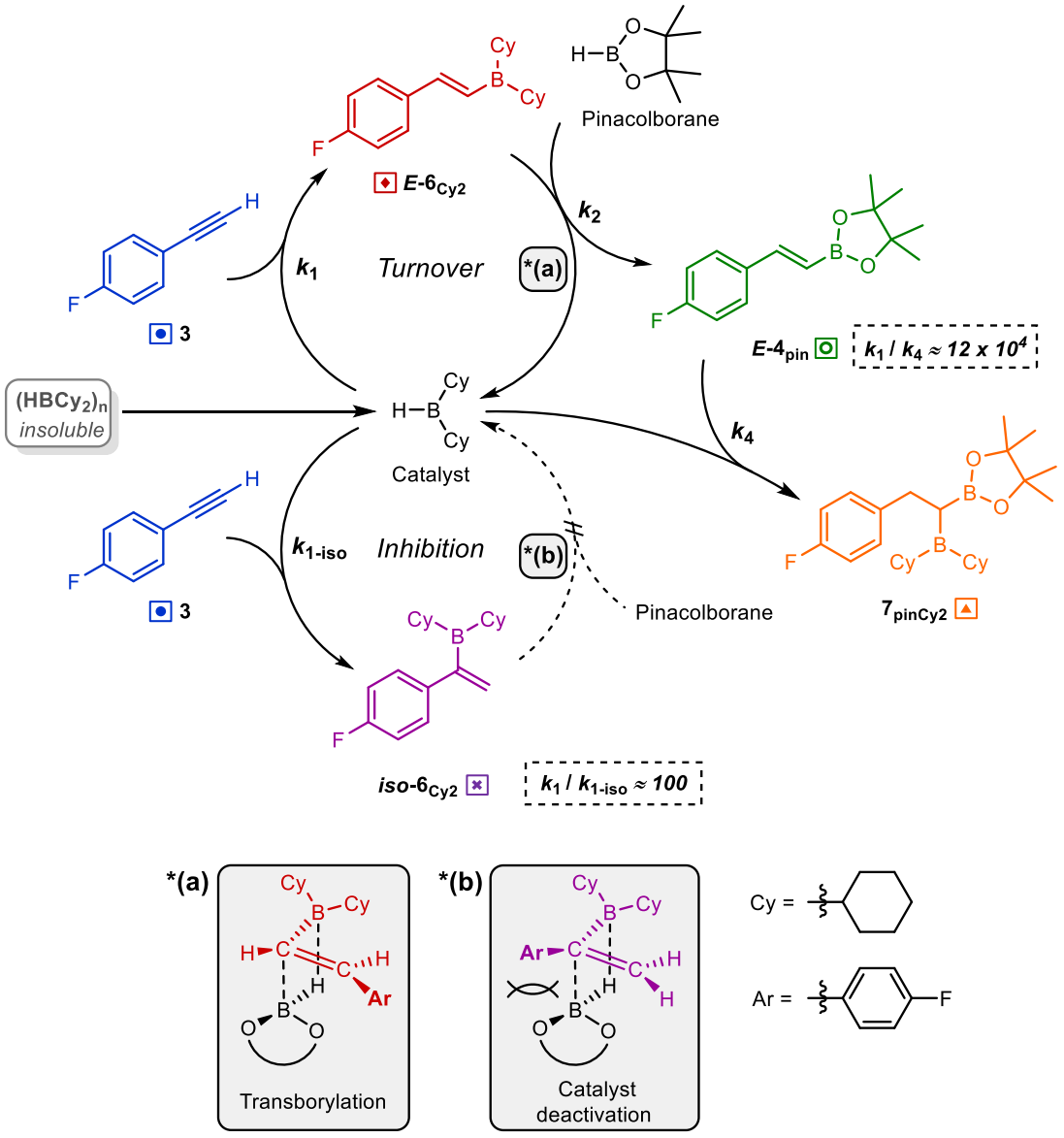


**Scheme 2.33** – Proposed catalytic cycle for dicyclohexylborane-catalysed hydroboration of 4-fluorophenylacetylene.

Stephan and co-workers reported a catalytic hydroboration of alkynes initiated by Piers' borane, $HB(C_6F_5)_2$. The published work reports the borane acting as a pre-catalyst generating dissymmetrically *gem*-diborylated species which is the

active catalyst.[112] This species is analogous to the double addition side-product, and while it is discussed how this species can catalyse the alkyne hydroboration *via* retro-hydroboration, no evidence of loss of $HB(C_5F_5)_2$ from the *gem*-diborylated species was presented. This retro-hydroboration proposal diverges from the results presented in this work, where it is showed the inability of the double addition side-product to undergo a backward reaction.

An alternative mechanistic proposal from Stephan and co-workers involves the *gem*-diborylated species, or its analogues, as a Lewis acid catalyst which activates the alkyne for hydroboration with HBpin.[112] The work by Stephan focuses on how an electrophilic borane can activate alkynes and a mechanistic proposal for this catalytic cycle, but not on the actual hydroboration and subsequent transborylation discussed in depth in this thesis.

### 2.4.7.1 Hydroboration of 4-Fluorophenylacetylene with Pinacolborane Catalysed by 9-Borabicyclo[3.3.1]nonane

A related secondary borane, 9-BBN, was used as an alternative to the air-sensitive $HBCy_2$, as the former is commercially available as a readily-handled solution in THF. An analogous reaction using 9-BBN to catalyse the hydroboration of 4-Fluorophenylacetylene **3** with HBpin was carried out and monitored by $^{19}F$ NMR spectroscopy as shown in Scheme 2.34.

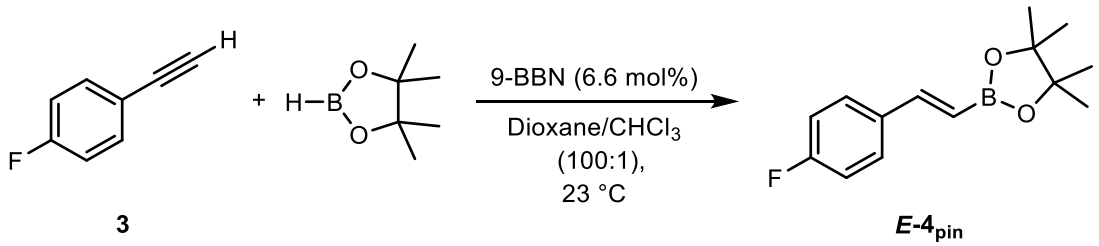


**3** **E-4pin**

**Scheme 2.34** – Reaction conditions used to investigate the kinetic profile of 9-BBN-catalysed alkyne hydroboration; [**3**]$_0$ = 0.6 M, [HBpin] = 0.6 M, [9-BBN] = 0.06 M and [1-fluoronaphthalene] = 0.256 M (IS).

The reaction reached completion within 5 h when carried out at 0.6 M in dioxane/$CHCl_3$ (100:1) at 23 °C with 6.6 mol% catalyst loading (Figure 2.12).

Temporal concentrations were calculated relative to the 1-fluoronaphthalene internal standard (IS) signal in the $^{19}F$ NMR spectra. Analysis of the reaction revealed a similar but not identical set of intermediates to those found for $HBCy_2$. Reaction of **3** with 9-BBN generated intermediate ***E*-6$_{BBN}$** (comparable to ***E*-6$_{Cy2}$**), and the double hydroboration product **7$_{(BBN)2}$**, which was also detected during the catalytic turnover.

Since 9-BBN is predominantly dimeric in solution (high association constant), there was a much lower pseudo-steady state concentration of intermediate ***E*-6$_{BBN}$** than is observed for ***E*-6$_{Cy2}$**. However, using higher catalyst loadings result in decreased selectivity for product ***E*-4$_{pin}$** over **7$_{(BBN)2}$**. The anti-Markovnikov selectivity in hydroboration of alkyne **3** with 9-BBN is substantially higher than that with $HBCy_2$. This is reflected in the absence of Markovnikov addition to **3**, thus inhibition *via* this pathway is negligible.

The rate of transborylation of ***E*-6$_{BBN}$** by HBpin is faster that for ***E*-6$_{Cy2}$**, leading to efficient turnover with 9-BBN even though the important dimerisation. Contrastingly, the rate of hydroboration of the product ***E*-4$_{pin}$** by 9-BBN is not significantly lower than the hydroboration of **3**, causing the irreversible generation of the double addition side-product **7$_{pinBBN}$** throughout the reaction. As a consequence of this, the maximum yield of ***E*-4$_{pin}$** gets significantly reduced under these conditions.

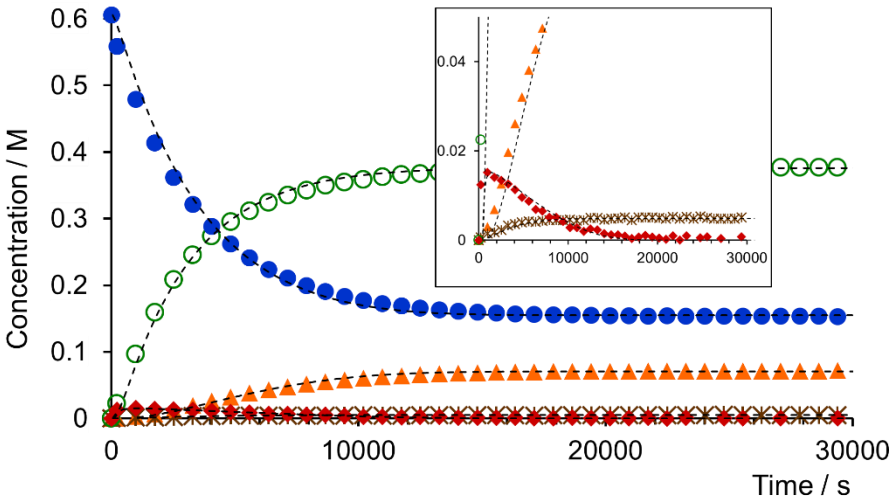


**Figure 2.12** – Simulated model fitted to experimental temporal concentration profile for hydroboration of **3** by 9-BBN monitored by $^{19}F$ NMR. Expansion window shows an amplified view of the intermediate and side-product precise fitting (blue circles: 3, outlined green circles: ***E*-4$_{pin}$**, red diamonds: ***E*-6$_{BBN}$**, purple crosses: **7$_{(BBN)2}$**, orange triangles: **7$_{pinBBN}$**, black dashed lines: simulated data according to the proposed model).

| Rate | Value | Units |
|---|---|---|
| $k_0$ | $1 \times 10^3$ | $s^{-1}$ |
| $k_{-0}$ | 1.7 | $mol^{-1}\ dm^3\ s^{-1}$ |
| $k_1$ | 1.6 | $mol^{-1}\ dm^3\ s^{-1}$ |
| $k_{1\text{-}iso}$ | $> k_2 / 400$ | $mol^{-1}\ dm^3\ s^{-1}$ |
| $k_2$ | $5.6 \times 10^{-1}$ | $mol^{-1}\ dm^3\ s^{-1}$ |
| $k_3$ | $k_1 / 2.9$ | $mol^{-1}\ dm^3\ s^{-1}$ |
| $k_4$ | $k_1 / 4.6$ | $mol^{-1}\ dm^3\ s^{-1}$ |

**Table 2.3** – Rate constants used for the modelling of 9-BBN-catalysed hydroboration of 4-fluorophenylacetylene.

# Chapter 3 Conclusions and Future Work

A mechanism has been proposed for the alcoholysis of tris-(*o*-tolyl)phosphine borane (Figure 3.1). After a slow initial nucleophilic attack, the phosphine ligand gets displaced causing a gradual and reproducible consumption of the phosphine borane complex. The product of this first attack, $H_2BOEt$, results in the exposure of the vacant *p*-orbital on boron, making it susceptible to a quick attack by a Lewis base (EtOH) preventing its accumulation. A third consecutive attack by EtOH produces an accumulation of $HB(OEt)_2$, this due to the low-favoured four-membered ring configuration the intermediate has to take to be able to achieve its last hydride elimination, after from which, $B(OEt)_3$ is obtained.

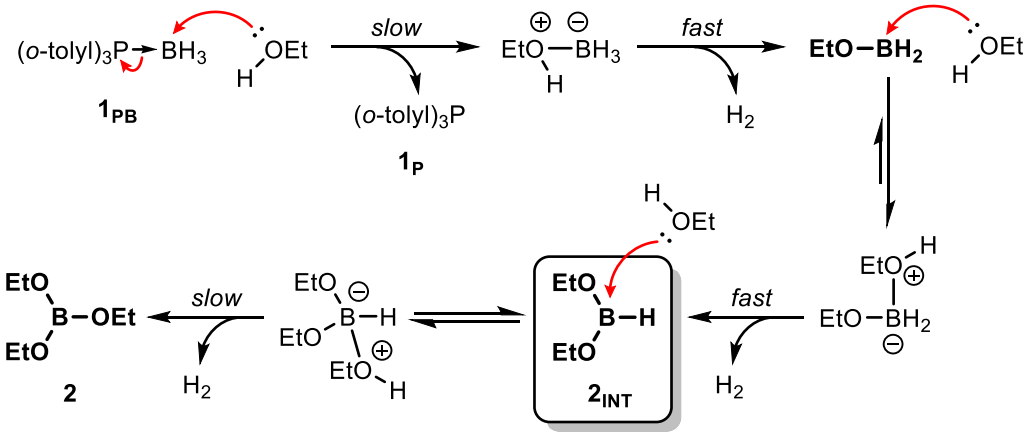


**Figure 3.1** – Proposed mechanism for ethanolysis of (*o*-tolyl)$_3$P·BH$_3$ (**1$_{PB}$**) in ethanol (5 M in toluene) at 30 °C. Intermediate highlighted inside the shadowed box (**2$_{INT}$**).

A system was developed to obtain and stabilise the dialkoxyborane almost quantitatively. The system is highly dependent on the nature of the solvents used, where a fine balance of mixture of them are needed to create a synergetic effect on dialkoxyborane stabilisation. The desired intermediate was obtained *in situ* by using a dioxane/$CHCl_3$ (100:1) solvent system with a relatively high concentration of the solvolytic agent. The cleanest and fastest reaction, that produced the highest concentration of the desired dialkoxyborane, was obtained when dimethyl sulfide borane complex was used as source of borane. The inconsistent generation of an ionic active species is likely to be causing the irreproducibility in the kinetic

stability of the intermediate $HB(OEt)_2$, however, it can be mitigated by selecting an appropriate solvent mixture.

A one-pot alkyne hydroboration reaction, where both the hydroborating agent (HBpin) and catalyst ($HBCy_2$) were synthesised *in situ* from DMSB, was developed (Figure 3.2). Alkenylboronic acid pinacol ester was obtained in good yield and stereoselectivity with reaction times under 24 hours.

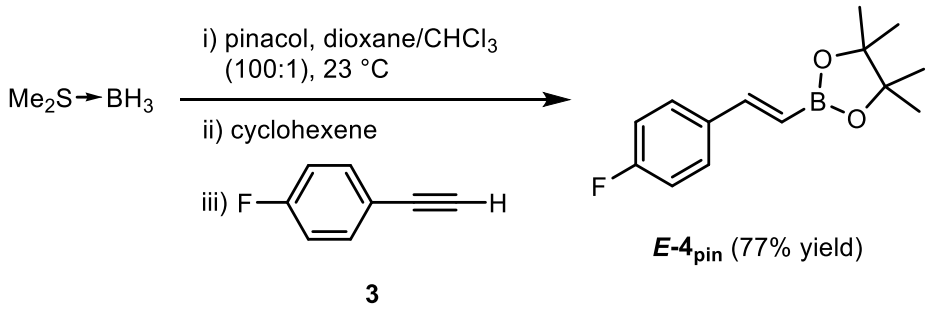


**Figure 3.2** – One-pot synthesis of alkenylboronic acid pinacol ester ***E*-4$_{pin}$**; hydroborating agent (pinacolborane) and catalyst (dicyclohexylborane) synthesised *in situ* from DMSB in dioxane/$CHCl_3$ (100:1) at 23 °C.

The mechanism of $HBCy_2$ catalysed hydroboration of 4-F-phenylacetylene has been investigated by *in situ* NMR spectroscopy and its kinetic profile has been successfully simulated. By performing isotope entrainment, single turnover labelling ($^{10}B$, $^{11}B$ and $^{2}H$) and density functional theory (DFT) calculations, the proposed mechanism has been verified.

$HBCy_2$ hydroborates 4-F-phenylacetylene giving rise to an intermediate that has been identified as (*E*)-1-alkenyldicyclohexylborane. This catalytically active species is generated by irreversible anti-Markovnikov addition whose alkenyl group is then replaced with the hydride of HBpin to furnish the final product. This last step is irreversible and turnover-rate limiting step that regenerates $HBCy_2$ back into the catalytic cycle *via* B−C−B transfer of the alkenyl group with retention of (*E*)-configuration (Figure 3.3, upper cycle).

A catalyst inhibition pathway caused by a competing and irreversible hydroboration by $HBCy_2$ has also been described. This can occur to the alkyne, in

a Markovnikov fashion, to produce an inactive iso-intermediate species. It can also include $HBCy_2$ addition to the hydroboration product that leads to a double addition side-product (Figure 3.3, lower cycle). These processes are reflected into an optimum catalyst loading to reduce these undesired reactions.

The mechanism of $HBCy_2$ was compared to another popular, commercially-available catalyst, 9-BBN. Where the subtle differences observed in their respective kinetic profiles, resided in the higher anti-Markovnikov selectivity of 9-BBN towards a triple bond, the high association constant for dimerisation and the rate of transborylation. This led to lower yields and higher side-product formation. Lastly, all details explained in this thesis, will aid in the design of new synthetic tools to offer more effective and selective boron-catalysed processes.

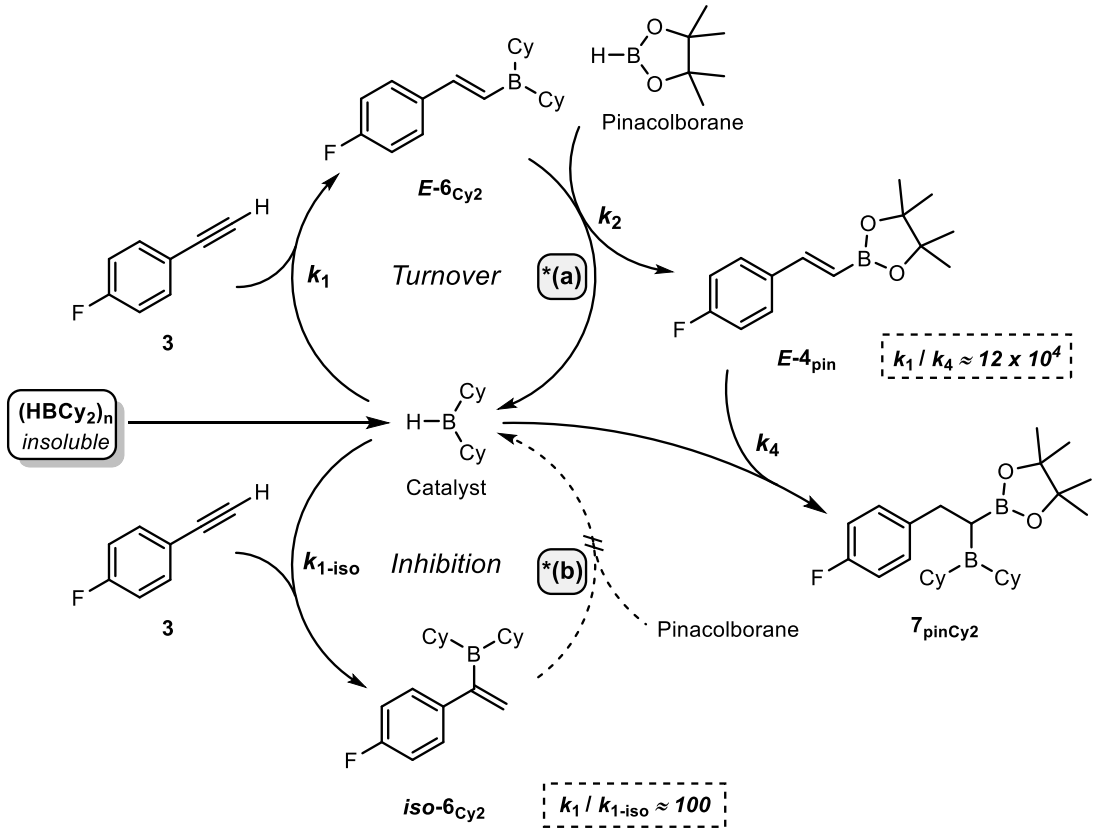


**Figure 3.3** – Proposed catalytic cycle for dicyclohexylborane-catalysed hydroboration of 4-fluorophenylacetylene.

Further work is needed to develop a catalysed alkyne hydroboration with $HB(OEt)_2$ and further ligand exchange to produce alkenylboronates in an easy, inexpensive

and straightforward fashion (Figure 3.4). A systematic computational study of $HBR_2$ and $HB(OR)_2$, allowing testing of the fastest pair of hydroboration/transborylation (or most selective), could provide further insight for the development of this reaction by testing the species identified that way, Additionally, as 9-BBN proved to be ineffective to catalyse the hydroboration reaction in the tested conditions, a wider screening of compatible catalysts (e.g. 1,8-naphthalenediaminatoborane) might offer a suitable option to carry out the desired transformation.

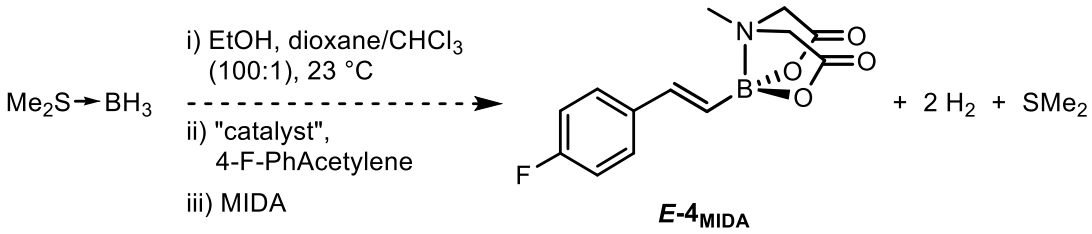


***E*-4$_{MIDA}$**

**Figure 3.4** – Proposed one-pot synthesis route to obtain MIDA boronate ester ***E*-4$_{MIDA}$** after ligand exchange with diethyl vinylboronate.

# Chapter 4 Experimental

## 4.1 General Experimental

### 4.1.1 Techniques

Unless otherwise stated, all reactions were performed in oven-dried glassware under an inter nitrogen atmosphere, using conventional Schlenk-line techniques on a vacuum line attached to a double manifold equipped with an oil pump (0.4 torr). Where required, needles and other glassware were dried in an oven (200 °C) and cooled under vacuum and purged with an inert atmosphere of nitrogen prior to use. All NMR tubes used as reaction vessels were prewashed sequentially with aqua regia, deionised water and acetone to remove any contaminants. The removal of solvents *in vacuo* was achieved using a Buchi rotary evaporator (with a water bath at temperatures up to 40 °C), or at 0.4 torr on a vacuum line at room temperature.

### 4.1.2 Reagents and Solvents

Unless stated otherwise, reagents were purchased from commercial sources (Acros Organics, Alfa Aesar, Fisher Scientific, Fluorochem, Sigma-Aldrich or VWR) and were used without purification. Triethylamine was distilled from $CaH_2$ and stored over 4 Å molecular sieves under nitrogen atmosphere. EtOH was dried over 4 Å molecular sieves in a Straus flask under inert nitrogen atmosphere and stored for future use. 1,4-Dioxane and chloroform were premixed in a 100:1 ratio, dried over 4 Å molecular sieves in a Straus flask under inert nitrogen atmosphere and stored for future use. Other anhydrous organic solvents were obtained by passage through a column of anhydrous alumina using an MBraun SPS-800 system situated in the School of Chemistry, University of Edinburgh. Straus flasks fitted with J. Young valves were used to collect an anhydrous solvent. Distilled water was obtained through a double distillation system. Deuterated solvents for NMR analysis were purchased from Sigma-Aldrich.

### 4.1.3 Chromatography

Analytical thin-layer chromatography was performed on precoated aluminium-backed plates (Silica gel 60 F254; Merck) and visualised using a combination of UV light ($\lambda = 254$ nm) and/or aqueous basic potassium permanganate ($KMnO_4$) solution. Flash column chromatography was performed using Merck Geduran® Si 60 (40-63 μm) silica gel.

### 4.1.4 Analysis

#### 4.1.4.1 NMR Spectroscopy

NMR spectra were recorded at 300 K (27 °C) unless stated otherwise; $^{1}H$, $^{13}C$ and $^{19}F$ spectra were recorded at 400 MHz, 101 MHz and 377 MHz respectively, using a Bruker Ascend spectrometer (400 MHz) with nitrogen cryoprobes. $^{1}H$ and $^{13}C\{^{1}H\}$ NMR spectra were referenced to TMS contained in $CDCl_3$. For $^{19}F$ NMR spectra used in characterization of compounds, a 30° pulse angle was employed with an acquisition time of 1.5 s and relaxation delay of 6 s. $^{11}B$ and $^{19}F$ NMR spectra recorded in $CDCl_3$ are both reported in ppm relative to $BF_3 \cdot OEt_2$ and $^{13}P$ NMR relative to 85% $H_3PO_4$ as an external standard. Coupling constants, *J*, are reported in Hertz (Hz), were calculated using MestReNova 9 or 10 to the nearest 0.1 Hz. Where reported, the phosphorous-boron coupling constants for phosphine boranes complexes were obtained from $^{11}B$ spectra. In $^{11}B$ spectra, the coupling constants were quoted to the nearest 1 Hz. The following abbreviations (and their combinations) are used to label the multiplicities: app (apparent), br (broad), s (singlet), d (doublet), t (triplet), q (quartet), p (pentent), sext (sextet), sept (septet) and m (multiplet). NMR tubes used to record spectra were made from borosilicate glass.

$^{11}B$ spectra contained large background signals. These were removed by applying a backward linear prediction function (MestReNova - Toeplitz method, 0 to 16, 32k basis points and 24 coefficients). $^{11}B$ baselines were corrected carefully to

ensure integrations were not affected (Whittaker smoother function, typically 40-80 Hz filter).

#### 4.1.4.2 Mass Spectrometry

Electron impact (EI+) spectra were recorded on a ThermoElectron MAT 900 mass spectrometer using a double focusing sector field mass analyser and HRMS was carried out using a Finnigan MAT 900 XLP high-resolution mass spectrometer, all performed by the Mass Spectrometry department at the School of Chemistry, University of Edinburgh. Data are reported in the form of m/z.

#### 4.1.4.3 Melting Points

Melting points (mp) were determined on a Griffin capillary apparatus in capillary melting point tubes and are uncorrected.

#### 4.1.4.4 Computational Studies

DFT calculations of dicyclohexylborane-catalysed hydroboration of phenylacetylene were performed using M06-2X/6-31+G* level of theory with solvation using a polarised continuum model (PCM) for dioxane. These studies were performed by Dr Andrew Leach (John Moores University) and were used to support various aspects of the experimental data presented in this work. All calculations were implemented in Gaussian 09.[169]

Kinetic multi-step simulations were performed on DynoChem 5.

## 4.2 Reaction Monitoring: Chapter 1

### 4.2.1 Borane Complexes Alcoholysis

The chosen borane complex was added to an NMR tube and dissolved with the solvent or mixture of solvents of choice (300 µL) followed by a pre-made solution of the chosen alcohol in the same solvent system (300 µL) to give a final borane concentration of 0.03 M. The NMR tube was closed and shaken thoroughly, then

it was loaded into a preheated NMR spectrometer at the selected temperature. The NMR probe was previously tuned ($^{11}B$) without a deuterium lock by using an equivalent mock sample of the borane complex in the same solvent system. The kinetic experiment was then initiated with the time between the alcohol addition and the first spectrum being recorded measured using a stopwatch. $^{11}B\{^{1}H\}$ NMR spectra were recorded at regular intervals without ejecting the sample between experiments.

*Note*: when an additional reagent needed to be added during the course of the reaction, the NMR tube was taken out from the spectrometer between data acquisitions, such reagent added and mixed into solution and the NMR tube was then placed back into the spectrometer to continue monitoring the reaction.

#### 4.2.1.1 Bubble Surface Effects − Modification

A modified version of procedure 4.2.1 was utilised to probe bubble surface effects on the phosphine borane complex alcoholysis. The deviation from the procedure consisted in the bubbling of either air or nitrogen at the chosen times. To bubble gas into the reaction mixture, an HPLC tubing attached to an elongated Pasteur pipette tip was used, this was fixed to a perforated NMR tube cap, so it reached the bottom of the NMR tube. The bubbling rate was adjusted using a manifold connected to the gas inlet.

### 4.2.2 Phosphine Borane Pinacolysis

Phosphine borane complex along with pinacol were added to an NMR tube and dissolved with dioxane/$CHCl_3$ (600 µL) to give a final concentration of 0.03 M. The NMR tube was closed and shaken thoroughly, then it was loaded into a preheated NMR spectrometer at 296 K. The NMR probe was previously tuned ($^{11}B$) without a deuterium lock by using a mock sample containing phosphine borane complex in the same solvent system. The kinetic experiment was then initiated with the time between the alcohol addition and the first spectrum being recorded measured using a stopwatch. $^{11}B\{^{1}H\}$ NMR spectra were recorded at set intervals.

### 4.2.3 Dimethyl Sulfide Borane Complex Pinacolysis

Pinacol was added to an NMR tube and dissolved with the solvent of choice (600 µL). To initiate the reaction, dimethyl sulfide borane complex was lastly added to give a final concentration of 0.8 M. The NMR tube was closed and shaken thoroughly, then it was loaded into a preheated NMR spectrometer at 303 K. The NMR probe was previously tuned ($^{11}$B) without a deuterium lock by using a mock sample containing DMSB in the same solvent system. The kinetic experiment was then initiated with the time between DMSB addition and the first spectrum being recorded measured using a stopwatch. $^{11}$B{$^{1}$H} NMR spectra were recorded at set intervals without ejecting the sample between experiments. After 3 hours, the reaction was intermittently monitored in automation leaving the sample at room temperature between data acquisitions.

### 4.2.4 Boronic Acid and MIDA Condensation

A small Schlenk flask was charged with boronic acid and 1-fluornaphthalene (IS) and then dissolved with DMF (5 mL) to give a final concentration of I.S. of 0.03 M and 0.05 of the boronic acid. The reaction was set up under an inert $N_2$ atmosphere at 40 °C; a $t$ = 0 sample was taken and analysed to find the true concentration of starting material. MIDA ligand was then added over a flow of $N_2$ to start the reaction. The mixture was stirred (700 rpm) and monitored by taking NMR aliquots and diluting them with DMF. The NMR samples were individually analysed by $^{19}$F NMR spectrometry to construct a multi-point kinetic profile.

## 4.3 Reaction Monitoring: Chapter 2

### 4.3.1 Dicyclohexylborane-Catalysed Alkyne Hydroboration

The catalyst, $HBCy_2$, was synthesised *in situ*; in a Young's tap NMR tube, cyclohexene (10 µL, 0.09 mmol, 0.2 equiv.) was added and diluted with dioxane/$CHCl_3$ (600 µL, 100:1) followed by addition of DMSB (4.3 µL,

0.045 mmol, 0.1 equiv.) under $N_2$ atmosphere; the tube was then closed, shaken to ensure well mixing and left open under $N_2$ atmosphere for 1 h; for these processes, a glass adapter was used where the NMR tube can be placed inside a larger, evacuable chamber to enable the atmosphere to be removed and replaced with the inert atmosphere. After this, HBpin (65 µL, 0.45 mmol, 1 equiv.) was added along with 1-fluoronaphthalene (25 µL, 0.194 mmol) as internal standard, lastly 4-fluorophenylacetylene (51.5 µL, 0.45 mmol, 1 equiv.) was added to start the reaction. The NMR tube was closed and shaken thoroughly, then it was loaded into the NMR spectrometer with a probe temperature of 296 K previously shimmed ($^1$H) and tuned ($^{19}$F) without a deuterium lock by using a mock sample containing (*E*)-2-(4-fluorostyryl)boronic acid pinacol ester and 1-fluoronaphthalene in the same solvent system. The kinetics experiment was then initiated with the time between 4-fluorophenylacetylene addition and the first spectrum being recorded using a stopwatch. $^{19}$F NMR spectra were recorded at different set time intervals without ejecting the sample between experiments.

*General considerations:* 4-fluorophenylacetylene was kept in a tepid water bath prior usage to maintain it in its liquid state (mp 26-27 °C).

### 4.3.2 DMSB-Catalysed Alkyne Hydroboration

A reaction was set up exactly as described in 4.3.1, except that no cyclohexene was added.

### 4.3.3 9BBN-Catalysed Alkyne Hydroboration

A reaction was set up exactly as described in 4.3.1, except 9-BBN was used as catalyst in the specified concentration.

### 4.3.4 Isotopic Entrainment

$HBCy_2$ was synthesised *in situ* in a Young's tap NMR tube, first cyclohexene (10 µL, 0.09 mmol, 0.2 equiv.) was added and diluted with dioxane/$CHCl_3$ (600 µL, 100:1) followed by addition of DMSB (4.3 µL, 0.045 mmol, 0.1 equiv.) under

$N_2$ atmosphere; the tube was then closed, shaken to ensure well mixing and left open under $N_2$ atmosphere for 1 h. After this, HBpin was added (75 µL, 0.517 mmol, 1.15 equiv.) along with 1-fluoronaphthalene (25 µL, 0.194 mmol) as internal standard, lastly [$H_4$]-4-fluorophenylacetylene (25.7 µL, 0.225 mmol, 0.5 equiv.) was added to start the reaction. The NMR tube was closed and shaken thoroughly, then it was loaded into the spectrometer to monitor the reaction by $^{19}$F NMR spectroscopy as mentioned in the representative procedure 4.3.1, after ~1800 s, the NMR tube was removed from the spectrometer and [$D_4$]-4-fluorophenylacetylene (30.7 µL, 0.225 mmol, 0.5 equiv.) was added under $N_2$ atmosphere, the sample was then returned to the spectrometer and the kinetic monitoring resumed.

### 4.3.5 Cross-over Experiment

$HBCy_2$ was synthesised *in situ* in a Young's tap NMR tube, first cyclohexene (10 µL, 0.09 mmol, 0.2 equiv.) was added and diluted with dioxane/$CHCl_3$ (560 µL, 100:1) followed by addition of DMSB (4.3 µL, 0.045 mmol, 0.1 equiv) under $N_2$ atmosphere; the tube was then closed, shaken to ensure well mixing and left open under $N_2$ atmosphere for 1 h. After this, HBpin was added (65 µL, 0.45 mmol, 1 equiv.) along with 1-fluoronaphthalene (25 µL, 0.194 mmol) as internal standard, lastly [$D_4$]-4-fluorophenylacetylene (63.5 µL, 0.45 mmol, 1 equiv.) was added to start the reaction. The NMR tube was closed and shaken thoroughly, then it was loaded into the spectrometer to monitor the reaction by $^{19}$F NMR spectroscopy as mentioned in the representative procedure 4.3.1. Towards the end of the reaction, the NMR tube was removed and additional HBpin (20 µL, 0.095 mmol, 0.2 equiv.) was added to drive the reaction to completion. After full consumption of the substrate, the NMR tube was removed from the spectrometer and [$H_4$]-(*E*)-2-(4-fluorostyryl)boronic acid pinacol ester (55.8 mg, 0.225 mmol, 0.5 equiv.) and freshly prepared $HBCy_2$ (250 µL, 0.112 mmol, 0.25 equiv) in dioxane/$CHCl_3$ (100:1) were added under $N_2$ atmosphere, the sample was then returned to the spectrometer and the kinetic monitoring continued.

## 4.4 Synthetic Procedures

**Tris(*o*-tolyl)phosphine borane $1_{PB}$**

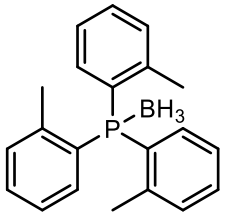


To a $N_2$ purged two-necked round bottom flask was loaded with tris(*o*-tolyl)phosphine (3.0 g, 10 mmol, 1 equiv.) over a flow of nitrogen and dissolved with $CH_2Cl_2$ (25 mL) followed by dropwise addition of DMSB (9.5 mL, 100 mmol, 10 equiv.), the reaction was left to stir at room temperature for 24 h. After this, the solution was quenched by slowly adding sat. aqueous $NH_4Cl$ (50 mL) and left to stir for further 2 h. A significant amount of effervescence was observed during this period, and consequently the vessel was opened to prevent an accumulation of pressure. The reaction mixture was then poured onto water (250 mL) and the aqueous phase was extracted with $CH_2Cl_2$ (3 x 250 mL); the combined organics were washed with sat. aqueous $NaHCO_3$ (250 mL) and dried over $MgSO_4$, filtered and solvent removal *in vacuo*. The residue was filtered through a pre-wetted silica gel plug (eluent: $CH_2Cl_2$) using nitrogen to push the solvent through the column. Evaporation of solvent under vacuum yielded the title compound as a white solid (2.8 g, 88% yield). **$^1$H NMR** (400 MHz, $CDCl_3$) $\delta_H$: 0.95-2.0 (br, 3H), 2.34 (s, 9H), 6.91 (m, 3H), 7.05 (t, *J* 7.4, 3H), 7.24 (m, 3H), 7.33 (t, *J* 7.3, 3H); **$^{13}$C{$^1$H} NMR** (101 MHz, $CDCl_3$) $\delta_C$: 23.12 (d, *J* 3.6), 125.97 (d, *J* 8.8), 127.12 (d, *J* 53.1), 131.34 (d, *J* 2.1), 132.11 (d, *J* 8.9), 133.47 (d, *J* 7.3), 143.96 (d, *J* 10.9); **$^{11}$B NMR** (128 MHz, $CDCl_3$) $\delta_B$: −31.96; **$^{31}$P{$^1$H} NMR** (162 MHz, $CDCl_3$) $\delta_P$: 22.87; mp 149-151 °C.

Data are in accordance with that previously reported.[78]

**(*E*)-2-(4-Fluorostyryl)boronic acid pinacol ester *E*-4$_{pin}$**

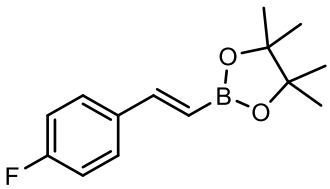

To a $N_2$ purged Schlenk tube, cyclohexene (20.5 µL, 0.2 mmol, 0.1 equiv.) was added and diluted with THF (2 mL, 100:1) followed by dropwise addition of DMSB (9.5 µL, 0.1 mmol, 0.1 equiv.). The reaction was left to stir for 1 h at 0 °C then for further 2 h at rt, then HBpin (290 µL, 2 mmol, 1 equiv.) was added followed by dropwise addition of 4-fluorophenylacetylene (230 µL, 2 mmol, 1 equiv.). After 16 h the crude mixture was diluted with hexane (50 mL) and poured onto water (20 mL), the organic phase was washed with water (3 x 30 mL); the organic fraction was set apart and the combined aqueous fractions were extracted with hexane (1 x 30 mL). The hexane fractions were combined and dried over $MgSO_4$, filtered and solvent removal *in vacuo* (300 mbar) to give the title product as a pale yellow oil that solidified upon cooling at rt (418 mg, 84.3% yield). **$^1$H NMR** (400 MHz, $CDCl_3$) $\delta_H$: 1.23 (s, 12H), 5.99 (d, *J* 18.4, 1H), 6.94 (m, 2H), 7.27 (d, *J* 18.4, 1H), 7.38 (m, 2H); **$^{13}$C{$^1$H} NMR** (101 MHz, $CDCl_3$) $\delta_C$: 24.80, 83.38, 115.55 (d, *J* 21.8), 128.71 (d, *J* 8.3), 133.75 (d, *J* 3.3), 148.16, 163.15 (d, *J* 248.7); **$^{11}$B NMR** (128 MHz, $CDCl_3$) $\delta_B$: 30.13; **$^{19}$F NMR** (377 MHz, $CDCl_3$) $\delta_F$: −112.39; **HRMS (EI$^+$)** $C_{14}H_{18}BFO_2^+$ $[M]^+$ found: 248.13753, requires: 248.13784 (−0.31 ppm).

Data are in accordance with that previously reported.[170]

**[D$_4$]-4-Fluorophenylacetylene [D$_4$]-3**

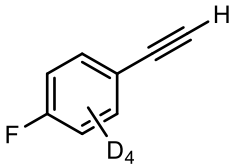

To a $N_2$ purged single-necked round bottom Schlenk flask, first, $PdCl_2(PPh_3)_2$ (291 mg, 0.415 mmol, 0.015 equiv.) and CuI (158 mg, 0.83 mmol, 0.03 equiv.) were added over a flow of nitrogen. THF (3.5 mL), followed by [$D_4$]-1-bromo-4-fluorobenzene (4.88 g, 27.3 mmol, 1 equiv.) and triethylamine (3.47 mL, 24.9 mmol, 0.91 equiv.) were added; the reaction mixture was degassed by three freeze-pump-thaw cycles. Finally, TMS acetylene (3.45 mL, 24.9 mmol, 0.91 equiv.) was added and the stirring solution heated at 70 °C for 16.5 h before

adding additional TMS acetylene (0.5 mL, 3.6 mmol, 0.13 equiv.) and THF (2 mL), the mixture was left to stir for 7 h at 70 °C. Extra TMS acetylene (0.5 mL, 3.6 mmol, 0.13 equiv.) and THF (2 mL) were added a second time, the reaction mixture was left to stir at 70 °C for 17.5 h. The mixture was then poured onto $HCl_{(aq)}$ (0.1 N, 20 mL) and the aqueous phase extracted with diethylether (3 x 30 mL); the combined organics were washed with water (2 x 20 mL), sat. aqueous $NaHCO_3$ (10 mL) and brine (10 mL). The organic layer was dried over $MgSO_4$, filtered through celite and solvent removal *in vacuo*.

The residue containing the TMS protected [$D_4$]-4-fluorophenylacetylene was dissolved in a mixture of MeOH (25 mL) and $K_2CO_3$ (0.87 mmol, 120 mg) and stirred at rt for 3 h. The mixture was poured onto a sat. aqueous $NH_4Cl$ (25 mL) and extracted with diethylether (3 x 25 mL); the combined organics were washed with brine (25 mL), dried over $MgSO_4$ and concentrated *in vacuo* (100 mbar). The crude material was purified by Kugelrohr distillation under reduced pressure (10-1 mbar) at 45 °C to give a clear and colourless oil (902 mg, 84% pure by $^{19}F$ NMR, 26.6% yield). **$^{1}H$ NMR** (400 MHz, $CDCl_3$) $\delta_H$: 2.96; **$^{13}C\{^{1}H\}$ NMR** (101 MHz, $CDCl_3$) $\delta_C$: 76.96, 82.56, 115.31 (td, *J* 25.6, 22.2), 117.99, 133.70 (td, *J* 25.1, 8.5), 162.76 (d, *J* 249.7); **$^{19}F$ NMR** (377 MHz, $CDCl_3$) $\delta_F$: −110.67; **HRMS (EI$^+$)** $C_8H_1D_4F^+$ $[M]^+$ found: 124.06269, requires: 124.06209 (+0.61 ppm).

Data are consistent with that expected based on published data for the same compound without deuterium labelling.[171,172]

**[$^{10}$B]-Triisopropoxyborane**

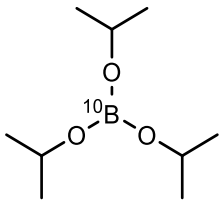


Synthetic procedure was followed as previously reported by a former group member.[173] To a $N_2$ purged two-necked round bottom flask equipped with a condenser, [$^{10}$B]-boric acid (4.88 g, 80 mmol, 1 equiv.) and $CaH_2$ (14.47 g, 93% w/w, 320 mmol, 4 equiv.) were added over a flow of nitrogen. Anhydrous isopropanol (18.4 mL, 240 mmol, 3 equiv.) was added dropwise down the condenser and over a stream of nitrogen. As the reaction is exothermic, additional isopropanol (20 mL,

261 mmol, 3.3 mmol) was required to ensure good stirring as some was evaporated during its addition. After bubbling had ceased, the mixture was heated to 90 °C for 16 h. After cooling to room temperature, volatiles were pumped off *in vacuo* and trapped at −78 °C. The condensate was distilled under reduced pressure: first at 105-100 mbar and 50 °C to remove a fraction richer in isopropanol and lastly at 40-20 mbar and 60 °C to give the title compound as a clear and colourless liquid. Stored over 4 Å molecular sieves under nitrogen atmosphere. **$^{1}$H NMR** (400 MHz, $CDCl_3$) $\delta_H$: 1.05 (d, *J* 6.2, 18H), 4.26 (sept, *J* 6.2, 3H); **$^{13}$C{$^{1}$H} NMR** (101 MHz, $CDCl_3$) $\delta_C$: 24.31, 64.69; **$^{10}$B NMR** (43 MHz, $CDCl_3$) $\delta_B$: 17.50.

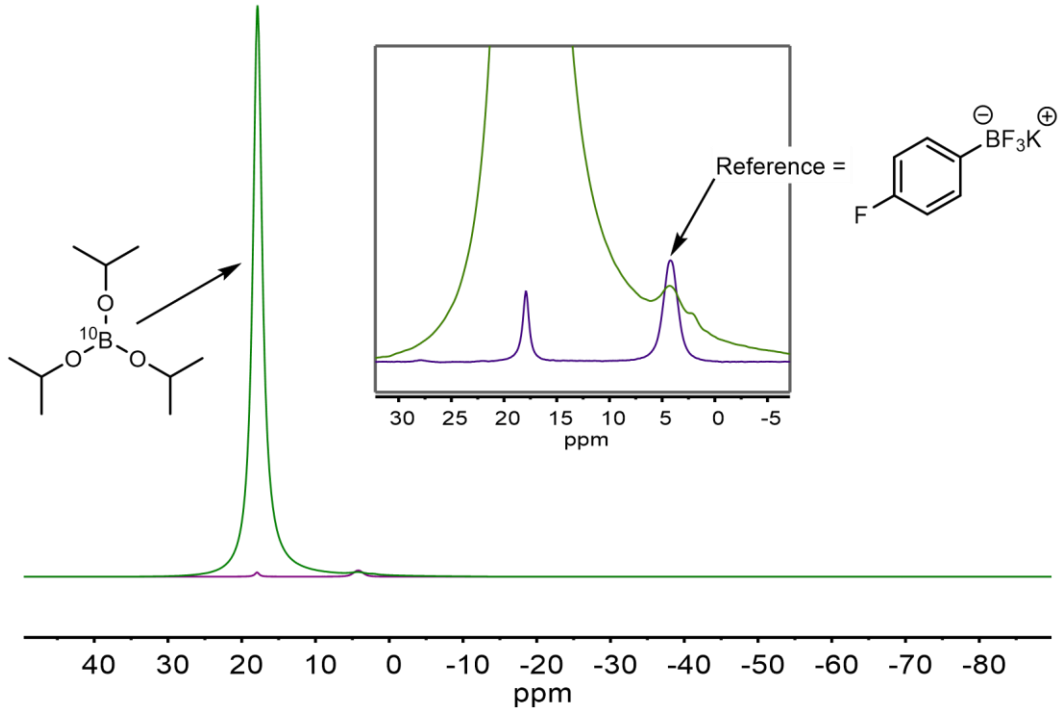


**Figure 4.1** – Superimposed $^{11}$B NMR (purple) and $^{10}$B NMR (green) spectra showing $^{11}$B/$^{10}$B ratios. Isolated labelled product displaying > 98% of $^{10}$B incorporation while typical 4:1 ratio is present in the reference compound.

Title compound > 99% pure by $^{1}$H NMR (based on isopropanol residual signal). $^{10}$B incorporation was determined using a natural abundance $ArBF_3K$ salt (Figure 4.1) and was estimated to be higher than 98%. Data is consistent with that expected based on published data for the same compound with natural abundance $^{10}$B/$^{11}$B (20/80).[174]

**[$^{10}$B]-Tris(*o*-tolyl)phosphine borane [$^{10}$B]-$\mathbf{1_{PB}}$**

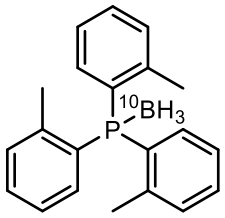


*General considerations:* Lithium aluminium hydride (95%) was used in its pellet form as it allowed a slow release into the reaction mixture permitting a gentler and step-wise reduction of [$^{10}$B]-triisopropoxyborane, a key feature for obtaining good yields (see Appendix for details on reaction optimisation).

To a $N_2$ purged two-necked round bottom flask was added tris(*o*-tolyl)phosphine (4.93 g, 16.2 mmol, 1.5 equiv.) over a flow of nitrogen and dissolved with THF (22 mL) followed by addition of [$^{10}$B]-triisopropoxyborane (2.5 mL, 10.8 mmol, 1 equiv.). The reaction mixture was then cooled down to 0 °C and $LiAlH_4$ (335 mg pellets, 8.6 mmol, 0.8 equiv.) was added over a flow of nitrogen. The ice-water bath used was left to thaw overnight so the reaction slowly reached room temperature. After 16 h the reaction was quenched by adding sat. aqueous potassium sodium tartrate (Rochelle salt) dropwise at 0 °C until bubbling ceased. Then, the mixture was diluted with $CH_2Cl_2$ (100 mL) and additional sat. aqueous potassium sodium tartrate (200 mL) added. The aqueous phase was extracted with $CH_2Cl_2$ (3 x 100 mL); the combined organics were washed with sat. aqueous $NaHCO_3$ (100 mL) and dried over $MgSO_4$, filtered and solvent removal *in vacuo*.

The crude solid obtained was redissolved with $CH_2Cl_2$ (600 mL) in a round bottom flask. The solution was treated with aqueous $H_2O_2$ (200 mL, 3% v/v) and stirred for 3 h; the experimental procedure to oxidise free phosphine was taken from literature.[175] The aqueous layer was discarded, and the organic fraction was washed with sat. aqueous $NaHCO_3$ (200 mL), dried over $MgSO_4$, filtered and concentrated *in vacuo*. The residue was filtered through a pre-wetted silica gel plug (eluent: $CH_2Cl_2$/petroleum ether 40-60, 1:1) using nitrogen to push the solvent through the column. Evaporation of solvent under vacuum yielded the title compound as a white solid (the content of free phosphine ranged from 3 to 23% by $^{31}P\{^1H\}$ NMR and crude yields from 52.2 to 71.9%). Representative $^{31}P$ spectra from samples taken during and after the oxidation and purification are shown in Figure 4.2. This

procedure was repeated six times to collect enough solid reagent for the H$^{10}$Bpin synthesis. **$^{1}$H NMR** (400 MHz, $CDCl_3$) $\delta_H$: 1.13-1.79 (br, 3H), 2.32 (s, 9H), 7.13 (m, 12H); **$^{13}$C{$^{1}$H} NMR** (101 MHz, $CDCl_3$) $\delta_C$: 23.12 (d, *J* 3.7), 126.0 (d, *J* 8.9), 254.16 (d, *J* 53.3), 131.37 (d, *J* 1.5), 132.16 (d, *J* 9.0), 133.48 (d, *J* 7.4), 143.92 (d, *J* 11.4); **$^{10}$B{$^{1}$H} NMR** (43 MHz, $CDCl_3$) $\delta_B$: −31.02; **$^{31}$P{$^{1}$H} NMR** (162 MHz, $CDCl_3$) $\delta_P$: 22.95; mp 149-151 °C.

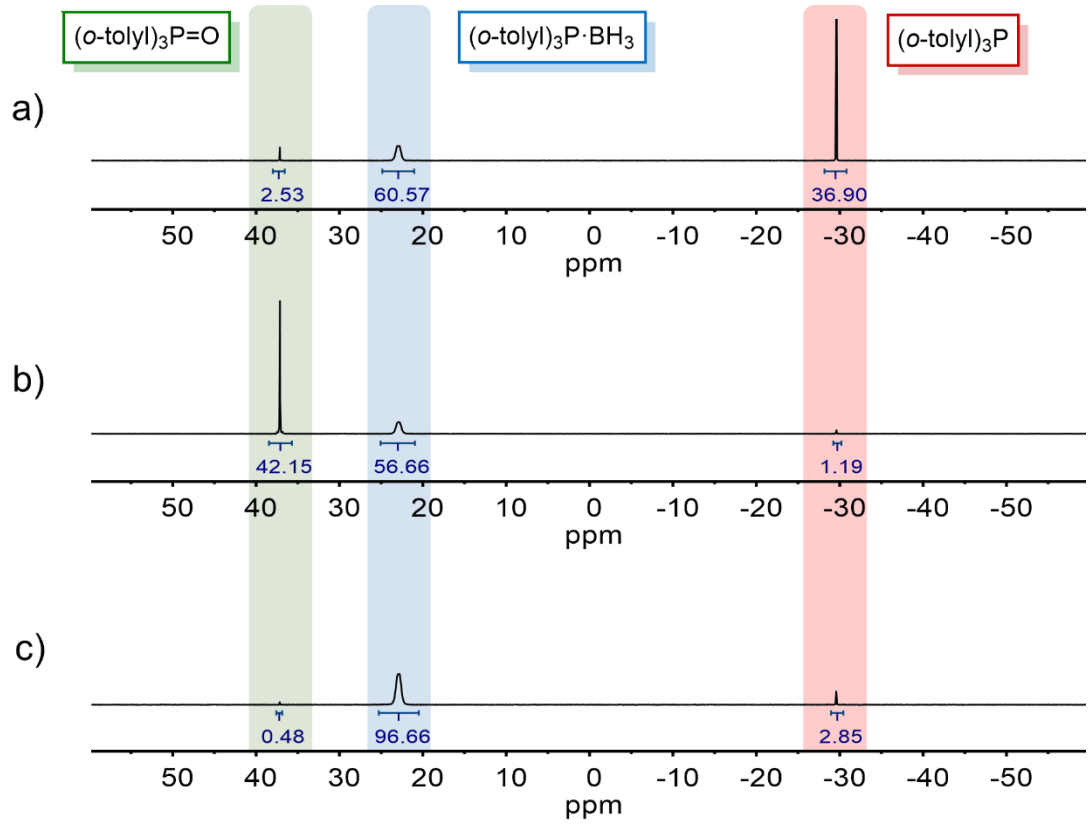


**Figure 4.2** – $^{31}$P{$^{1}$H} NMR spectra showing the fate of the species before (a) and after (b) the oxidation step; free phosphine is selectively oxidised in the presence of $H_2O_2$ (3% v/v) while phosphine borane complex remains unaffected, the former is then easily removed by silica gel filtration (c).

Data is consistent with that expected based on published data for the same compound with natural abundance $^{10}$B/$^{11}$B (20/80).[78]

**[$^{10}$B]-Pinacolborane**

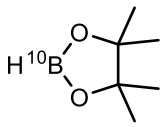

Individual batches from [$^{10}$B]-tris(*o*-tolyl)phosphine borane synthesis were combined and used without further purification. To a $N_2$ purged two-necked round bottom flask was added [$^{10}$B]-tris(*o*-tolyl)phosphine borane (13.5 g, 42.5 mmol, 1.3 equiv.) and pinacol (3.86 g, 32.7 mmol, 1 equiv.) over a flow of nitrogen followed by addition of dioxane/$CHCl_3$ (23 mL, 100:1). The mixture was left to stir for 16 h at 57 °C. The reaction was cooled down to 40 °C and the supernatant was pumped off *in vacuo* (90-60 mbar) and trapped at -78 °C into a dry Schlenk tube; the trapped solution was kept under dry nitrogen as a clear and colourless liquid. **$^1$H NMR** [400 MHz, dioxane/$CHCl_3$ (100:1) spiked with $CDCl_3$] $\delta_H$: 0.87; **$^{13}$C{$^1$H} NMR** [101 MHz, dioxane/$CHCl_3$ (100:1) spiked with $CDCl_3$] $\delta_C$: 24.12, 82.56; **$^{10}$B NMR** [43 MHz, dioxane/$CHCl_3$ (100:1) spiked with $CDCl_3$] $\delta_B$: 28.05 (d, *J* 54.8).

Title compound was obtained in a 1.09 M solution; volume estimated to be 15 mL to give a total yield of ~50%. The concentration was calculated by using the newly synthesised labelled compound in a standard kinetic reaction where H$^{10}$Bpin was the limiting reagent as explained below.

First, $^1$H NMR spectroscopy with solvent signal suppression was used to calculate an estimate concentration of the H$^{10}$Bpin solution. An aliquot of the H$^{10}$Bpin solution (100 μL) was accurately measured volumetrically and added into a Young's Tap NMR tube under $N_2$ atmosphere. Additionally, a solution of 1,3,5-trimethoxybenzene in $CDCl_3$ (0.133 M, 400 μL) was added as internal standard, the tube was then closed and shaken to ensure well mixing and the spectrum recorded. Molarity of the isolated H$^{10}$Bpin solution was calculated to be 1.53 M based on this experiment (Figure 4.3).

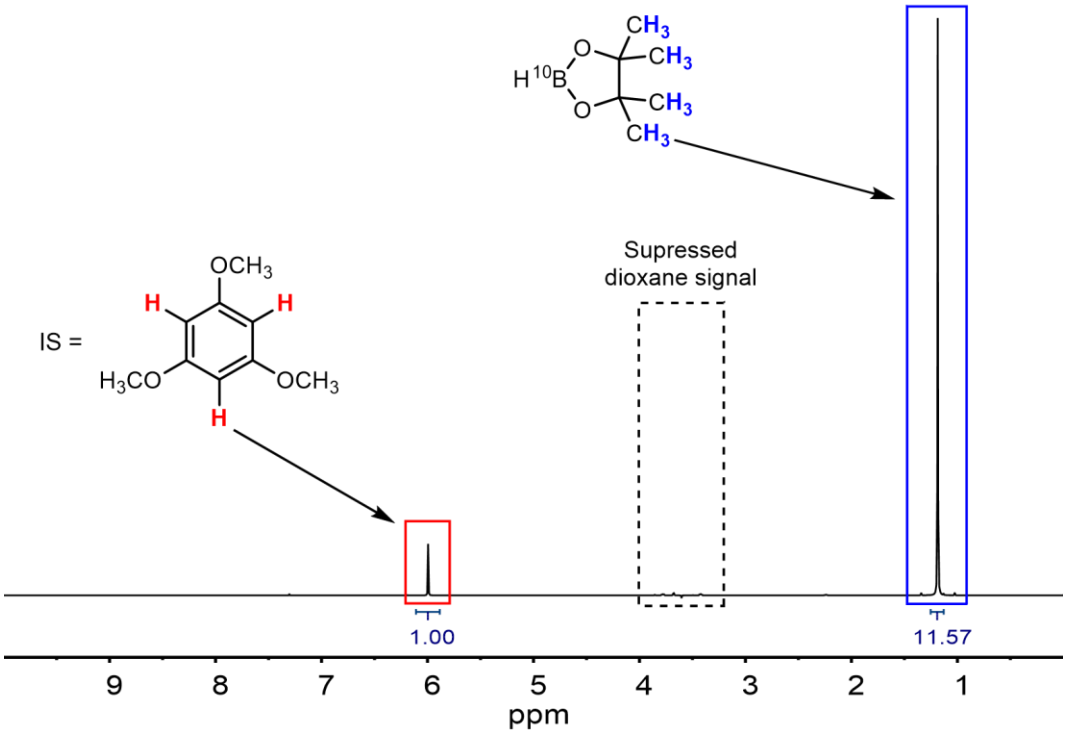


**Figure 4.3** – $^{1}$H NMR spectrum for quantification of [$^{10}$B]-pinacolborane showing the integration of the benzylic protons from the IS (red) against the methyl protons from [$^{10}$B]-pinacolborane (blue).

To rectify the calculated molarity from the H$^{10}$Bpin solution, a dicyclohexylborane-catalysed hydroboration of 4-fluorophenylacetylene **3** reaction was set up and monitored as described in the representative procedure in section 4.3.1 on page 114. For this purpose, the freshly prepared H$^{10}$Bpin was used (295 μL, 0.45 mmol, 1 equiv.) using the solution's molarity estimation previously calculated (1.53 M). As depicted in Figure 4.4, only 0.321 mmol of H$^{10}$BPin reacted based on $[\mathbf{3}]_0$ = 0.538 M, $[\mathbf{3}]_{end}$ = 0.154 M; the reactive molarity of the H$^{10}$BPin solution can then be calculated to be 1.09 M.

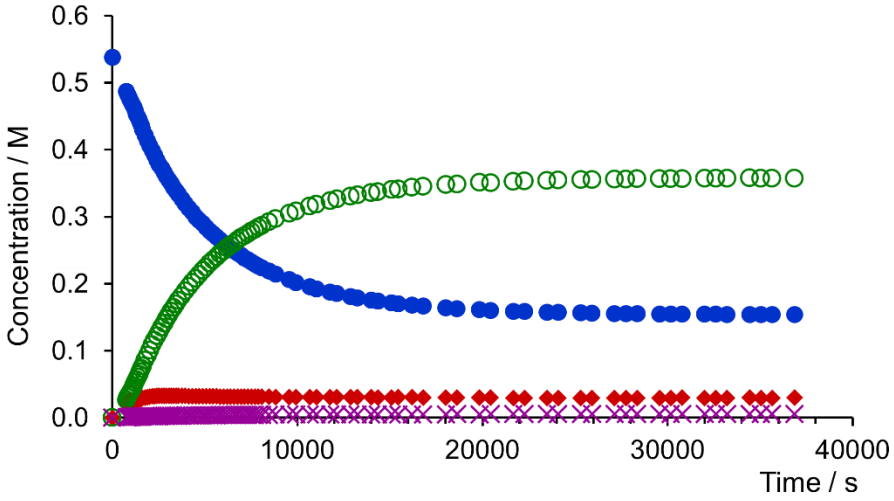


**Figure 4.4** – Temporal concentration profile for hydroboration of **3** by $HBCy_2$ using labelled $H^{10}Bpin$ showing incomplete consumption of the substrate (blue circles: **3**, outlined green circles: ***E*-4$_{pin}$**, red diamonds: ***E*-6$_{Cy2}$**, purple crosses: ***iso*-6$_{Cy2}$**).

# References


1. Brown, H. C.; Rao, B. C. S. *J. Am. Chem. Soc.* **1956**, *78* (11), 2582–2588.

2. Brown, H. C.; Benjamin, W. A. *Angew. Chemie* **1963**, *75* (3), 179–179.

3. Suzuki, A.; Dhillon, R. S. *Top. Curr. Chem.* **1986**, *130*, 23–88.

4. Yamamoto, H. In *Lewis Acids in Organic Synthesis*; Wiley-VCH, 2000; pp 191–281.

5. Kim, B. M.; Williams, S. F.; Masamune, S. In *Comprehensive Organic Synthesis*; Pergamon, 1991; p 239.

6. Miyaura, N.; Suzuki, A. *Chem. Rev.* **1995**, *95* (7), 2457–2483.

7. Miyaura, N. In *Cross-Coupling Reactions: A Practical Guide (Topics in Current Chemistry)*; Springer, 2002; p 11.

8. Miyaura, N. In *Metal-catalyzed cross-coupling reactions*; Wiley-VCH, 2004; p 41.

9. Torborg, C.; Beller, M. *Adv. Synth. Catal.* **2009**, *351* (18), 3027–3043.

10. Crabtree, R. H. *The Organometallic Chemistry of the Transition Metals*; Wiley, 2005.

11. Cooper, T. W. J.; Campbell, I. B.; MacDonald, S. J. F. *Angew. Chemie - Int. Ed.* **2010**, *49* (44), 8082–8091.

12. Lennox, A. J. J.; Lloyd-Jones, G. C. *Chem. Soc. Rev.* **2014**, *43* (1), 412–443.

13. Molander, G. A.; Biolatto, B. *J. Org. Chem.* **2003**, *68* (11), 4302–4314.

14. Molander, G. A.; Canturk, B.; Kennedy, L. E. *J. Org. Chem.* **2009**, *74* (3), 973–980.

15. Knapp, D. M.; Gillis, E. P.; Burke, M. D. *J. Am. Chem. Soc.* **2009**, *131* (20), 6961–6963.

16. Li, J.; Grillo, A. S.; Burke, M. D. *Acc. Chem. Res.* **2015**, *48* (8), 2297–2307.

17. Warren, C. B.; Malec, E. J. *Science* **1972**, *176* (4032), 277–279.

18. Gillis, E. P.; Burke, M. D. *Aldrichimica Acta* **2009**, *42* (1), 17–27.

19. Gillis, E. P.; Burke, M. D. *J. Am. Chem. Soc.* **2007**, *129* (21), 6716–6717.

20. Suk, J. L.; Gray, K. C.; Paek, J. S.; Burke, M. D. *J. Am. Chem. Soc.* **2008**, *130* (2), 466–468.

21. Mancilla, T.; Contreras, R.; Wrackmeyer, B. *J. Organomet. Chem*. **1986**, *307* (1), 1–6.

22. Ballmer, S. G.; Gillis, E. P.; Burke, M. D. *Org. Synth.* **2009**, *86* (September), 344–359.

23. Brice, E. U.; Gillis, E. P.; Burke, M. D. *Tetrahedron* **2009**, *65* (16), 3130–3138.

24. Woerly, E. M.; Cherney, A. H.; Davis, E. K.; Burke, M. D. *J. Am. Chem. Soc.* **2010**, *132* (20), 6941–6943.

25. Struble, J. R.; Lee, S. J.; Burke, M. D. *Tetrahedron* **2010**, *66* (26), 4710–4718.

26. Lee, S. J.; Anderson, T. M.; Burke, M. D. *Angew. Chemie Int. Ed.* **2010**, *49* (47), 8860–8863.

27. Dick, G. R.; Knapp, D. M.; Gillis, E. P.; Burke, M. D. *Org. Lett.* **2010**, *12* (10), 2314–2317.

28. Gillis, E. P.; Burke, M. D. *J. Am. Chem. Soc.* **2008**, *130* (43), 14084–14085.

29. Mancilla, T.; Zamudio-rivera, L. S.; Beltrán, I.; Santillan, R. *Arkivoc* **2005**, *2005* (6), 366–376.

30. Dhillon, R. S. *Hydroboration and Organic Synthesis*; Springer, 2007.

31. Pereira, S.; Srebnik, M. *Organometallics* **1995**, *14* (7), 3127–3128.

32. He, X.; Hartwig, J. F.; He, X.; Hartwig, J. F. *J. Am. Chem. Soc.* **1996**, *118* (7), 1696–1702.

33. Kim, H. R.; Jung, I. G.; Yoo, K.; Jang, K.; Lee, E. S.; Yun, J.; Son, S. U. *Chem. Commun.* **2010**, *46* (5), 758–760.

34. Obligacion, J. V.; Neely, J. M.; Yazdani, A. N.; Pappas, I.; Chirik, P. J. *J. Am. Chem. Soc.* **2015**, *137* (18), 5855–5858.

35. Greenhalgh, M. D.; Jones, A. S.; Thomas, S. P. *ChemCatChem* **2015**, *7* (2), 190–222.

36. Tucker, C. E.; Davidson, J.; Knochel, P. *J. Org. Chem*. **1992**, *57* (12), 3482–3485.

37. Hoshi, M.; Arase, A. *Synth. Commun.* **1997**, *27* (4), 567–572.

38. Shirakawa, K.; Arase, A.; Hoshi, M. *Synthesis* **2004**, 11, 1814–1820.

39. Miyaura, N.; Suzuki, A. *J. Chem. Soc. Chem. Commun.* **1979**, No. 866, 866–867.

40. Miyaura, N.; Yamada, K.; Suzuki, A. *Tetrahedron Lett.* **1979**, *20* (36), 3437–3440.

41. Pelter, A.; Smith, K.; Brown, H. C. *Borane Reagents: Best Synthetic Methods*; Academic Press, 1988.

42. Suzuki, A. *Angew. Chemie - Int. Ed.* **2011**, *50* (30), 6723–6733.

43. Suzuki, A. *J. Organomet. Chem.* **1999**, *576* (1–2), 147–168.

44. Brown, H. C.; Bhat, N. G.; Somayaji, V. *Org. Synth.* **1983**, *2* (10), 1311–1316.

45. Brown, H. C.; Imai, T. *Organometallics* **1984**, *3* (8), 1392–1395.

46. Hoffmann, R. W.; Dresely, S. *Synthesis* **1988**, *2*, 103–106.

47. Martinez-Fresneda, P.; Vaultier, M. *Tetrahedron Lett.* **1989**, *30* (22), 2929–2932.

48. Rasset-Deloge, C.; Martinez-Fresneda, P.; Vaultier, M. *Bull. Soc. Chim. Fr.* **1992**, *129*, 285–290.

49. Hara, S.; Hyuga, S.; Aoyama, M.; Sato, M.; Suzuki, A. *Tetrahedron Lett.* **1990**, *31* (2), 247–250.

50. Knizek, J.; Nöth, H.; Schmidt-Amelunxen, M. *Eur. J. Inorg. Chem.* **2011**, *2011* (36), 5548–5557.

51. Woerly, E. M.; Struble, J. R.; Palyam, N.; O'Hara, S. P.; Burke, M. D. *Tetrahedron* **2011**, *67* (24), 4333–4343.

52. Alnajjar, M.; Quigley, D.; Kuntamukkula, M.; Simmons, F.; Freshwater, D.; Bigger, S. *J. Chem. Heal. Saf.* **2011**, *18* (1), 5–10.

53. Burg, A. B.; Wagner, R. I. *J. Am. Chem. Soc.* **1952**, *75* (6), 3872–3877.

54. Frisch, H. A.; Heal, H. G.; Mackle, H.; Madden, I. O. *J. Chem. Soc.* **1965**, 899–907.

55. Nguyen, D. H.; Bayardon, J.; Salomon-Bertrand, C.; Jugé, S.; Kalck, P.; Daran, J. C.; Urrutigoity, M.; Gouygou, M. *Organometallics* **2012**, *31* (3), 857–869.

56. Denmark, S. E.; Werner, N. S. *Org. Lett.* **2011**, *13* (17), 4596–4599.

57. Grabulosa, A. *P-Stereogenic Ligands in Enantioselective Catalysis*; Royal Society Of Chemistry, 2010.

58. Adams, R. M.; Beres, J.; Dodds, A.; Morabito, A. J. *Inorg. Chem.* **1971**, *10* (9), 2072–2074.

59. Imamoto, T.; Kusumoto, T.; Suzuki, N.; Sato, K. *J. Am. Chem. Soc.* **1985**, *107*, 5301–5303.

60. Corey, E. J.; Chen, Z.; Tanoury, G. J. *J. Am. Chem. Soc.* **1993**, *115* (1), 11000–11001.

61. McNulty, J.; Zhou, Y. *Tetrahedron Lett.* **2004**, *45* (2), 407–409.

62. Moulin, D.; Bauduin, C.; Darcel, C.; Jugé, S. *Tetrahedron: Asymmetry* **2000**, *11*, 3939–3956.

63. Jugé, S.; Stephan, M.; Laffitte, J. A.; Genet, J. P. *Tetrahedron Lett.* **1990**, *31* (44), 6357–6360.

64. Imamoto, T.; Sugita, K.; Yoshida, K. *J. Am. Chem. Soc.* **2005**, *127* (34), 11934–11935.

65. Heath, H.; Wolfe, B.; Livinghouse, T.; Bae, S. K. *Synthesis* **2001**, No. 15, 2341–2347.

66. Katagiri, K.; Danjo, H.; Yamaguchi, K.; Imamoto, T. *Tetrahedron* **2005**, *61* (19), 4701–4707.

67. Grabulosa, A.; Muller, G.; Ordinas, J. I.; Mezzetti, A.; Maestro, M. A.; Font-Bardia, M.; Solans, X. *Organometallics* **2005**, *24* (21), 4961–4973.

68. Yamago, S.; Yanagawa, M.; Mukai, H.; Nakamura, E. *Tetrahedron* **1996**, *52* (14), 5091–5102.

69. Morisaki, Y.; Imoto, H.; Tsurui, K.; Chujo, Y. *Org. Lett.* **2009**, *11* (11), 2241–2244.

70. McKinstry, L.; Livinghouse, T. *Tetrahedron Lett.* **1994**, *35* (50), 9319–9322.

71. McKinstry, L.; Livinghouse, T. *Tetrahedron* **1995**, *51* (28), 7655–7666.

72. McKinstry, L.; Overberg, J. J.; Soubra-Ghaoui, C.; Walsh, D. S.; Robins, K. A.; Toto, T. T.; Toto, J. L. *J. Org. Chem.* **2000**, *65* (7), 2261–2263.

73. Muhlberg, M.; Jaradat, D. M. M.; Kleineweischede, R.; Papp, I.; Dechtrirat, D.; Muth, S.; Broncel, M.; Hackenberger, C. P. R. *Bioorganic Med. Chem.* **2010**, *18* (11), 3679–3686.

74. Knühl, G.; Sennhenn, P.; Helmchen, G. *J. Chem. Soc. Chem. Commun.* **1995**, *5*, 1845–1846.

75. Imamoto, T.; Watanabe, J.; Wada, Y.; Masuda, H.; Yamada, H.; Tsuruta, H. *J. Am. Chem. Soc.* **1998**, *120*, 1635–1636.

76. Yang, Z.; Liu, D.; Liu, Y.; Sugiya, M.; Imamoto, T.; Zhang, W. *Organometallics* **2015**, *34* (7), 1228–1237.

77. Schröder, M.; Nozaki, K.; Hiyama, T. *Bull. Chem. Soc. Jpn.* **2004**, *77* (10), 1931–1932.

78. Van Overschelde, M.; Vervecken, E.; Modha, S. G.; Cogen, S.; Van der Eycken, E.; Van der Eycken, J. *Tetrahedron* **2009**, *65* (32), 6410–6415.

79. Camus, J. M.; Andrieu, J.; Richard, P.; Poli, R.; Darcel, C.; Jugé, S. *Tetrahedron Asymmetry* **2004**, *15* (13), 2061–2065.

80. Nöth, H.; Wrackmeyer, B. *Nuclear Magnetic Resonance Spectroscopy of Boron Compounds*; Springer-Verlag, 1978.

81. Eisenberger, P.; Crudden, C. M. *Dalt. Trans.* **2017**, *46* (15), 4874–4887.

82. Potyen, M.; Josyula, K. V. B.; Schuck, M.; Lu, S.; Gao, P.; Hewitt, C. *Org. Process Res. Dev.* **2007**, *11* (2), 210–214.

83. Graham, W. A. G.; Stone, F. G. A. *J. Inorg. Nucl. Chem.* **2003**, *3* (3–4), 164–177.

84. Brown, H. C. *Hydroboration, W. A. Benjamin: New York*; 1962.

85. Brown, H. C. *Pure Appl. Chem.* **1976**, *47* (8), 49–60.

86. Brown, H. C.; Chandrasekharan, J.; Wang, K. K. *Pure Appl. Chem.* **1983**, *55* (9), 1387–1414.

87. Pelter, A.; Smith, K.; Brown, H. C. *Borane Reagents; Academic Press Inc.: San Diego CA*; 1988.

88. Trost, B. M.; Ball, Z. T. *Synthesis* **2005**, 6, 853–887.

89. Brown, H. C.; Zweifel, G. *J. Am. Chem. Soc.* **1960**, *82* (17), 4708–4712.

90. Woods, W. G.; Bengelsdorf, I. S.; Hunter, D. L. *J. Org. Chem.* **1966**, *31* (9), 2766–2768.

91. Brown, H. C.; Gupta, S. K. *J. Am. Chem. Soc.* **1972**, *94* (12), 4370–4371.

92. Brown, H. C.; Gupta, S. K. *J. Am. Chem. Soc.* **1975**, *97* (18), 5249–5255.

93. Zaidlewicz, M.; Meller, J. *Collect. Czech. Chem. Commun.* **1999**, *64* (6), 1049–1056.

94. Kanth, J. V. B.; Periasamy, M.; Brown, H. C. *Org. Process Res. Dev.* **2002**, *4* (6), 550–553.

95. Morrill, T. C.; D'Souza, C. A.; Yang, L.; Sampognaro, A. J. *J. Org. Chem.* **2002**, *67* (8), 2481–2484.

96. Westcott, S. A.; Blom, H. P.; Marder, T. B.; Baker, R. T.; Calabrese, J. C. *Inorg. Chem.* **1993**, *32* (10), 2175–2182.

97. Brown, H. C.; Basavaiah, D.; Kulkarni, S. U. *J. Organomet. Chem.* **1982**, *225* (1), 63–69.

98. Li, P.; Li, J.; Arikan, F.; Ahlbrecht, W.; Dieckmann, M.; Menche, D. *J. Org. Chem.* **2010**, *75* (8), 2429–2444.

99. Chen, Q.; Schweitzer, D.; Kane, J.; Davisson, V. J.; Helquist, P. *J. Org. Chem.* **2011**, *76* (13), 5157–5169.

100. Kamabuchi, A.; Moriya, T.; Miyaura, N.; Suzuki, A. *Synth. Commun.* **1993**, *23* (20), 2851–2859.

101. Handa, M.; Scheldt, K. A.; Bossart, M.; Zheng, N.; Roush, W. R. *J. Org. Chem.* **2008**, *73* (3), 1031–1035.

102. Kalinin, A. V.; Scherer, S.; Snieckus, V. *Angew. Chemie - Int. Ed.* **2003**, *42* (29), 3399–3404.

103. Molander, G. A.; Dehmel, F. *J. Am. Chem. Soc.* **2004**, *126* (33), 10313–10318.

104. Luithle, J. E. A.; Pietruszka, J.; Witt, A. *Chem. Commun.* **1998**, *4* (23), 2651–2652.

105. Arase, A.; Hoshi, M.; Mijin, A.; Nishi, K. *Synth. Commun.* **1995**, *25* (13), 1957–1962.

106. Evans, D. A.; Starr, J. T. *J. Am. Chem. Soc.* **2003**, *125* (44), 13531–13540.

107. Fürstner, A.; Flügge, S.; Larionov, O.; Takahashi, Y.; Kubota, T.; Kobayashi, J. *Chem. Eur. J.* **2009**, *15* (16), 4011–4029.

108. Pellicena, M.; Krämer, K.; Romea, P.; Urpí, F. *Org. Lett.* **2011**, *13* (19), 5350–5353.

109. Bassan, E. M.; Baxter, C. A.; Beutner, G. L.; Emerson, K. M.; Fleitz, F. J.; Johnson, S.; Keen, S.; Kim, M. M.; Kuethe, J. T.; Leonard, W. R.; et al. *Org. Process Res. Dev.* **2012**, *16* (1), 87–95.

110. Napolitano, C.; Palwai, V. R.; Eriksson, L. A.; Murphy, P. V. *Tetrahedron* **2012**, *68* (27–28), 5533–5540.

111. Scaggs, W. R.; Snaddon, T. N. *Chem. Eur. J.* **2018**, *24* (54), 14378–14381.

112. Fleige, M.; Möbus, J.; vom Stein, T.; Glorius, F.; Stephan, D. W. *Chem. Commun.* **2016**, *52* (72), 10830–10833.

113. Lawson, J. R.; Wilkins, L. C.; Melen, R. L. *Chem. Eur. J.* **2017**, *23* (46), 10997–11000.

114. Ang, N. W. J.; Buettner, C. S.; Docherty, S.; Bismuto, A.; Carney, J. R.; Docherty, J. H.; Cowley, M. J.; Thomas, S. P. *Synthesis* **2018**, *50* (4), 803–808.

115. Wen, K.; Chen, J.; Gao, F.; Bhadury, P. S.; Fan, E.; Sun, Z. *Org. Biomol. Chem.* **2013**, *11* (37), 6350–6356.

116. Ho, H. E.; Asao, N.; Yamamoto, Y.; Jin, T. *Org. Lett.* **2014**, *16* (17), 4670–4673.

117. Hong, S.; Zhang, W.; Liu, M.; Yao, Z. J.; Deng, W. *Tetrahedron Lett.* **2016**, *57* (1), 1–4.

118. Wu, Y.; Shan, C.; Ying, J.; Su, J.; Zhu, J.; Liu, L. L.; Zhao, Y. *Green Chem.* **2017**, *19* (17), 4169–4175.

119. Boussonnière, A.; Pan, X.; Geib, S. J.; Curran, D. P. *Organometallics* **2013**, *32* (24), 7445–7450.

120. McGough, J. S.; Butler, S. M.; Cade, I. A.; Ingleson, M. J. *Chem. Sci.* **2016**, *7* (5), 3384–3389.

121. Hoffmann, R. W.; Krüger, J.; Brückner, D. *New J. Chem.* **2001**, *25*, 102–107.

122. Wang, Y. D.; Kimball, G.; Prashad, A. S.; Wang, Y. *Tetrahedron Lett.* **2005**, *46* (50), 8777–8780.

123. Pereira, S.; Srebnik, M. *Tetrahedron Lett.* **1996**, *37* (19), 3283–3286.

124. Ohmura, T.; Yamamoto, Y.; Miyaura, N. *J. Am. Chem. Soc.* **2000**, *122* (20), 4990–4991.

125. Cid, J.; Carbó, J. J.; Fernández, E. *Chem. Eur. J.* **2012**, *18* (5), 1512–1521.

126. Neilson, B. M.; Bielawski, C. W. *Organometallics* **2013**, *32* (10), 3121–3128.

127. von Hahmann, C. N.; Talavera, M.; Xu, C.; Braun, T. *Chem. Eur. J.* **2018**, *24* (43), 11131–11138.

128. Curto, S. G.; Esteruelas, M. A.; Oliván, M.; Oñate, E. *Organometallics* **2019**, *38* (9), 2062–2074.

129. Dietz, M.; Johnson, A.; Martínez-Martínez, A.; Weller, A. S. *Inorganica Chim. Acta* **2019**, *491* (February), 9–13.

130. Takahashi, K.; Ishiyama, T.; Miyaura, N. *J. Organomet. Chem.* **2001**, *625* (1), 47–53.

131. Moure, A. L.; Gómez Arrayás, R.; Cárdenas, D. J.; Alonso, I.; Carretero, J. C. *J. Am. Chem. Soc.* **2012**, *134* (17), 7219–7222.

132. He, T.; Li, B.; Liu, L. C.; Wang, J.; Ma, W. P.; Li, G. Y.; Zhang, Q. W.; He, W. *Chem. - A Eur. J.* **2019**, *25* (4), 966–970.

133. Yoshida, H.; Takemoto, Y.; Takaki, K. *Chem. Commun.* **2014**, *50* (61), 8299–8302.

134. Jang, W. J.; Lee, W. L.; Moon, J. H.; Lee, J. Y.; Yun, J. *Org. Lett.* **2016**, *18* (6), 1390–1393.

135. Romero, E. A.; Jazzar, R.; Bertrand, G. *J. Organomet. Chem.* **2017**, *829*, 11–13.

136. Zhao, F.; Jia, X.; Li, P.; Zhao, J.; Zhou, Y.; Wang, J.; Liu, H. *Org. Chem. Front.* **2017**, *4* (11), 2235–2255.

137. Netsu, Y.; Tsukada, N. *Org. Chem.* **2017**, *14* (4), 243–247.

138. Song, L.; Ma, X.; Xu, S.; Shi, M.; Zhang, J. *New J. Chem.* **2018**, *42* (11), 8342–8345.

139. Lipshutz, B. H.; Bošković, Ž. V.; Aue, D. H. *Angew. Chemie Int. Ed.* **2008**, *47* (52), 10183–10186.

140. Lee, J. E.; Kwon, J.; Yun, J. *Chem. Commun.* **2008**, No. 6, 733–734.

141. Kim, H. R.; Jung, I. G.; Yoo, K.; Jang, K.; Lee, E. S.; Yun, J.; Son, S. U. *Chem. Commun.* **2010**, *46* (5), 758–760.

142. Sasaki, Y.; Horita, Y.; Zhong, C.; Sawamura, M.; Ito, H. *Angew. Chemie Int. Ed.* **2011**, *50* (12), 2778–2782.

143. Jang, H.; Zhugralin, A. R.; Lee, Y.; Hoveyda, A. H. *J. Am. Chem. Soc.* **2011**, *133* (20), 7859–7871.

144. Kim, H. R.; Yun, J. *Chem. Commun.* **2011**, *47* (10), 2943–2945.

145. Yuan, W.; Ma, S. *Org. Biomol. Chem.* **2012**, *10* (36), 7266–7268.

146. Semba, K.; Fujihara, T.; Terao, J.; Tsuji, Y. *Chem. Eur. J.* **2012**, *18* (14), 4179–4184.

147. Park, J. K.; Ondrusek, B. A.; McQuade, D. T. *Org. Lett.* **2012**, *14* (18), 4790–4793.

148. Jung, H. Y.; Feng, X.; Kim, H.; Yun, J. *Tetrahedron* **2012**, *68* (17), 3444–3449.

149. Moure, A. L.; Mauleón, P.; Arrayás, R. G.; Carretero, J. C. *Org. Lett.* **2013**, *15* (8), 2054–2057.

150. Stavber, G.; Časar, Z. *Appl. Organomet. Chem.* **2013**, *27* (3), 159–165.

151. Bidal, Y. D.; Lazreg, F.; Cazin, C. S. J. *ACS Catal.* **2014**, *4* (5), 1564–1569.

152. Zaidlewicz, M.; Meller, J. *Main Gr. Met. Chem.* **2000**, *23* (12), 765–772.

153. Lee, C. I.; Zhou, J.; Ozerov, O. V. *J. Am. Chem. Soc.* **2013**, *135* (9), 3560–3566.

154. Merola, J. S.; Knorr, J. R. *J. Organomet. Chem.* **2014**, *750*, 86–97.

155. Lee, C. I.; Shih, W. C.; Zhou, J.; Reibenspies, J. H.; Ozerov, O. V. *Angew. Chemie Int. Ed.* **2015**, *54* (47), 14003–14007.

156. Yoshida, H.; Kimura, M.; Tanaka, H.; Murashige, Y.; Kageyuki, I.; Osaka, I. *Chem. Commun.* **2019**, *55* (38), 5420–5422.

157. Sundararaju, B.; Fürstner, A. *Angew. Chemie - Int. Ed.* **2013**, *52* (52), 14050–14054.

158. Szyling, J.; Franczyk, A.; Stefanowska, K.; Klarek, M.; Maciejewski, H.; Walkowiak, J. *ChemCatChem* **2018**, *10* (3), 531–539.

159. Haberberger, M.; Enthaler, S. *Chem. Asian J.* **2013**, *8* (1), 50–54.

160. Greenhalgh, M. D.; Thomas, S. P. *Chem. Commun.* **2013**, *49* (95), 11230–11232.

161. Rawat, V. S.; Sreedhar, B. *Synlett* **2014**, *25* (8), 1132–1136.

162. Cabrera-Lobera, N.; Rodríguez-Salamanca, P.; Nieto-Carmona, J. C.; Buñuel, E.; Cárdenas, D. J. *Chem. Eur. J.* **2018**, *24* (4), 784–788.

163. Leyva, A.; Zhang, X.; Corma, A. *Chem. Commun.* **2009**, No. 33, 4947–4949.

164. Wang, Q.; Motika, S. E.; Akhmedov, N. G.; Petersen, J. L.; Shi, X. *Angew. Chemie Int. Ed.* **2014**, *53* (21), 5418–5422.

165. Bismuto, A.; Thomas, S. P.; Cowley, M. J. *Angew. Chem. Int. Ed.* **2016**, No. 55, 1–5.

166. Bismuto, A.; Cowley, M. J.; Thomas, S. P. *ACS Catal.* **2018**, *8* (3), 2001–2005.

167. Harinath, A.; Banerjee, I.; Bhattacharjee, J.; Panda, T. K. *New J. Chem.* **2019**, 10531–10536.

168. Lee, G. M.; Vogels, C. M.; Decken, A.; Westcott, S. A. *Eur. J. Inorg. Chem.* **2011**, No. 15, 2433–2438.

169. Frisch, M. J.; Trucks, G. W.; Schlegel, H. B.; Scuseria, G. E.; Robb, M. A.; Cheeseman, J. R.; Scalmani, G.; Barone, V.; Mennucci, B.; Petersson, G. A.; Nakatsuji, H.; Caricato, M.; Li, X.; Hratchian, H. P.; Izmaylov, A. F.; Bloino, J.; Zheng, G.; Sonnenberg, J. L.; Hada, M.; Ehara, M.; Toyota, K.; Fukuda, R.; Hasegawa, J.; Ishida, M.; Nakajima, T.; Honda, Y.; Kitao, O.; Nakai, H.; Vreven, T.; Montgomery, J. A., Jr.; Peralta, J. E.; Ogliaro, F.; Bearpark, M.; Heyd, J. J.; Brothers, E.; Kudin, K. N.; Staroverov, V. N.; Kobayashi, R.; Normand, J.; Raghavachari, K.; Rendell, A.; Burant, J. C.; Iyengar, S. S.; Tomasi, J.; Cossi, M.; Rega, N.; Millam, J. M.; Klene, M.; Knox, J. E.; Cross, J. B.; Bakken, V.; Adamo, C.; Jaramillo, J.; Gomperts, R.; Stratmann, R. E.; Yazyev, O.; Austin, A. J.; Cammi, R.; Pomelli, C.; Ochterski, J. W.; Martin, R. L.; Morokuma, K.; Zakrzewski, V. G.; Voth, G. A.; Salvador, P.; Dannenberg, J. J.; Dapprich, S.; Daniels, A. D.; Farkas, Ö.; Foresman, J. B.; Ortiz, J. V.; Cioslowski, J.; Fox, D. J. *Gaussian, Inc., Wallingford CT*, **2009**.

170. Hemelaere, R.; Caijo, F.; Mauduit, M.; Carreaux, F.; Carboni, B. *J. Org. Chem*. **2014**, 16, 3328–3333.

171. Park, Y. T.; Chiesel, N.; Economy, J. *Mol. Cryst. Liq. Cryst. Sci. Technol. Sect. A. Mol. Cryst. Liq. Cryst.* **1994**, *247* (1), 351–363.

172. Barsoum, D. N.; Brassard, C. J.; Deeb, J. H. A.; Okashah, N.; Sreenath, K.; Simmons, J. T.; Zhu, L. *Synthesis* **2013**, *45* (17), 2372–2386.

173. Cox, P. A.; Leach, A. G.; Campbell, A. D.; Lloyd-Jones, G. C. *J. Am. Chem. Soc.* **2016**, 138 (29), 9145–9157.

174. Cole, T. E.; Quintanilla, R.; Rodewald, S. *Synth. React. Inorg. Met. Chem*. **1990**, *20* (1), 55–63.

175. Dubován, L.; Pöllnitz, A.; Silvestru, C. *Eur. J. Inorg. Chem*. **2016**, *2016* (10), 1521–1527.

176. Todd, R. C.; Hossain, M. M.; Josyula, K. V.; Gao, P.; Kuo, J.; Tan, C. T. *Tetrahedron Lett.* **2007**, *48* (13), 2335–2337.

# Chapter 5 Appendix

## 5.1 Chapter 1

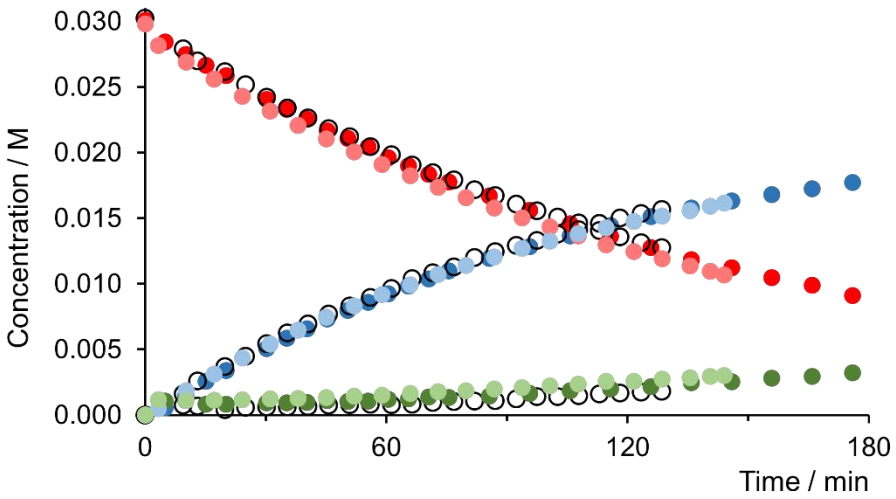


**Figure 5.1** – Temporal concentration profile for ethanolyses of $\mathbf{1_{PB}}$ in $CHCl_3$ (filled circles) and $CDCl_3$ (outlined circles) showing acceptable reproducibility; monitored by $^{11}B\{^1H\}$ NMR (red circles: $\mathbf{1_{PB}}$, blue circles: $\mathbf{2_{INT}}$, green circles: **2**). Conditions: $[\mathbf{1_{PB}}]_0$ = 0.03 M, $[EtOH]_0$ = 5 M at 30 °C.

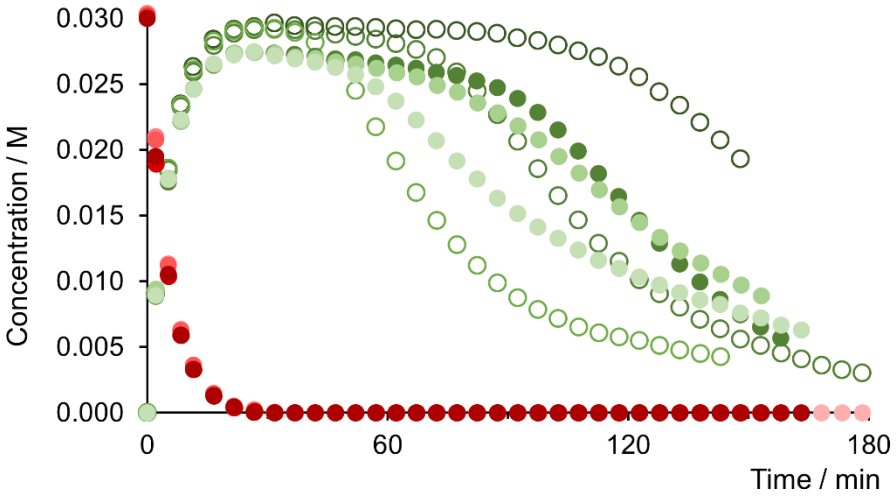


**Figure 5.2** – Temporal concentration profile for ethanolyses of $\mathbf{1_{PB}}$ in dioxane/$CHCl_3$ (80,000:1, filled circles) and dioxane/$CDCl_3$ (80,000:1, outlined circles) showing highly variable intermediate consumption; monitored by $^{11}B\{^1H\}$ NMR (red circles: $\mathbf{1_{PB}}$, green circles: $\mathbf{2_{INT}}$). Conditions: $[\mathbf{1_{PB}}]_0$ = 0.03 M, $[EtOH]_0$ = 5 M at 30 °C.

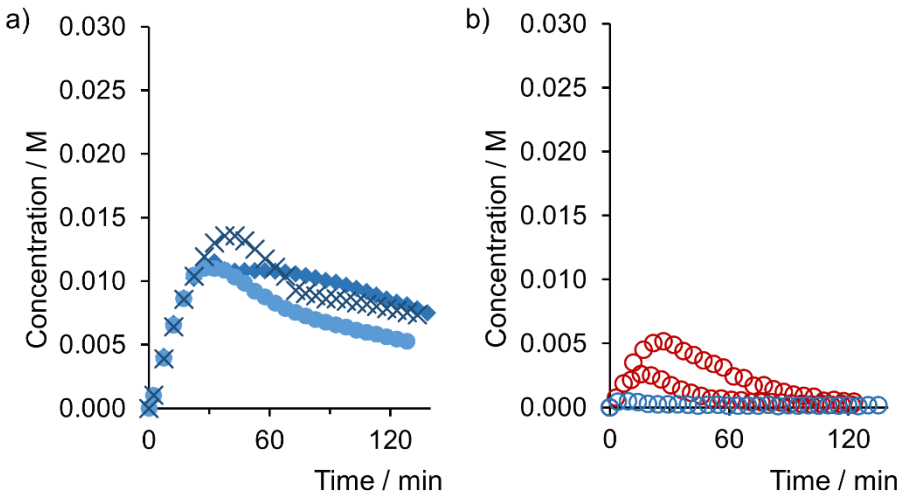


**Figure 5.3** – Temporal concentration profile for different ethanolyses of $\mathbf{1_{PB}}$ displaying the effect bubbling has on the intermediate $\mathbf{2_{INT}}$ build-up; monitored by $^{11}B\{^1H\}$ NMR. **a)** Bubbling $N_2$ starting at 20 min (circles), 30 min (diamonds) and 60 min (crosses); **b)** $N_2$ (blue) and $O_2$ (red) continuous bubbling since the beginning of the reaction. Conditions: $[\mathbf{1_{PB}}]_0$ = 0.03 M, $[EtOH]_0$ = 5 M in toluene at 30 °C.

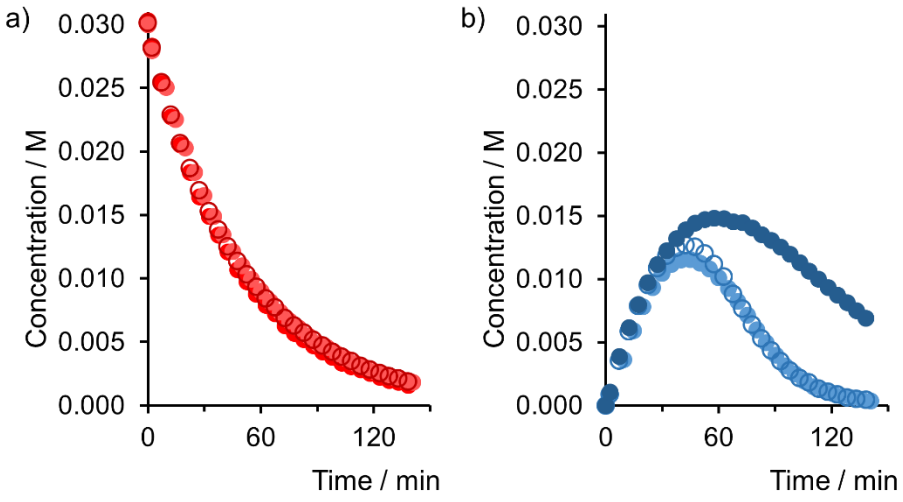


**Figure 5.4** – Temporal concentration profile for ethanolyses of $\mathbf{1_{PB}}$ with benzoyl peroxide as additive at 5 mol% (filled circles) and 10 mol% (outlined circles); monitored by $^{11}B\{^1H\}$ NMR. **a)** Reproducible pseudo-first order decay of $\mathbf{1_{PB}}$; **b)** Irreproducible $\mathbf{2_{INT}}$ build-up. Conditions: $[\mathbf{1_{PB}}]_0$ = 0.03 M, $[EtOH]_0$ = 5 M in toluene at 30 °C.

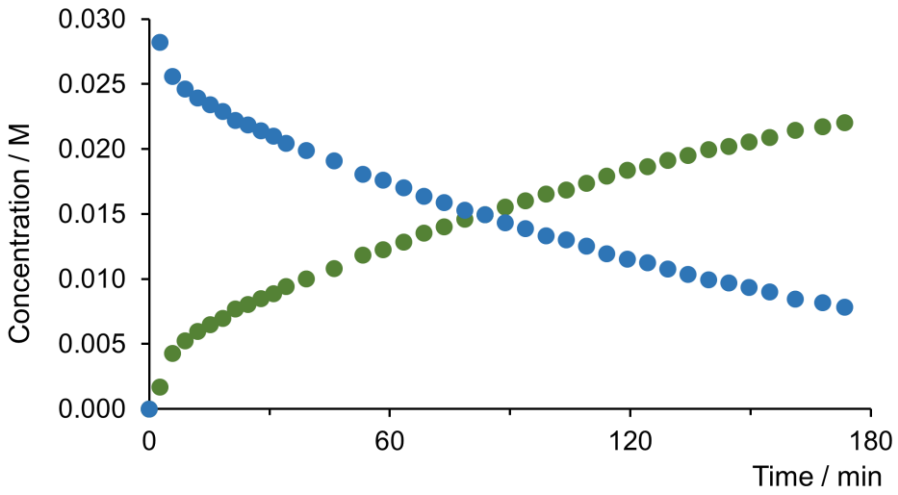


**Figure 5.5** – Temporal concentration profile for ethanolysis of DMSB in the presence of free phosphine; monitored by $^{11}B\{^{1}H\}$ NMR (blue circles: $\mathbf{2_{INT}}$, green circles: **2**). Conditions: $[\mathbf{1_{PB}}]_0$ = 0.03 M, $[(o\text{-tolyl})_3P]$ = 0.03 M, $[EtOH]_0$ = 5 M in dioxane at 30 °C.

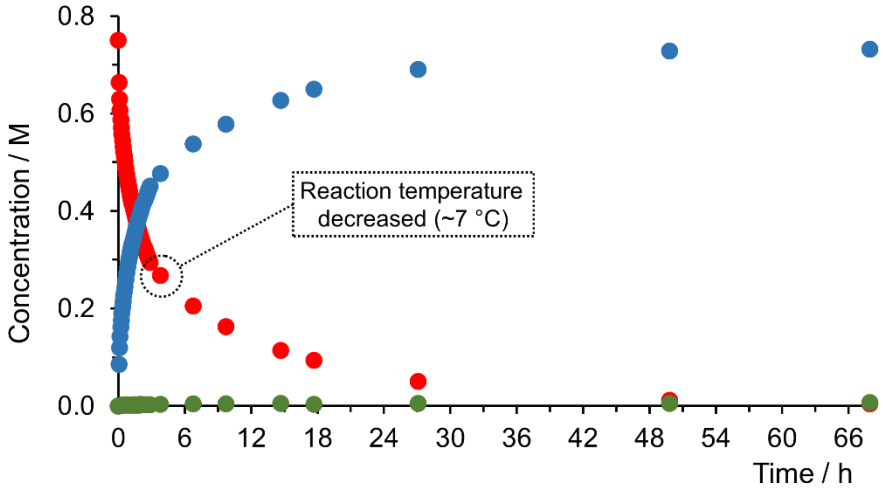


**Figure 5.6** – Temporal concentration profile for pinacolysis of DMSB monitored by $^{11}B\{^{1}H\}$ NMR (red circles: DMSB, blue circles: HBpin, green circles: $B_2pin_3$). Conditions: $[DMSB]_0$ = 0.03 M, [pinacol] = 0.03 M in dioxane at 30 °C for 3 h then lowered to 23 °C.

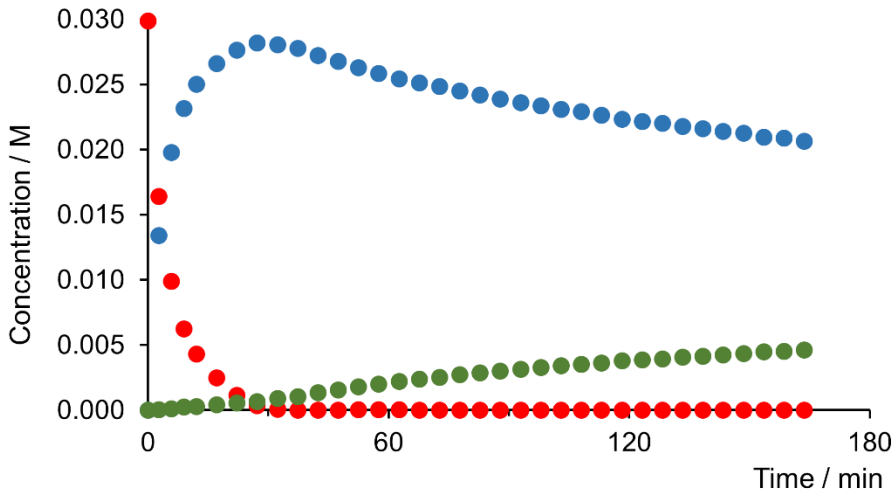


**Figure 5.7** – Temporal concentration profile for pinacolysis of DMSB monitored by $^{11}B\{^{1}H\}$ NMR (red circles: DMSB, blue circles: HBpin, green circles: $B_2pin_3$). Conditions: $[DMSB]_0$ = 0.03 M, [pinacol] = 0.27 M in dioxane at 30 °C.

## 5.2 Chapter 2

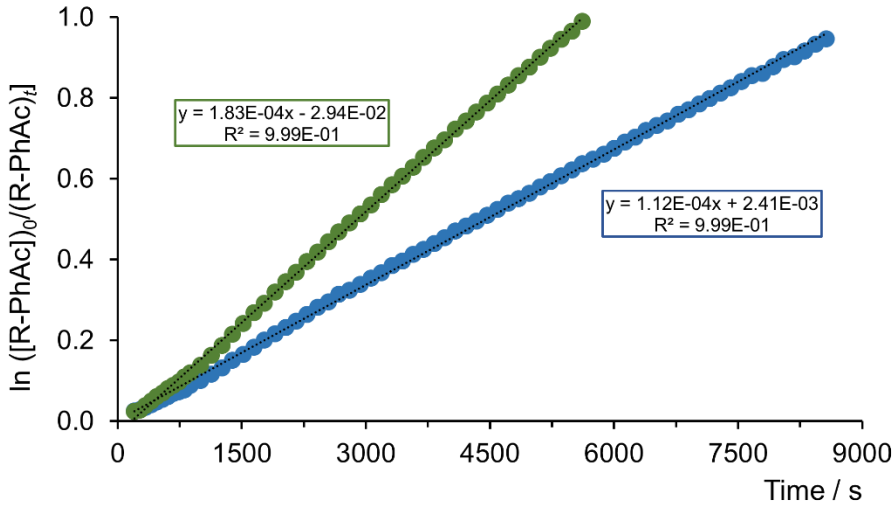


**Figure 5.8** – Pseudo-first order rate constants ($k_{obs}$) calculated from the decay of 4-fluorophenylacetylene (blue data) and 4-(trifluoromethyl)phenylacetylene (green data). Conditions: $[F\text{-}PhAcetylene]_0$ = 0.3 M, $[F_3C\text{-}PhAcetylene]_0$ = 0.3 M, [HBpin] = 0.06, $[HBCy_2]$ = 0.06 M and [1-fluoronaphthalene] = 0.253 M in dioxane/$CHCl_3$ (100:1) at 23 °C.

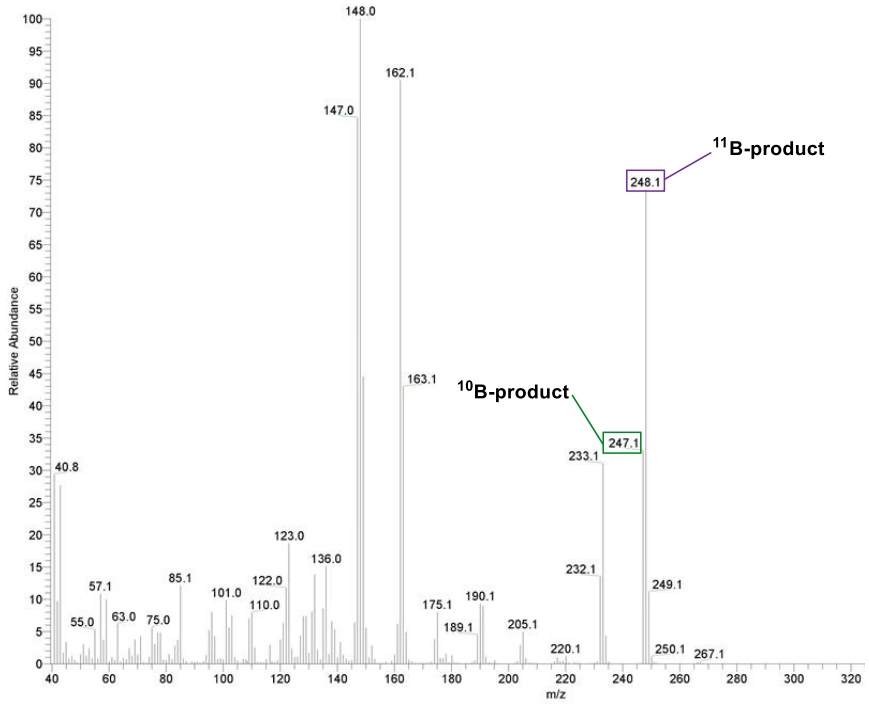


**Figure 5.9** – EI-MS spectrum of product ***E*-4$_{pin}$** from control reaction using HBpin; $^{11}$B represents the mayor isotope incorporated in the product.

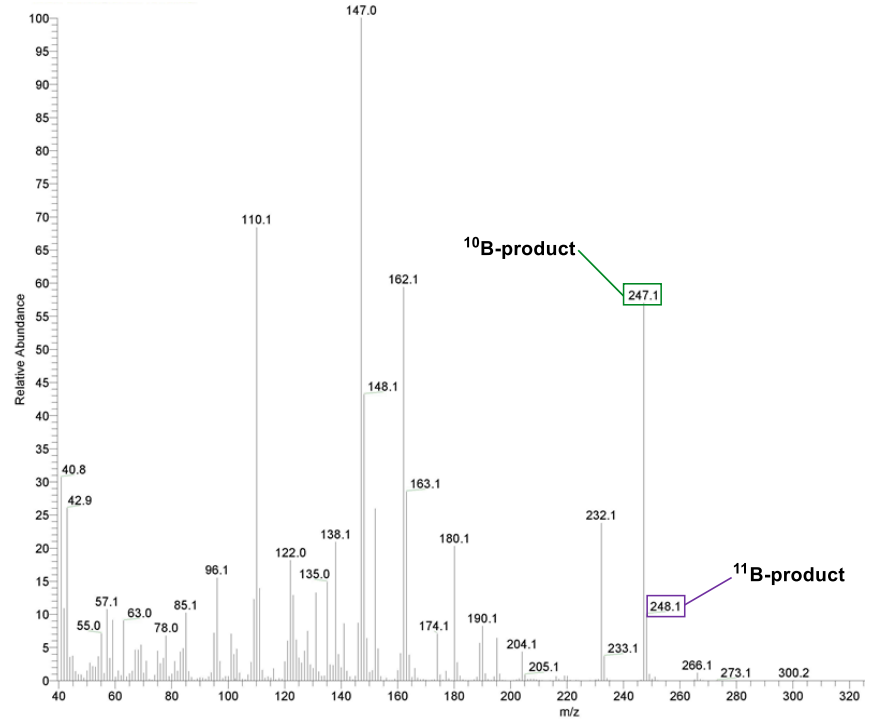


**Figure 5.10** – EI-MS spectrum of product [$^{10}$B]-***E*-4$_{pin}$** from single turnover experiment using H$_{10}$Bpin indicating enrichment of $^{10}$B into the product.

## 5.2.1 Deuteration Efficiency of [$D_3$]-THFB

In order to assess if the non-complete deuterated product obtained when $DBCy_2$ was used (Figure 2.9) arose from using an incomplete deuterated THF [$D_3$]-borane complex or from the reaction *per se*, an experiment was set up where [$D_3$]-THFB was used in an *in situ* alkene hydroboration/oxidation reaction (Scheme 5.1). After the work up, $^1$H NMR spectroscopy was used to calculate deuterium content in the product. A control reaction was again carried out where non-labelled reagents were used instead.

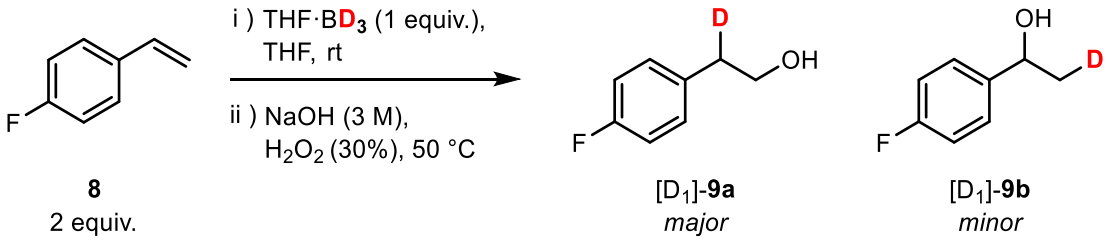


**8**
2 equiv.

[$D_1$]-**9a**
*major*

[$D_1$]-**9b**
*minor*

**Scheme 5.1** – Alkene hydroboration/oxidation. Conditions: $[8]_0$ = 0.45 M, [$D_3$-THFB] = 0.23 M in THF at 50 °C.

To a $N_2$ purged two-necked round bottom flask, THF [$D_3$]-borane complex was added (750 µL, 0.75 mmol, 1 equiv.) and diluted with anhydrous THF (1.2 mL). The diluted solution was cooled down to 0 °C followed by dropwise addition of 4-fluorostyrene **8** (179 µL, 1.5 mmol, 2 equiv.). The reaction mixture was stirred at room temperature for 2 h. After that, the reaction was cooled down to 10 °C and NaOH solution (3 M, 900 µL) followed by $H_2O_2$ (30% in water, 300 µL) were sequentially added. The reaction mixture was stirred further at 50 °C for 2 h and then let it cool down to room temperature.

The crude mixture was diluted with ether (20 mL). Then, the organic phase was consecutively washed with sat. aqueous $Na_2S_2O_3$ (10 mL), water (10 mL) and brine (10 mL), dried over $MgSO_4$ and filtered and solvent removal *in vacuo* (300 mbar). The residue was passed through a silica gel plug (eluent: ether, 30 mL) to give a clear liquid after solvent removal.[176]

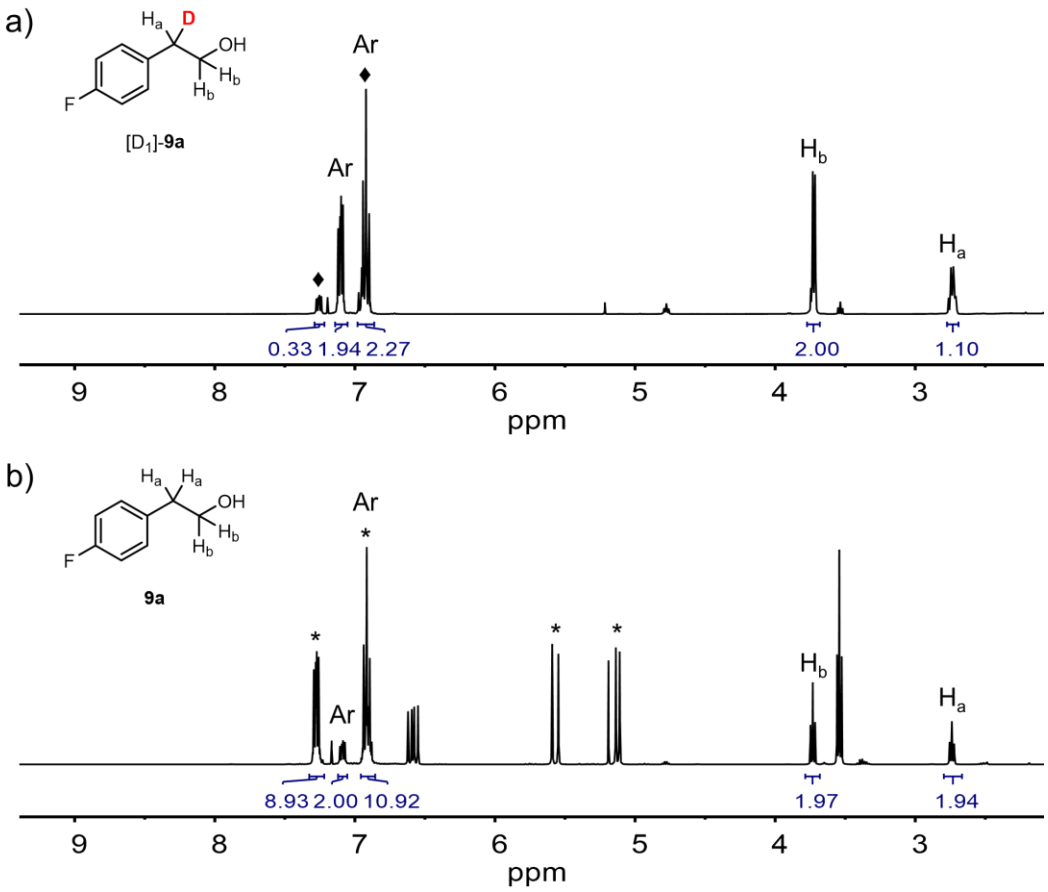


**Figure 5.11** – $^{1}$H NMR spectra; **a)** Isolated labelled product [D$_1$]-**9a** where integration of proton H$_a$ exceeds the expected value by 0.10 due to an incomplete deuteration. Minor regioisomer peaks from [D$_1$]-**9b** are also present (♦); **b)** Isolated product **9a** from control reaction displaying matching integration values for both protons H$_a$ and H$_b$. Peaks from unreacted 4-fluorostyrene are also shown (*).

In addition to NMR spectroscopy, product [D$_1$]-**9a** was analysed by HRMS (EI$^+$) where $C_8H_8DFO^+$ $[M]^+$ found was: 141.07067 m/z, requires: 141.06947 m/z (+1.20 ppm).

## 5.2.2 Synthesis Optimisation Summary for [$^{10}$B]-Tris(o-tolyl)-phosphine borane

The challenging reaction for obtaining [$^{10}$B]-tris(o-tolyl)phosphine borane [$^{10}$B]-**1$_{PB}$** in useful purity and good yields, (needed for the non-trivial synthesis of [$^{10}$B]-pinacolborane) required careful optimization of specific conditions that are

summarised in Table 5.1. Unlabelled materials were used for these series of experiments (Scheme 5.2).

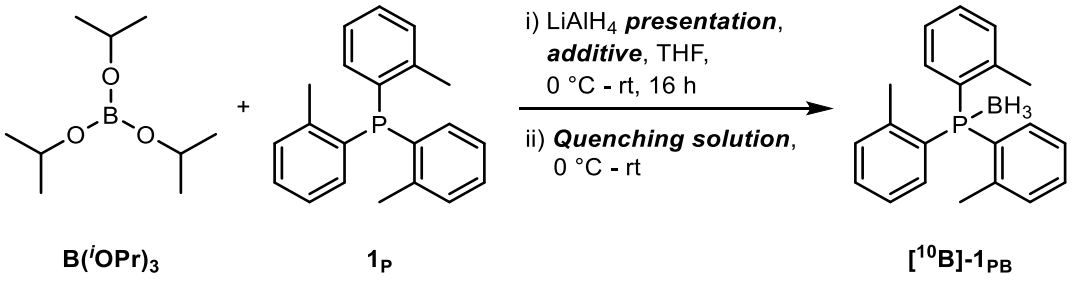


**Scheme 5.2** – Reaction conditions for synthesis optimisation for the preparation of [$^{10}$B]-**1$_{PB}$**.

| Entry | equiv. of B($^{i}$OPr)$_3$ | equiv. of **1$_P$** | equiv. of $LiAlH_4$ | $LiAlH_4$ presentation | Additive | Quenching solution | Crude yield[a] [$^{10}$B]-**1$_{PB}$** (%) | Free phosphine[a] (%) |
|---|---|---|---|---|---|---|---|---|
| 1[b] | 1 | 0.77 | 1.15 | 1 M solution | none | AcOH/THF over 15 min | 70.2 | 27 |
| 2[b] | 1 | 0.77 | 1.15 | 1 M solution | none | AcOH/THF over **30 min** | 75.1 | 16 |
| 3[b] | 1 | 0.77 | 1.15 | 1 M solution | none | AcOH/THF over **2.5 h** | 44.8 | 44 |
| 4[c] | 1 | 0.77 | **0.77** | 1 M solution | **$AlCl_3$** | **Sat. aqueous Rochelle salt** | 40.0 | 51 |
| 5 | 1 | 0.77 | 0.77 | **Pellet** | **none** | Sat. aqueous Rochelle salt | 70.3 | 17 |
| 6 | 1 | **0.9** | **0.9** | Pellet | none | Sat. aqueous Rochelle salt | 41.2 | 60 |
| 7 | 1 | **1.5** | **0.8** | Pellet | none | Sat. aqueous Rochelle salt | 95.7 | 36 |

**Table 5.1** – Optimisation summary for [$^{10}$B]-**1$_{PB}$** synthesis in THF (10 mL). [a]Percentage of free phosphine present in the product calculated from $^{31}P\{^{1}H\}$ NMR. [b]1.7 equiv. of acetic acid in THF (10 mL). [c]0.5 equiv. of $AlCl_3$ in THF (9 mL) were sequentially added three times to give a total of 1.5 equiv used. Changes from the previous entry are shown highlighted.

Particular importance should be given to $LiAlH_4$ addition into the reaction mixture as it takes an overriding role in the triisopropoxyborane reduction. Slow addition

allowed a stepwise and more controlled reduction as seen in Figure **5.12**. This could be achieved by using the required amount of $LiAlH_4$ as solid and slowly dissolving it at cold temperatures. Contrastingly, using a solution of $LiAlH_4$ in conjunction with $AlCl_3$ produced the more reactive $AlH_3$ which reduced triisopropoxyborane affording a borohydride species as the major product (Figure 5.13). This species is not capable of coordinating to free phosphine thus lowering the yield of the desired product.

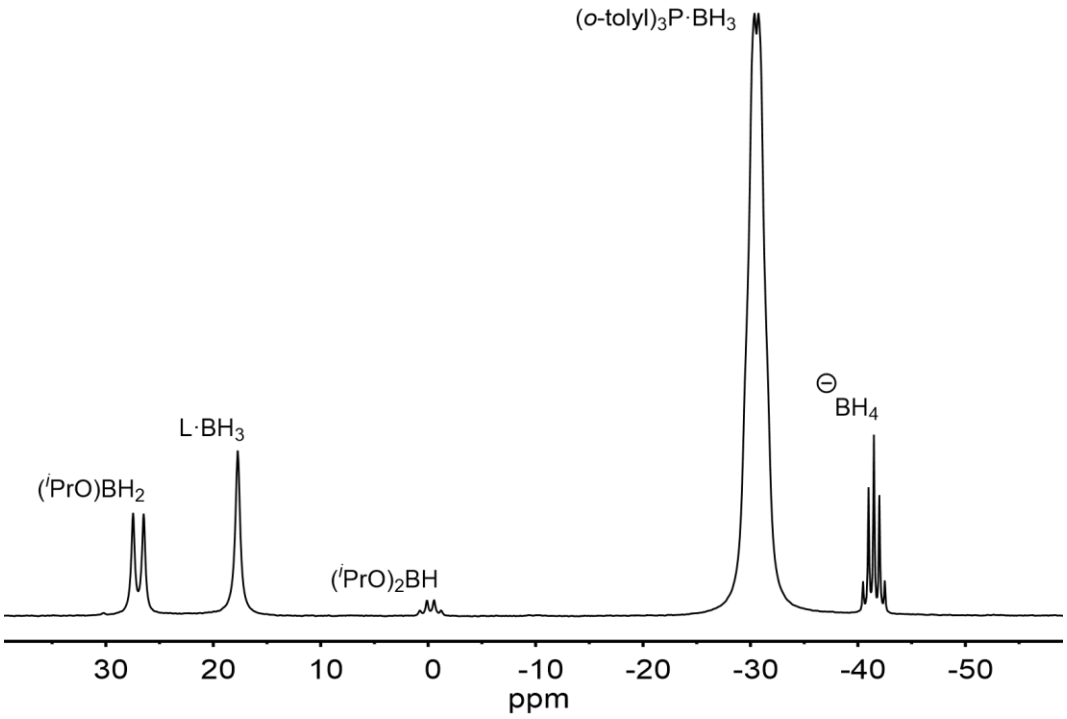


**Figure 5.12** – $^{11}B$ NMR spectrum from an ongoing triisopropoxyborane reduction reaction using the slow release $LiAlH_4$ pellet. All the distinct species are observed in solution before the reaction reached completion indicating a controlled stepwise process.

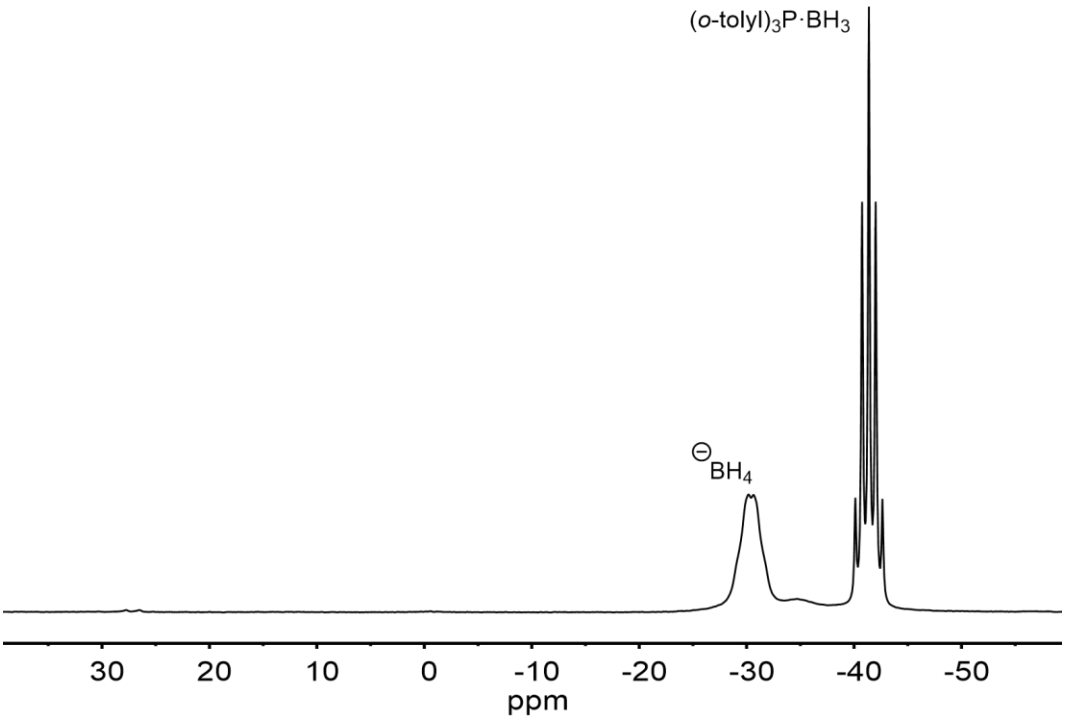


**Figure 5.13** – $^{11}B$ NMR spectrum from an ongoing triisopropoxyborane reduction reaction using a $LiAlH_4$ solution and $AlCl_3$ as an additive, just the product and the borohydride byproduct can be observed suggesting a more aggressive reduction taking place.

## 5.2.3 Double addition side-product NMR data

In a $N_2$ purged Schlenk tube, freshly prepared $HBCy_2$ was used to titrate a solution of (*E*)-2-(4-fluorostyryl)boronic acid pinacol ester (2 mmol) in dioxane/$CHCl_3$ (100:1, 1 mL) in order to increase the concentration of the double addition side-product. Aliquots of the crude mixture were taken (0.1 mL) and diluted with the same solvent system (0.5 mL) to be analysed by $^{19}F$ NMR until the highest signal corresponded to the desired product. Various NMR experiments were run and are shown below.

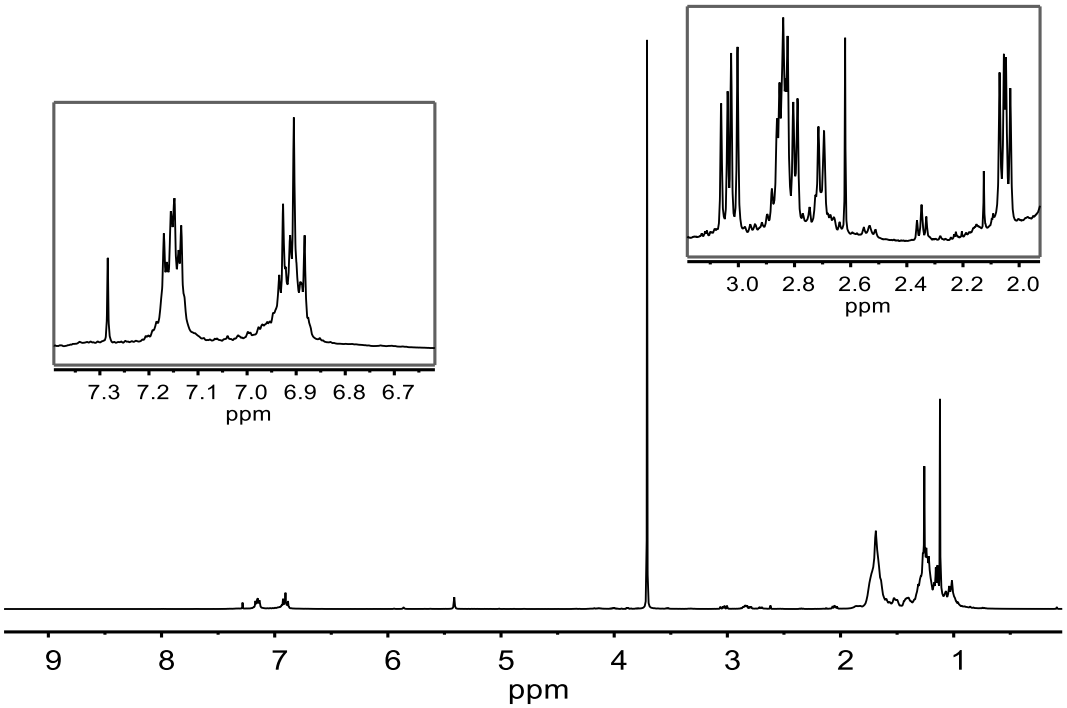


**Figure 5.14** – $^{1}H$ NMR spectrum of double addition side-product titration.

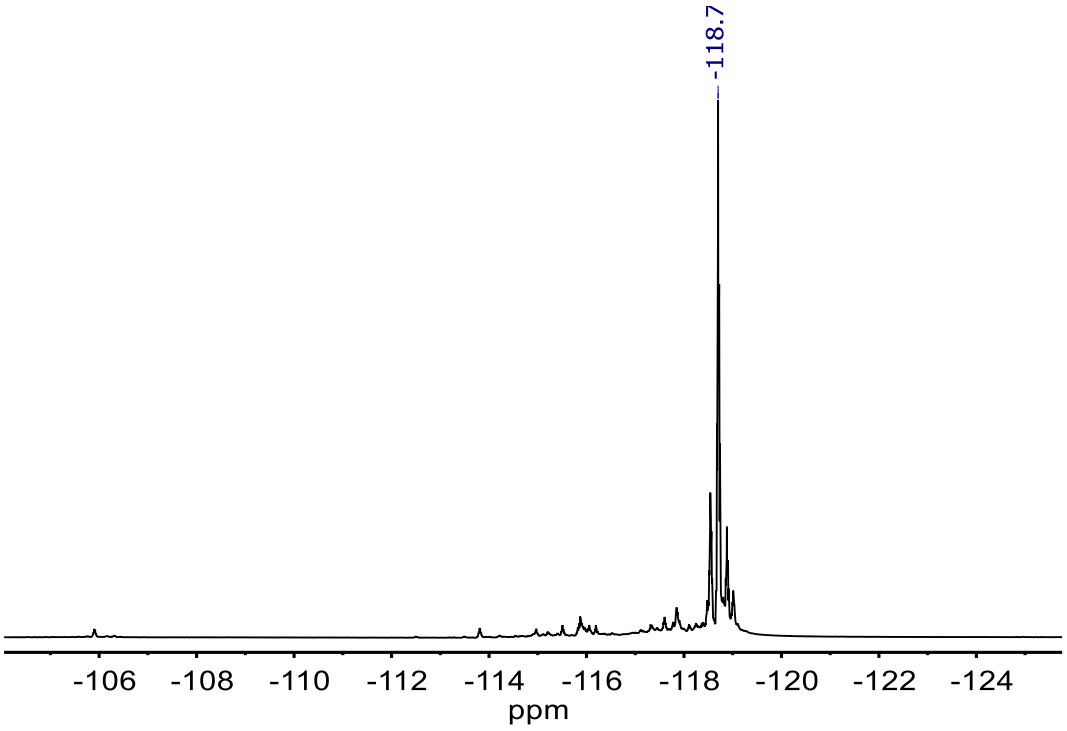


**Figure 5.15** – $^{19}F$ NMR spectrum of double addition side-product titration.

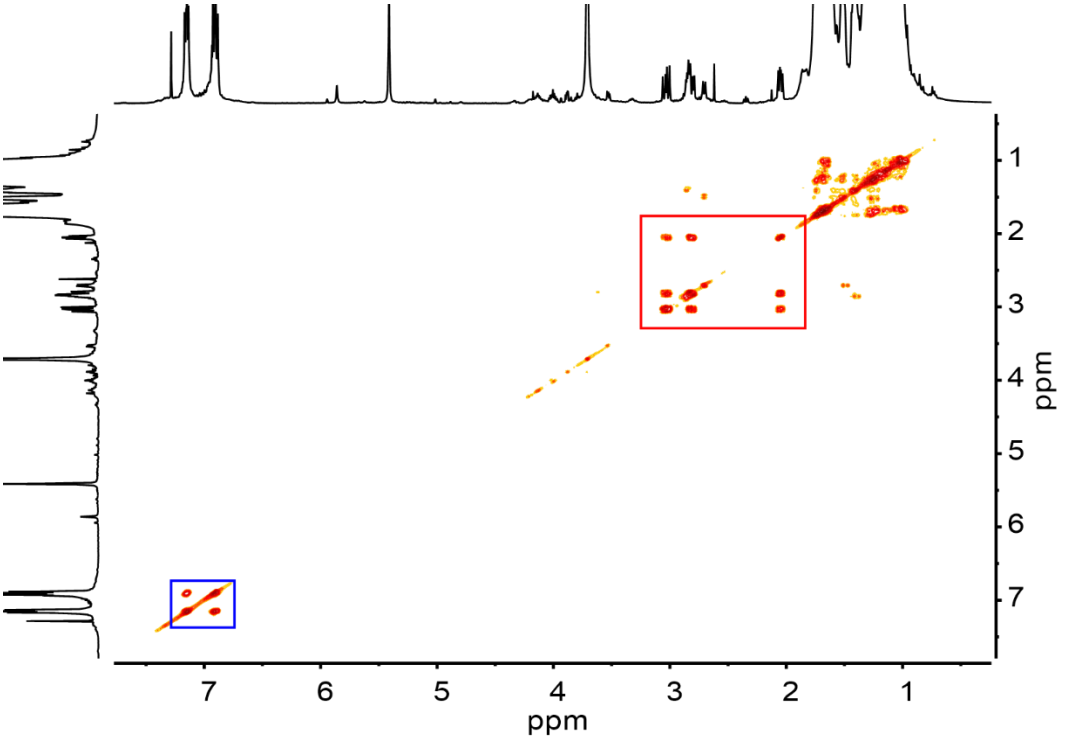


**Figure 5.16** – $^{1}H$-$^{1}H$ COSY spectrum of double addition side-product titration showing aryl protons coupled to each (blue rectangle) other and alkyl protons coupled to each other (red rectangle) (being the -$CH_2$- protons diastereotopic protons, hence three distinct signals).